Wilson, P.A., Lyle, M., and Firth, J.V. (Eds.)
Proceedings of the Ocean Drilling Program, Scientific Results Volume 199

3. Cenozoic Radiolarian Biostratigraphy: A Magnetobiostratigraphic Chronology of Cenozoic Sequences from ODP Sites 1218, 1219, and 1220, Equatorial Pacific[1]

Catherine Nigrini,[2] Annika Sanfilippo,[3] and Theodore J. Moore Jr.[2]

ABSTRACT

A generally rich radiolarian fauna ranging in age from Quaternary to early Eocene (Zone RP7) was found at five of the eight sites drilled during Ocean Drilling Program (ODP) Leg 199. Of particular interest are the stratigraphically complete assemblages that range in age from middle Miocene (Zone RN5) to early Eocene (Zone RP7), composites of Sites 1218, 1219, and 1220. At the same sites, multisensor track (MST) data show consistent cycles in gamma ray attenuation density, color, and carbonate content that can be correlated on a submeter scale from the early Miocene to early Eocene. In addition, the magnetic reversal records from these three sites allow construction of an absolute timescale. A series of 305 radiolarian morphologic first and last occurrences and evolutionary transitions for radiolarians were determined and correlated directly with the accompanying MST and paleomagnetic data, resulting in a detailed and accurate dating of events. Since many of the bioevents are found at more than one site, it was also possible to test their reliability within the study area. Twelve new species are described: *Calocycletta (Calocycletta) anekathen*, *Dorcadospyris anastasis*, *Dorcadospyris copelata*, *Dorcadospyris cyclacantha*, *Dorcadospyris ombros*, *Dorcadospyris scambos*, *Eucyrtidium mitodes*, *Theocyrtis careotuberosa*, *Theocyrtis*

[1] Nigrini, C., Sanfilippo, A., and Moore, T.J., Jr., 2005. Cenozoic radiolarian biostratigraphy: a magnetobiostratigraphic chronology of Cenozoic sequences from ODP Sites 1218, 1219, and 1220, equatorial Pacific. *In* Wilson, P.A., Lyle, M., and Firth, J.V. (Eds.), *Proc. ODP, Sci. Results,* 199, 1–76 [Online]. Available from World Wide Web: <http://www-odp.tamu.edu/publications/199_SR/VOLUME/CHAPTERS/225.PDF>. [Cited YYYY-MM-DD]
[2] Department of Geological Sciences, University of Michigan, 3514B C.C. Little Building, 425 East University, Ann Arbor MI 48109-1063, USA.
[3] Scripps Institution of Oceanography, University of California at San Diego, La Jolla CA 92093-0244, USA. asanfilippo@ucsd.edu

Initial receipt: 2 August 2004
Acceptance: 18 May 2005
Web publication: 11 January 2006
Ms 199SR-225

perpumila, *Theocyrtis perysinos*, *Theocyrtis setanios*, and *Thyrsocyrtis (Pentalacorys) orthotenes*.

INTRODUCTION

The objective of Ocean Drilling Program (ODP) Leg 199 was to drill a transect of sites across the equator along crust that was created at ~56 Ma. In so doing we endeavored to recover well-preserved sections of Paleogene sediments that would give us a history of the strength of the equatorial divergence, the equatorial currents, and the winds that drove them from mid-Miocene through early Eocene times. Although the calcite compensation depth (CCD) was quite shallow (CCD = ~3300 m) during the Eocene, we hoped that the basal part of the recovered section would contain carbonate material that would allow us to compare radiolarian and calcareous nannofossil stratigraphies. Toward that end we also drilled one site (Site 1218) on ~40-Ma crust in order to recover some upper to middle Eocene sediments containing carbonate. We recovered the sections needed for studying the Paleogene history of the equatorial current system; however, poor preservation of the basal sections prevented a detailed comparison of the calcareous and siliceous stratigraphies. The paleomagnetic stratigraphies developed for these sites (Lanci et al., 2004, in press; Pares et al., 2004) did enable us to establish a robust chronostratigraphy for most of the section recovered. This represents the first time that most of the radiolarian stratigraphic datums of the Paleogene have been tied directly to the paleomagnetic timescale.

The primary focus of this investigation is to precisely quantify the timing and duration of radiolarian events in the sedimentary record. A remarkable number of problems can be addressed with a highly calibrated timescale, from rates of biological evolution to evaluating diachrony of extinction events, to connections between evolution and tectonics. The success depends on the application of a well-calibrated magnetostratigraphy. Development of a high-resolution temporal framework for Paleogene radiolarians will benefit macroevolutionary studies of mass extinctions, post-extinction recoveries, evolutionary radiations, patterns of migration, and diversification.

MATERIALS

Because of the overwhelming amount of radiolarian-rich material collected during Leg 199, the subsequent shore-based investigation was divided among the three authors. Dr. T.C. Moore examined the Neogene sections, Dr. C. Nigrini looked at the Oligocene material, and Dr. A. Sanfilippo examined the Eocene sections. For the shore-based report, only Sites 1218, 1219, and 1220 were studied. As a result, there is some variation in the method of reporting abundances, but where uncertainties in relative abundances of some species within a sample exist, they have been recorded simply as present or absent.

At Site 1218 (8.889°N, 135.367°W), we examined almost 300 m of sediment ranging in age from 0.06 to 42.82 Ma and encompassing radiolarian Zones RN16–RP14. Samples were taken from each section of Hole 1218A, and additional samples taken from Holes 1218B and 1218C were integrated into the stratigraphic sequence using multisensor track (MST) data (primarily gamma ray attenuation [GRA] poros-

ity and magnetic susceptibility) to correlate between cores of adjacent holes at the site. During *Maurice Ewing* cruise EW9709, site survey piston core EW9709-7P (8.794°N, 135.366°W) (Moore et al., 2002) was collected and subsequently correlated to the composite MST record of Site 1218 using both magnetic susceptibility (Fig. F1) and GRA data, checked against a comparison of the radiolarian stratigraphies of piston core EW9709-7P and Site 1218. This correlation allowed us to associate each sample depth in core EW9709-7P with an equivalent depth in the Site 1218 composite. The uppermost sections of both Site 1218 and EW9709-7P contain relatively few and generally poorly preserved radiolarians, and it was not possible to determine definite zonal assignments above Zone RN7. Below that, in the Neogene, the fauna became increasingly more abundant and better preserved, making zonal assignments possible. The Oligocene section (Zones RP22–RP20) contains a rich fauna that is generally well preserved but suffers from dissolution from time to time. Although the abundances in the Eocene material are quite high, the preservation is often poor to moderate. This may be due either to the dissolution of delicate forms that one might normally expect to find or to a local paleoenviromental effect. In addition, we observed that some samples contain both well-preserved delicate forms and highly dissolved forms.

At Site 1219 (7.800°N, 142.016°W) we examined ~275 m of sediment ranging in age from 7.27 to 49.99 Ma and encompassing radiolarian Zones RN7–RP12. Sample spacing was variable but usually included three samples and the core catcher from each core. Additional samples from Holes 1219B and 1219C were integrated into the stratigraphic sequence using MST data (primarily GRA porosity and magnetic susceptibility) to correlate between cores of adjacent holes at the site. During *Maurice Ewing* cruise EW9709, site survey piston core EW9709-12P (7.765°N, 141.934°W) (Moore et al., 2002) was collected and subsequently correlated to the composite MST record of Site 1219 using both magnetic susceptibility (Fig. F2) and GRA data, checked against a comparison of the radiolarian stratigraphies of piston core EW9709-12P and Site 1219. This correlation allowed us to associate each sample depth in core EW9709-12P with an equivalent depth in the composite of Site 1219.

Pälike et al. (this volume) also correlated the composite section of Site 1219 to that of Site 1218, checking the correlation against both paleomagnetic data and biostratigraphies. This enabled us to place all the samples from Sites 1218, 1219, and cores EW9709-7P and EW9709-12P on a common depth (revised meters composite depth; rmcd) and timescale. Zones RN3–RN7 contain common but only moderately well preserved radiolarians. Both abundance and preservation improve downhole (Zones RN2–RP12), although there are occasional partially dissolved intervals, particularly in the Oligocene.

At Site 1220 (10.177°N, 142.758°W) we examined ~190 m of sediment ranging in age from 20.83 to 53.25 Ma. The uppermost samples belong to Zone RN2 and the lowermost sample in Zone RP7 represents the oldest radiolarian-rich material found during Leg 199. The Neogene and Oligocene material contain common but only moderately well preserved radiolarians, whereas the Eocene sections contain a common to abundant population in which the preservation is locally idiosyncratic, varying from moderate to good. Sample intervals varied from three to six samples per core with the addition of integrated samples from Holes 1220B and 1220C, particularly in the older Eocene intervals.

F1. Site 1218 vs. core EW9709-7P magnetic susceptibility, p. 58.

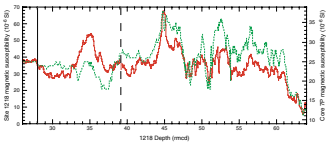

F2. Site 1219 vs. core EW9709-12P magnetic susceptibility, p. 59.

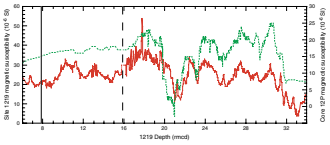

METHODS

Samples were prepared on board ship and sieved at 63 µm following the procedures outlined in Sanfilippo et al. (1985). In some cases we also treated samples with NaOH to aid in the disaggregation of the sediments. Subsequent tests showed that this method did not result in further dissolution of the samples.

The preservation of the assemblages are noted as follows:

G = good (individual specimens exhibit little dissolution and delicate parts of the skeleton are preserved).
M = moderate (dissolution and breakage of individual specimens apparent but identification of species not impaired).
P = poor (individual specimens exhibit considerable dissolution and breakage and identification of some species is not possible).

Total abundances are recorded on a relative scale given as follows:

A = abundant.
C = common.
F = few.
R = rare.
VR = very rare.
B = barren.

Abundances of individual taxa relative to the entire slide are tabulated as follows (symbols contained within parentheses represent suspected reworking):

A = abundant (>10%).
C = common (>1%–10%).
F = few (>0.5%–1%).
VF = very few (>0.1%–0.5%).
MR = moderately rare (>0.05%–0.1%).
R = rare (>0.01%–0.05%).
VR = very rare (2 specimens).
\+ = 1 specimen.
– = looked for but not found.

A range chart of all stratigraphically useful radiolarians was constructed for each of the three sites (Tables **T1, T2, T3**) and for the two site survey piston cores studied (Tables **T4, T5**). The tables include the sample designation, number of meters below seafloor (mbsf), meters composite depth (mcd), revised meters composite depth (rmcd) (except for Site 1220), and the calculated age in millions of years. First and last morphotypic occurrences and a number of evolutionary transitions at each site are recorded sequentially according to their age in Table **T6.** The table includes the top (T) and bottom (B) intervals, the depths in mcd and rmcd, and the calculated age in millions of years for each event. Where closer age constraints could be achieved by using data from the integration of the several holes and nearby piston cores (Figs. **F1, F2**) into composite stratigraphies, we recorded only the more precise interval. In our summary Table **T7** we give average ages for each biostratigraphic datum at each site, together with a mean age for each datum that makes use of the detailed correlation of Sites 1218 and 1219 based on MST data,

T1. Range chart, Site 1218, p. 64.
T2. Range chart, Site 1219, p. 65.
T3. Range chart, Site 1220, p. 66.
T4. Range chart, piston core EW9709-7P, p. 67.
T5. Range chart, piston core EW9709-12P, p. 68.
T6. Chronological list of radiolarian events, p. 69.
T7. Average biostratigraphic datum ages, p. 70.

paleomagnetic stratigraphy, and biostratigraphy (**Pälike et al.,** this volume). The timescale for the detailed correlations of these two sites was further refined by tuning of the MST data to calculated orbital parameters (**Pälike et al.,** this volume; Wade and Pälike, 2004; Shackleton et al., 1999; Berggren et al., 1995).

Figure **F3** shows the radiolarian zonal boundaries and radiolarian events, adjusted to match the new ages for the defining datums presented herein. This figure also shows the paleomagnetic chrons and zonal boundaries for calcareous nannofossils and foraminifers primarily from Berggren et al. (1995), with adjustments cited in Shipboard Scientific Party (2002a).

F3. Radiolarian datum correlation chart for 11.7–52.6 Ma, p. 60.

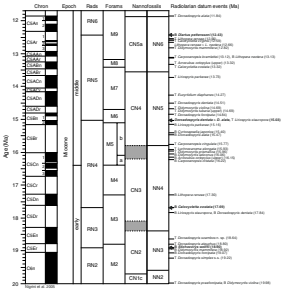

BIOSTRATIGRAPHY

Relevant Zones

Relevant zones are taken from Sanfilippo and Nigrini (1998). The sequence of tropical radiolarian zones, from youngest to oldest, their definitions, and a list of events in approximate stratigraphic order within each zone is given below. First morphotypic occurrences are shown below as FO, last morphotypic occurrences are LO, and evolutionary transitions are indicated by an arrow. Radiolarian zonal boundaries, adjusted to match the new ages for the defining datums presented herein, and events are shown in Figure **F3.**

RN6—*Diartus petterssoni* Interval Zone (Riedel and Sanfilippo, 1970, emend. Riedel and Sanfilippo, 1978)

Top: evolutionary transition from *Diartus petterssoni* to *Diartus hughesi*; this event is now known to be a diachronous event (Johnson and Nigrini, 1985); coincident with the lower limit of the *Didymocyrtis antepenultima* Zone.

Base: morphotypic lowest occurrence of *Diartus petterssoni;* this event is now known to be a diachronous event (Johnson and Nigrini, 1985); coincident with the upper limit of the *Dorcadospyris alata* Zone.

Events in the zone include the following:

Lithopera (Lithopera) neotera →*Lithopera (Lithopera) bacca*
LO *Stichocorys wolffii* *
LO *Cyrtocapsella japonica*; LO *Lithopera (Glomaria) thornburgi*
LO *Cyrtocapsella cornuta*; LO *Cyrtocapsella tetrapera*
LO *Carpocanopsis cristata*
FO *Phormostichoartus doliolum*
LO *Dorcadospyris alata*; LO *Liriospyris parkerae*; FO *Cyrtocapsella japonica*; *Calocycletta (Calocycletta) virginis* →*Calocycletta (Calocycletta) cladara*

Remarks: This zone corresponds to the stratigraphic range of *D. petterssoni* below its evolutionary transition to *D. hughesi*.

*In some Pacific Ocean sections the morphotypic highest occurrence of *Stichocorys wolffii* is below the morphotypic highest occurrence of *Cyrtocapsella cornuta* and the morphotypic lowest occurrence of *Phormostichoartus doliolum*.

RN5—*Dorcadospyris alata* Interval Zone (Riedel and Sanfilippo, 1970, emend. Riedel and Sanfilippo, 1971, emend. Riedel and Sanfilippo, 1978)

Top: morphotypic lowest occurrence of *Diartus petterssoni*; this event is now known to be a diachronous event (Johnson and Nigrini, 1985); coincident with the lower limit of the *Diartus petterssoni* Zone.

Base: evolutionary transition from *Dorcadospyris dentata* to *Dorcadospyris alata;* coincident with the upper limit of the *Calocycletta (Calocyclissima) costata* Zone.

Events in the zone include the following:

LO *Carpocanopsis bramlettei*
Lithopera (Lithopera) renzae →*Lithopera (Lithopera) neotera*
Didymocyrtis mammifera →*Didymocyrtis laticonus*
FO *Lithopera (Glomaria) thornburgi*; FO *Phormostichoartus corbula*; FO *Dictyocoryne ontongensis*
LO *Calocycletta (Calocyclissima) costata*; LO *Didymocyrtis tubaria*; LO *Didymocyrtis violina*; FO *Lithopera (Lithopera) renzae*
The lower limit of the zone is approximately synchronous with LO *Dorcadospyris forcipata*

Remarks: This zone corresponds to the stratigraphic range of *D. alata* (above its evolutionary transition from *D. dentata*) and below the lowest occurrence of *Diartus petterssoni*.

RN4—*Calocycletta (Calocyclissima) costata* Interval Zone (Riedel and Sanfilippo, 1970, 1978)

Top: evolutionary transition from *Dorcadospyris dentata* to *Dorcadospyris alata*; coincident with the lower limit of the *Dorcadospyris alata* Zone.

Base: morphotypic lowest occurrence of *Calocycletta (Calocyclissima) costata*; coincident with the upper limit of the *Stichocorys wolffii* Zone.

Events in the zone include the following:

LO *Eucyrtidium diaphanes*
Liriospyris stauropora →*Liriospyris parkerae*
LO *Carpocanopsis favosa*
LO *Didymocyrtis prismatica*
LO *Carpocanopsis cingulata*; FO *Carpocanopsis cristata*
The lower limit of the zone is approximately synchronous with LO *Lychnocanoma elongata*

Remarks: This zone corresponds to the stratigraphic range of *D. dentata* (below its evolutionary transition to *D. alata*) above the lowest occurrence of *C. costata*.

RN3—*Stichocorys wolffii* Interval Zone (Riedel and Sanfilippo, 1978)

Top: morphotypic lowest occurrence of *Calocyletta (Calocyclissima) costata*; coincident with the lower limit of the *Calocycletta (Calocyclissima) costata* Zone.

Base: morphotypic lowest occurrence of *Stichocorys wolffii*; coincident with the upper limit of the *Stichocorys delmontensis* Zone.

Events in the zone include the following:

FO *Didymocyrtis mammifera*
FO *Calocycletta (Calocyclior) caepa*
FO *Dorcadospyris dentata*
FO *Liriospyris stauropora*
The lower limit is approximately synchronous with LO *Dorcadospyris ateuchus;* FO *Siphostichartus corona*.

RN2—*Stichocorys delmontensis* Interval Zone (Riedel and Sanfilippo, 1978)

Top: morphotypic lowest occurrence of *Stichocorys wolffii*; coincident with the lower limit of the *Stichocorys wolffii* Zone.
Base: morphotypic highest occurrence of *Theocyrtis annosa*; coincident with the upper limit of the *Cyrtocapsella tetrapera* Zone.
The lower limit of the zone is approximately synchronous with the following events:

FO *Didymocyrtis tubaria;* FO *Didymocyrtis violina;* FO *Stichocorys delmontensis;* FO *Carpocanopsis bramlettei*

Remarks: This zone corresponds to the interval between the lowest occurrence of *S. wolffii* and the highest occurrence of *T. annosa*. In most sections it can be recognized by the presence of *S. delmontensis* and the absence of *S. wolffii* and *T. annosa*. However, at the base of the zone *S. delmontensis* may also be absent, but one would expect to find any of the species mentioned above as well as *Eucyrtidium diaphanes*, *Cyrtocapsella cornuta*, *C. tetrapera, Calocycletta virginis,* and *Lychnocanoma elongata*.

RN1—*Cyrtocapsella tetrapera* Concurrent Range Zone (Riedel and Sanfilippo, 1978)

Top: morphotypic highest occurrence of *Theocyrtis annosa*; coincident with the lower limit of the *Stichocorys delmontensis* Zone.
Base: morphotypic lowest occurrence of *Cyrtocapsella tetrapera*; coincident with the upper limit of the *Lychnocanoma elongata* Zone.
Events in the zone include the following:

LO *Calocycletta (Calocyclopsis) serrata*
LO *Calocycletta (Calocycletta) robusta*
FO *Carpocanopsis favosa*
FO *Cyrtocapsella cornuta*
The lower limit of the zone is approximately synchronous with FO *Calocycletta (Calocyclopsis) serrata*; FO *Calocycletta (Calocycletta) virginis*; FO *Botryostrobus miralestensis*

RP22—*Lychnocanoma elongata* Interval Zone (Riedel and Sanfilippo, 1970, emend. Riedel and Sanfilippo, 1978)

Top: morphotypic lowest occurrence of *Cyrtocapsella tetrapera*; coincident with the lower limit of the *Cyrtocapsella tetrapera* Zone.
Base: morphotypic lowest occurrence of *Lychnocanoma elongata;* coincident with the upper limit of the *Dorcadospyris ateuchus* Zone.
Events in the zone include the following:

LO *Artophormis gracilis*
FO *Eucyrtidium diaphanes*

LO *Dorcadospyris papilio*
The lower limit of the zone is approximately synchronous with FO *Carpocanopsis cingulata*

RP21—*Dorcadospyris ateuchus* Interval Zone (Riedel and Sanfilippo, 1971; Riedel and Sanfilippo, 1978)

Top: morphotypic lowest occurrence of *Lychnocanoma elongata*; coincident with the lower limit of the *Lychnocanoma elongata* Zone.
Base: evolutionary transition from *Tristylospyris triceros* to *Dorcadospyris ateuchus*; coincident with the upper limit of the *Theocyrtis tuberosa* Zone.
Events in the zone include the following:

FO *Dorcadospyris forcipata*; LO *Lychnocanoma trifolium*
FO *Calocycletta (Calocycletta) robusta*
FO *Dorcadospyris papilio*
LO *Lithocyclia angusta*

Remarks: This zone corresponds to the stratigraphic range of *D. ateuchus* (above its evolutionary transition from *T. triceros*) below the lowest occurrence of *L. elongata*.

RP20—*Theocyrtis tuberosa* Interval Zone (Riedel and Sanfilippo, 1970, emend. Riedel and Sanfilippo, 1971, emend. Riedel and Sanfilippo, 1978)

Top: evolutionary transition from *Tristylospyris triceros* to *Dorcadospyris ateuchus*; coincident with the lower limit of the *Dorcadospyris ateuchus* Zone.
Base: evolutionary transition from *Lithocyclia aristotelis* group to *Lithocyclia angusta*; coincident with the upper limit of the *Cryptocarpium ornatum* Zone.
Events in the zone include the following:

FO *Theocyrtis annosa;* LO *Theocyrtis tuberosa*
LO *Lithocyclia crux*
FO *Lychnocanoma trifolium*
FO *Didymocyrtis prismatica*; LO *Dorcadospyris pseudopapilio*
Centrobotrys petrushevskayae →*Centrobotrys thermophila*
FO *Lychnodictyum audax*
Centrobotrys gravida →*Centrobotrys petrushevskayae*; FO *Dorcadospyris pseudopapilio*
FO *Lithocyclia crux*; *Artophormis barbadensis* →*Artophormis gracilis*
FO *Centrobotrys gravida*
LO *Dictyoprora pirum*; FO *Phormostichoartus fistula*
The lower limit of the zone is approximately synchronous with LO *Cryptocarpium ornatum*; LO *Dictyoprora mongolfieri*; LO *Lychnocanoma amphitrite*

Remarks: This zone corresponds approximately to the stratigraphic range of *T. tuberosa* below the evolutionary transition of *T. triceros* to *D. ateuchus* and above the evolutionary transition of the *L. aristotelis* group to *L. angusta*.

RP19—*Cryptocarpium ornatum* Interval Zone (Maurrasse and Glass, 1976)

Top: evolutionary transition of the *Lithocyclia aristotelis* group to *Lithocyclia angusta*; coincident with the lower limit of the *Theocyrtis tuberosa* Zone.

Base: morphotypic highest occurrence of *Thyrsocyrtis (Pentalacorys) tetracantha*; coincident with the upper limit of the *Calocyclas bandyca* Zone.

Events in this zone include the following:

LO *Dictyoprora armadillo*
LO *Lophocyrtis (Lophocyrtis) jacchia*
LO *Calocyclas turris*; LO *Thyrsocyrtis (Thyrsocyrtis) bromia*; LO *Thyrsocyrtis (Thyrsocyrtis) rhizodon*; LO *Cryptocarpium azyx*
The lower limit of the zone is approximately synchronous with LO *Thyrsocyrtis (Pentalacorys) lochites*; LO *Calocyclas bandyca*; LO *Calocyclas hispida*; LO *Lychnocanoma bellum*; LO *Podocyrtis (Podocyrtis) papalis*

Remarks: This zone corresponds to the stratigraphic range of *C. ornatum* below the evolutionary transition of the *L. aritotelis* group to *L. angusta* and above the highest occurrence of *T. (P.) tetracantha*.

RP18—*Calocyclas bandyca* Concurrent Range Zone (Sanfilippo and Riedel in Saunders et al., 1985)

Top: morphotypic highest occurrence of *Thyrsocyrtis (Pentalacorys) tetracantha*; coincident with the lower limit of the *Cryptocarpium ornatum* Zone.

Base: morphotypic lowest occurrence of *Calocyclas bandyca*; coincident with the upper limit of the *Cryptocarpium azyx* Zone.

Events in this zone include the following:

LO *Thyrsocyrtis (Pentalacorys) triacantha*
FO *Theocyrtis tuberosa*
LO *Eusyringium fistuligerum*
LO *Podocyrtis (Lampterium) goetheana*

RP17—*Cryptocarpium azyx* Interval Zone (Sanfilippo and Riedel in Saunders et al., 1985)

Top: morphotypic lowest occurrence of *Calocyclas bandyca*; coincident with the lower limit of the *Calocyclas bandyca* Zone.

Base: morphotypic lowest occurrence of *Cryptocarpium azyx*; coincident with the upper limit of the *Podocyrtis (Lampterium) goetheana* Zone.

Events in this zone include the following:

LO *Podocyrtis (Lampterium) chalara*
FO *Lychnocanoma amphitrite*
Calocyclas hispida →*Calocyclas turris*

RP16—*Podocyrtis (Lampterium) goetheana* Interval Zone (Moore, 1971, emend. Riedel and Sanfilippo, 1978)

Top: morphotypic lowest occurrence of *Cryptocarpium azyx*; coincident with the lower limit of the *Cryptocarpium azyx* Zone.

Base: morphotypic lowest occurrence of *Podocyrtis (Lampterium) goetheana*; coincident with the upper limit of the *Podocyrtis (Lampterium) chalara* Zone.

Events in the zone include the following:

LO *Spongatractus pachystylus*
FO *Thyrsocyrtis (Thyrsocyrtis) bromia*
FO *Thyrsocyrtis (Pentalacorys) tetracantha*; FO *Dictyoprora pirum*; LO *Theocotylissa ficus*
LO *Sethochytris triconiscus*
FO *Dictyoprora armadillo*
The lower limit of the zone is approximately synchronous with the evolutionary transition from the *Lithocyclia ocellus* group to the *Lithocyclia aristotelis* group.

RP15—*Podocyrtis (Lampterium) chalara* Lineage Zone (Riedel and Sanfilippo, 1970; Riedel and Sanfilippo, 1978)

Top: morphotypic lowest occurrence of *Podocyrtis (Lampterium) goetheana*; coincident with the lower limit of the *Podocyrtis (Lampterium) goetheana* Zone.

Base: evolutionary transition from *Podocyrtis (Lampterium) mitra* to *Podocyrtis (Lampterium) chalara*; coincident with the upper limit of the *Podocyrtis (Lampterium) mitra* Zone.

Events in the zone include the following:

LO *Podocyrtis (Lampterium) trachodes*
The lower limit of the zone is approximately synchronous with LO *Phormocyrtis striata striata*; FO *Tristylospyris triceros*

RP14—*Podocyrtis (Lampterium) mitra* Lineage Zone (Riedel and Sanfilippo, 1970; Riedel and Sanfilippo, 1978)

Top: evolutionary transition from *Podocyrtis (Lampterium) mitra* to *Podocyrtis (Lampterium) chalara*; coincident with the lower limit of the *Podocyrtis (Lampterium) chalara* Zone.

Base: evolutionary transition from *Podocyrtis (Lampterium) sinuosa* to *Podocyrtis (Lampterium) mitra*; coincident with the upper limit of the *Podocyrtis (Podocyrtoges) ampla* Zone.

Events in the zone include the following:

FO *Cryptocarpium ornatum*
LO *Podocyrtis (Podocyrtoges) ampla*
LO *Eusyringium lagena*; FO *Artophormis barbadensis*; FO *Thyrsocyrtis (Pentalacorys) lochites*; FO *Sethochytris triconiscus*; LO *Podocyrtis (Lampterium) fasciolata*; LO *Podocyrtis (Lampterium) helenae*

RP13—*Podocyrtis (Podocyrtoges) ampla* Lineage Zone (Riedel and Sanfilippo, 1970; Riedel and Sanfilippo, 1978)

Top: evolutionary transition from *Podocyrtis (Lampterium) sinuosa* to *Podocyrtis (Lampterium) mitra*; coincident with the lower limit of the *Podocyrtis (Lampterium) mitra* Zone.

Base: evolutionary transition from *Podocyrtis (Podocyrtoges) phyxis* to *Podocyrtis (Podocyrtoges) ampla*; coincident with the upper limit of the *Thyrsocyrtis (Pentalacorys) triacantha* Zone.

Events in the zone include the following:

FO *Podocyrtis (Lampterium) trachodes*
LO *Podocyrtis (Podocyrtoges) dorus*
Eusyringium lagena →*Eusyringium fistuligerum*
FO *Podocyrtis (Lampterium) fasciolata*; FO *Podocyrtis (Lampterium) helenae*
The lower limit of the zone is approximately synchronous with LO *Theocotyle venezuelensis*

RP12—*Thyrsocyrtis (Pentalacorys) triacantha* Interval Zone (Riedel and Sanfilippo, 1970, emend. Riedel and Sanfilippo, 1978)

Top: evolutionary transition from *Podocyrtis (Podocyrtoges) phyxis* to *Podocyrtis (Podocyrtoges) ampla*; coincident with the lower limit of the *Podocyrtis (Podocyrtoges) ampla* Zone.

Base: morphotypic lowest occurrence of *Eusyringium lagena*; coincident with the upper limit of the *Dictyoprora mongolfieri* Zone.

Events in the zone include the following:

FO *Eusyringium fistuligerum*
LO *Theocotyle nigriniae*; LO *Theocotyle conica*; *Podocyrtis (Podocyrtoges) diamesa* →*Podocyrtis (Podocyrtoges) phyxis*; LO *Theocorys anaclasta*; LO *Lamptonium fabaeforme constrictum*; *LO Lamptonium fabaeforme chaunothorax*; LO *Thyrsocyrtis (Thyrsocyrtis) hirsuta*; LO *Thyrsocyrtis (Thyrsocyrtis) robusta*
The lower limit of the zone is approximately synchronous with *Thyrsocyrtis (Pentalacorys) tensa* →*Thyrsocyrtis (Pentalacorys) triacantha*

Remarks: This zone corresponds to the stratigraphic range of *T. triacantha* below the evolutionary transition of *P. (P.) phyxis* to *P. (P.) ampla* and above the lowest occurrence of *E. lagena*.

RP11—*Dictyoprora mongolfieri* Interval Zone (Riedel and Sanfilippo, 1970, emend. Riedel and Sanfilippo, 1978)

Top: morphotypic lowest occurrence of *Eusyringium lagena*; coincident with the lower limit of the *Thyrsocyrtis (Pentalacorys) triacantha* Zone.

Base: morphotypic lowest occurrence of *Dictyoprora mongolfieri*; coincident with the upper limit of the *Theocotyle cryptocephala* Zone.

Events in the zone include the following:

LO *Lamptonium fabaeforme fabaeforme*; FO *Podocyrtis (Podocyrtoges) dorus*
Theocotyle cryptocephala →*Theocotyle conica*
The lower limit of the zone is approximately synchronous with LO *Calocycloma castum*.

RP10—*Theocotyle cryptocephala* Interval Zone (Foreman, 1973)

Top: morphotypic lowest occurrence of *Dictyoprora mongolfieri*; coincident with the lower limit of the *Dictyoprora mongolfieri* Zone.

Base: evolutionary transition from *Theocotyle nigriniae* to *Theocotyle cryptocephala*; coincident with the upper limit of the *Phormocyrtis striata striata* Zone.

Events in the zone include the following:

Podocyrtis (Lampterium) acalles →*Podocyrtis (Lampterium) sinuosa*
FO *Thyrsocyrtis (Thyrsocyrtis) robusta*
FO *Theocotyle venezuelensis*
The lower limit of the zone is approximately synchronous with LO *Buryella clinata*

Remarks: This zone corresponds to the stratigraphic range of *T. cryptocephala* (above its evolutionary transition from *T. nigriniae*) below lowest occurrence of *D. mongolfieri*.

RP9—*Phormocyrtis striata striata* Interval Zone (Foreman, 1973; emend. Riedel and Sanfilippo, 1978)

Top: evolutionary transition from *Theocotyle nigriniae* to *Theocotyle cryptocephala*; coincident with the lower limit of the *Theocotyle cryptocephala* Zone.

Base: morphotypic lowest occurrence of *Theocorys anaclasta*; coincident with the upper limit of the *Buryella clinata* Zone.

Events in the zone include the following:

Spongatractus balbis →*Spongatractus pachystylus*
LO *Lamptonium sanfilippoae*
FO *Thyrsocyrtis (Thyrsocyrtis) rhizodon*
FO *Podocyrtis (Podocyrtoges) diamesa*
The lower limit of the zone is approximately synchronous with FO *Lamptonium fabaeforme constrictum; Phormocyrtis striata exquisita* → *Phormocyrtis striata striata*; FO *Podocyrtis (Lampterium) acalles*; LO *Phormocyrtis cubensis*; FO *Lychnocanoma bellum*.

RP8—*Buryella clinata* Interval Zone (Foreman, 1973, emend. Foreman, 1975, emend. Riedel and Sanfilippo, 1978)

Top: morphotypic lowest occurrence of *Theocorys anaclasta*; coincident with the lower limit of the *Phormocyrtis striata striata* Zone.

Base: evolutionary transition from *Pterocodon anteclinata* to *Buryella clinata*; coincident with the upper limit of the *Bekoma bidartensis* Zone.

Events in the zone include the following:

LO *Pterocodon ampla*; LO *Bekoma bidartensis*; LO *Buryella tetradica*; LO *Thyrsocyrtis (Thyrsocyrtis) tarsipes*
FO *Lithocyclia ocellus* group; FO *Thyrsocyrtis (Pentalacorys) tensa*; *Theocotylissa alpha* →*Theocotylissa ficus*
FO *Calocyclas hispida*
The lower limit of the zone is approximately synchronous with FO *Spongatractus balbis*; FO *Lamptonium sanfilippoae*; FO *Theocotyle nigriniae*; FO *Thyrsocyrtis (Thyrsocyrtis) hirsuta*

Remarks: This zone corresponds to the stratigraphic range of *B. clinata* (above its evolutionary transition from *P. anteclinata*) below lowest occurrence of *T. anaclasta*.

RESULTS

A series of 305 radiolarian morphologic first and last occurrences and evolutionary transitions between radiolarian species were determined in the material collected in association with Leg 199. Among these are 12 newly described species from Leg 199 material (see the **"Appendix,"** p. 24). These results are listed for each of the five sections studied (Sites 1218, 1219, and 1220 and piston cores EW9709-7P and EW9709-12P) (Tables **T1, T2, T3, T4, T5**). In Tables **T1, T2,** and **T3,** the full suite of species used in this study are tabulated; however, some of the species were not traced through their entire range. For these species an upward arrow and "?" indicate that its upper limit is not documented in this study. Tables **T4** and **T5** list only those species that are considered both in this study and contained within the more limited stratigraphic range of the piston cores. The revised meters composite depth (rmcd) for each of the samples studied is based on a correlation of the piston cores to their associated nearby ODP sites (Figs. **F1, F2**) and the correlation of Site 1219 to Site 1218 (**Pälike et al.,** this volume). Thus, all samples are related to a depth at Site 1218. The associated age of each of the samples is based on the correlations and timescale developed by **Pälike et al.** (this volume).

Table **T6** gives the sample control and sample ages that constrain each of the radiolarian datum levels at Sites 1218, 1219, and 1220. We feel that Sites 1218 and 1219 contain the most complete well-preserved sections recovered during Leg 199 and have been integrated into a very robust composite section (**Pälike et al.,** this volume). This table also makes use of samples from the nearby site survey piston cores to more tightly constrain datum levels and ages. These data are taken from Tables **T1, T2, T4,** and **T5.**

The results shown in Table **T6** are summarized in Table **T7,** which gives the average age estimate (and error of estimate) for each datum at Sites 1218, 1219, and 1220. A mean age (and error) is also given, based on the oldest top and youngest bottom samples of the entire (1218, 1219, 1220, EW9709-7P, and EW9709-12P) data set. We leave it to future researchers to decide which of these datum age estimates are the most appropriate to use in their work.

Radiolarian zonal boundaries and radiolarian events, adjusted to match the new ages for the defining datums presented herein are shown in Figure **F3.** Included in this figure are the paleomagnetic chrons and zonal boundaries for calcareous nannofossils and foraminifers primarily from Berggren et al. (1995), with adjustments cited in Shipboard Scientific Party (2002a). Leg 199 provided the first opportunity to tie tropical radiolarian biostratigraphic events directly to magnetochronology and the absolute timescale of the Paleogene. Most Paleogene radiolarian bioevents have in the past been calibrated indirectly to the absolute timescale by correlation to calcareous nannofossil biostratigraphy. During Leg 199, radiolarian bioevents were accompanied by high-resolution magnetostratigraphy, which initially allowed the ages of zonal boundaries to be determined directly from the Cande and Kent (1995) and Shackleton et al. (1995) timescales. In the Figure **F23** of Shipboard Scientific Party (2002b) and Figure **F7** of Shipboard Scientific Party, 2002a) show a comparison between the newly determined zonal boundary ages calibrated using the reversal stratigraphy from Sites 1218, 1219, and 1220 with those estimated by Sanfilippo and Nigrini (1998). Note that the results presented in Figure **F3** herein su-

persede the results presented in Lyle, Wilson, Janecek, et al. (2002). Also note that the chronology of Paleogene radiolarian zonal boundary events presented by Sanfilippo and Nigrini (1998) was, according to the authors, a good approximation at best.

DISCUSSION

As might be expected in the sites from the northern side of the equatorial Pacific sedimentary mound presented in this work, the preservation of the upper Neogene section is generally poor and contains numerous reworked older microfossils. Once the site locations drifted north of ~3°–4°N paleolatitude, the drop in preservation of biogenic silica is marked. Given this long-term trend in preservation, there appears to be an additional variation in preservation and in the abundance of larger (>63 µm) diatoms found in the samples. Through the lower Miocene and Oligocene zones, moderately well preserved radiolarians appear to be spaced at intervals of 0.5 to 1.5 m.y. (Tables **T1, T2, T3, T4, T5**). In the Eocene sediment accumulations drop, as all carbonate was dissolved from the section and the preservation of the radiolarians—even in this very siliceous section—is usually moderate. Very well preserved assemblages are frequently found only in the more rapidly accumulating sediments of the middle Eocene (Zones RP15 and RP16).

There does seem to be a logical association between higher accumulation of sediments and better preservation; however, in some samples we have observed both well-preserved and rather poorly preserved specimens in the same sample. It is commonly believed that deep-sea pelagic ooze sediments are bioturbated to depths of 5 to 10 cm. These are pelagic (not laminated) oozes and no subcentimeter scale layering is noted. Thus, over 2 cm the sediment should be well mixed.We believe that this enigma may be explained by the differential deposition that appears to be taking place near these sites. We suggest that some specimens are transported from nearby slowly accumulating, more poorly preserved assemblages and deposited in areas where average accumulation is more rapid, resulting in assemblages with widely varying preservation in the more rapidly accumulating section. This suggestion is borne out by a comparison of the material recovered at Sites 1218 and 1219 to that of the nearby site survey piston cores. Although the piston cores recovered during the survey for Sites 1218 and 1219 were taken at water depths only ~50 m shoaler than the sites themselves, the apparent sediment accumulation rates for these cores were four to five times slower than at the adjacent drill sites (Tables **T1, T2, T3, T4, T5**). And, as might be expected, preservation of the radiolarian fauna is generally poorer in the piston cores than in the associated drill sites. It is difficult to generalize about the minimum sediment accumulation rate needed to preserve siliceous microfossils. The bottom waters of the oceans are presumed to have always been undersaturated with respect to silica; thus, the longer a shell is exposed to these waters the more dissolution takes place. If the amount of biogenic silica delivered to the seafloor forms a high proportion of the total sediment flux to the seafloor, then the pore waters of these sediments may become close to saturation with respect to silica and serve to retard dissolution of the tests—even though the total sediment flux is fairly low. Thus ODP Site 1215 (located well north of the Eocene equatorial divergence) is devoid of siliceous microfossils even though lower Eocene sediments here are accumulating at 4–10 m/m.y.; whereas Site 1220 (near the Eocene equa-

torial divergence) recovered a middle–lower Eocene section that was useful for radiolarian studies even though total sediment accumulation rates were of about the same magnitude as those at Site 1215.

Perhaps the most important contribution of the work presented in this paper is the development of a detailed radiolarian biostratigraphy for the lower Neogene and much of the Paleogene. Tying this stratigraphy to time was made possible by the paleomagnetic stratigraphy developed for the sites (Lanci et al., in press; Pares and Lanci, 2004; Shipboard Scientific Party, 2002c). The time resolution achieved in this study is a result of both the large number of samples studied and the integration of the stratigraphies from Sites 1218 and 1219 (**Pälike et al.,** this volume), along with those of cores EW9709-7P and EW9709-12P (Figs. **F1, F2**). As a result, our average time resolution for radiolarian Zones RN5–RN2 is 86 k.y., for Zones RN1–RP20 is 57 k.y., and for Zones RP19–RP12 is 110 k.y. (Tables **T1, T2, T3, T4, T5**). This resolution encompasses the magnitude of diachrony seen in many of the radiolarian biostratigraphic events in the upper Neogene sections of the eastern equatorial Pacific (Moore et al., 1993).

This degree of resolution not only improves upon the preexisting radiolarian stratigraphy for the tropical Pacific, but also it gives us confidence in commenting on some of the peculiarities noted in ranges of the individual species studied. For example, we feel confident that we have narrowly defined the stratigraphic range for several (some newly described) short-lived species in this region:

a. Eocene: *Dorcadospyris anastasis* n. sp. and *Calocycletta* (*Calocycletta*) *anekathen* n. sp.;
b. Oligocene: *Centroboytris gravida, Dorcadospyris spinosa, Dorcadospyris cyclacantha* n. sp., and *Liriospyris longicornuta*; and
c. Miocene: *Calocycletta* (*Calocyclopsis*) *serrata* and *Acrocubus octopylus*.

Acrocubus octopylus is a prime example of a peculiar anomaly seen in our data. It has a clearly discontinuous range. This robust and easily identifiable species first occurs at the base of Zone RP22 and ranges up for ~0.5 m.y. before disappearing from the assemblage. It reoccurs in the middle part of Zone RN4 and continues upsection for ~2.6 m.y. into Zone RN5 before becoming very rare. *Lithocyclia angusta, Didymocyrtis tubaria,* and *Centrobotrys thermophila* also show such discontinuous ranges. In some cases (e.g., for *Didymocyrtis tubaria*), the discontinuity of the range may indicate a taxonomic problem in which the species concept is too broad. In other cases, the true range of the species may be continuous but paleoenvironmental conditions at the edge of the South Equatorial Current may have varied sufficiently to cause small shifts in the zoogeography of the species. This seems to be the case with *Dorcadospyris riedeli,* a typically very rare species that reaches its highest abundances near its upper limit in the middle part of Zone RP22. However, specimens of *Dorcadospyris riedeli* occasionally occur in samples throughout Zones RP22, RP21, and down into the uppermost part of Zone RP20. This pattern suggests that Sites 1218 and 1219 are located near the fringes of the distribution of this species. Similarly, the brief reoccurrence of *Lithocyclia angusta* in the middle part of Zone RP22 at both Sites 1218 and 1219 after its last consistent occurrence in Zone RP21 (some 4 m.y. earlier) suggests either a significant change in environmental conditions or a shift in the environmental tolerances of the species. Although the preservation of the assemblage might also play a role in the "temporary" dis-

appearance of more delicate species, we do not believe this is the case for the material studied here. For example, we searched for *Lithocyclia angusta* in ~180 samples between its last occurrence in the lower Oligocene and its recurrence in the middle part of Zone RP22 and most of these samples had abundant or common well-preserved radiolarians. When it did reappear briefly within Zone RP22 its abundance was comparable to that found in its "normal" range within Zone RP20.

Such discontinuous occurrences and sporadic reoccurrences of species may have been observed in the past and attributed to reworking of sediments, downhole contamination, or laboratory contamination. Because we have observed these phenomena at more than one site in sections representing comparable intervals of time and in multiple, closely spaced samples, we feel that contamination of the samples is not a reasonable explanation.

Just as our tightly controlled stratigraphy gives us confidence in identifying the apparent ranges of even short-lived species, it also gives us confidence that some species that we might expect to be present in the assemblages, but were not found, really are absent from the material collected. These "missing species" tend to be concentrated in the Eocene. For example, *Lychnocanoma bellum* is not found in our material. Species of the genera *Thyrsocyrtis* and *Theocotyle* are not as abundant as seen in other tropical sections and tend to have abbreviated ranges. Similarly, *Podocyrtis (Lampterium) goetheana, Lophocyrtis (Lophocyrtis) jacchia,* and *Phormocyrtis striata striata* appear sporadically and have abbreviated ranges. In contrast, *Podocyrtis (Podocyrtoges) ampla* is abnormally abundant in samples that encompass its normal range.

Eocene sections have not been so frequently sampled and studied that we can draw firm conclusions about the unusual nature of the Eocene assemblages noted above. However, a recent synthesis of the Paleogene sediments in the equatorial Pacific (Moore et al., 2004) indicates the following:

a. The location of all the sites studied are close to the equatorial zone of divergence in the Eocene;
b. Their rotated paleopositions also place them in the extreme eastern equatorial Pacific Basin; and
c. During the Eocene, the eastern equatorial Pacific was connected to the Caribbean by means of at least two Central American gateways.

Thus, the sites studied were located within the paleo-South Equatorial Current, within the influence of equatorial divergence, downstream from the paleo-Peru-Chile Current, and just downstream from the Central American gateways. All of these factors would have tended to increase the nutrient supply to the near-surface waters and to increase the rates of accumulation of biogenic sediments at these site locations (Moore et al., 2004).

A qualitative evaluation of the Eocene assemblages at sites located in the Pacific equatorial zone farther to the west (e.g., Deep Sea Drilling Project [DSDP] Sites 462, 167, and 163) suggests that they too show some of the anomalous characteristics of the Eocene assemblages noted above (e.g., *Podocyrtis (Lampterium) goetheana* and *Lychnocanoma bellum* are rare or absent). This may indicate that the noted differences in Eocene assemblages are a result of ecological differences associated with higher-productivity regions. It is well known that higher-productivity regions have distinctive radiolarian assemblages in the late Neogene

(e.g., Nigrini and Caulet, 1992). We suggest that this holds for Eocene assemblages as well; however, we do not attempt in this study to establish the degree to which individual Eocene species are sensitive to such environmental differences.

Comparatively large variations in abundance of other Paleogene species typically used in biostratigraphy also indicate the sensitivity of these species to environmental conditions. A good example of this is *Lychnocanoma elongata*. This species ranges from the base of Zone NP22 to the middle part of Zone RN4 (~9 m.y.). Within this range it varies in abundance from 0 (absent) to >350 specimens per slide in a series of cycles that appear to be a few hundred thousand years in duration. We suspect that these abundance cycles, as well as less pronounced cycles in the abundance of other species, reflect a response to cyclic variations in environmental conditions.

Hiatus

In the lower part of the Eocene section at Site 1220, the interval representing Zones RP9 and RP10 is missing. This apparent hiatus of ~2 m.y. is comparable to a similar (somewhat shorter) hiatus found at ODP Site 1051 in the North Atlantic (Sanfilippo and Blome, 2001) and associated with a widespread lower Eocene–middle Eocene hiatus. Norris et al. (2001) related this unconformity to seismic Reflector A^c in the western North Atlantic, which formed at the end of early Eocene time and may be correlative with unconformities in every major ocean basin. There is little evidence for the exact cause of this widespread unconformity, but it is seen in both the siliceous and calcareous microfossils. Bralower et al. (1995) note that a sharp drop in water temperatures occurred at the end of the early Eocene at Allison Guyot in the Mid-Pacific Mountains (ODP Site 865). Sanfilippo and Blome (2001) attribute this hiatus to unspecified changes in oceanic circulation and temperature gradients. The early–middle Eocene reconstructions of the equatorial Pacific (Moore et al., 2004) show a much reduced development of equatorial divergence associated with lower overall sediment accumulation rates in the equatorial zone. Although the early–middle Eocene reconstruction averages over a much longer time interval (~4 m.y.), it may indicate that the development of the hiatus is associated with a lower overall tropical temperature gradient, lower wind-induced upwelling, and lower sediment accumulation rates. Site 1220 is located very close to the paleoequator of early–middle Eocene time, whereas Site 865 lay some 5°–6° latitude north of the equator, near the boundary between the North Equatorial Current and the North Equatorial Counter Current (Moore et al., 2004). Both regions have relatively high sediment accumulation rates compared to sites lying outside these two regions of divergence, but both sites show this relatively brief hiatus.

ACKNOWLEDGMENTS

The manuscript has benefited from helpful comments and thoughtful reviews by John A. Barron (U.S. Geological Survey) and Christopher J. Hollis (Institute of Geological and Nuclear Sciences, New Zealand). This research used samples provided by the Ocean Drilling Program (ODP). ODP is sponsored by the U.S. National Science Foundation (NSF) and participating countries under management of Joint Oceanographic Institutions (JOI), Inc. Funding for this research was provided

by the U.S. Science Support Program. We would like to thank our many scientific and technical colleagues on board the *JOIDES Resolution* during ODP Leg 199. Their hard work and support has helped make this research possible. One of us (C.N.) would like to thank most sincerely her colleagues and her children for being there when she really needed them. The bibliography was prepared using RadRefs, a comprehensive computer-based library of all radiolarian literature.

REFERENCES

Berggren, W.A., Kent, D.V., Swisher, C.C., III, and Aubry, M.-P., 1995. A revised Cenozoic geochronology and chronostratigraphy. *In* Berggren, W.A., Kent, D.V., Aubry, M.-P., and Hardenbol, J. (Eds.), *Geochronology, Time Scales and Global Stratigraphic Correlation*. Spec. Publ.—SEPM (Soc. Sediment. Geol.), 54:129–212.

Bralower, T.J., Zachos, J.C., Thomas, E., Parrow, M., Paull, C.K., Kelly, D.C., Premoli Silva, I., Sliter, W.V., and Lohmann, K.C., 1995. Late Paleocene to Eocene paleoceanography of the equatorial Pacific Ocean: stable isotopes recorded at Ocean Drilling Program Site 865, Allison Guyot. *Paleoceanography,* 10(40):841–865.

Brandt, R., 1935. Die Mikropalaeontologie des Heiligenhafener, Kieseltones (Ober-Eozän) Radiolarien, Systematik. *In* Wetzel, E.O. (Ed.), *Jahresbericht des Niedersachsischen Geologischen Vereins,* 27:48-59.

Campbell, A.S., and Clark, B.L., 1944. Miocene radiolarian faunas from Southern California. *Spec. Pap.—Geol. Soc. Am.,* 51:1–76.

Cande, S.C., and Kent, D.V., 1995. Revised calibration of the geomagnetic polarity timescale for the Late Cretaceous and Cenozoic. *J. Geophys. Res.,* 100:6093–6095.

Carnevale, P., 1908. Radiolarie e silicoflagellati di Bergonzano (Reggio Emilia). *Veneto Sci. Lett. Arti Mem.,* 28(3):1–46.

Cita, M.B., Nigrini, C., and Gartner, S., 1970. Biostratigraphy. *In* Peterson, M.N.A., et al., *Init. Repts. DSDP,* 2: Washington (U.S. Govt. Printing Office), 391–411.

Clark, B.L., and Campbell, A.S., 1942. Eocene radiolarian faunas from the Mt. Diablo area, California. *Spec. Pap.—Geol. Soc. Am.,* 39:1–112.

Ehrenberg, C.G., 1847. Über die mikroskopischen kieselschaligen Polycystinen als mächtige Gebirgsmasse von Barbados und über das Verhältniss deraus mehr als 300 neuen Arten bestehenden ganz eigenthümlichen Formengruppe jener Felsmasse zu den jetzt lebenden Thieren und zur Kreidebildung. Eine neue Anregung zur Erforschung des Erdlebens. *K. Preuss. Akad. Wiss. Berlin, Ber.,* Jahre 1847:40–60.

Ehrenberg, C.G., 1854. *Mikrogeologie: Das Erden und Felsen schaffende Wirken des unsichtbar kleinen selbständigen Lebens auf der Erde:* Leipzig (Leopold Voss).

Ehrenberg, C.G., 1873. Grössere Felsproben des Polycystinen-Mergels von Barbados mit weiteren Erläuterungen. *K. Preuss. Akad. Wiss. Berlin, Monatsberichte,* 1873:213–263.

Ehrenberg, C.G., 1875. Fortsetzung der mikrogeologischen Studien als Gesammt-Uebersicht der mikroskopischen Paläontologie gleichartig analysirter Gebirgsarten der Erde, mit specieller Rücksicht auf den Polycystinen-Mergel von Barbados. *Abh. K. Akad. Wiss. Berlin,* 1875:1–225.

Foreman, H.P., 1968. Upper Maestrichtian Radiolaria of California. *Palaeontol. Assoc. London, Spec. Pap. Palaeontol.,* 3:1–82.

Foreman, H.P., 1973. Radiolaria of Leg 10 with systematics and ranges for the families Amphipyndacidae, Artostrobiidae, and Theoperidae. *In* Worzel, J.L., Bryant, W., et al., *Init. Repts. DSDP,* 10: Washington (U.S. Govt. Printing Office), 407–474.

Foreman, H.P., 1975. Radiolaria from the North Pacific, Deep Sea Drilling Project, Leg 32. *In* Larson, R.L., Moberly, R., et al., *Init. Repts. DSDP,* 32: Washington (U.S. Govt. Printing Office), 579–676.

Goll, R.M., 1968. Classification and phylogeny of Cenozoic Trissocyclidae (Radiolaria) in the Pacific and Caribbean basins, Part I. *J. Paleontol.,* 42(6):1409–1432.

Goll, R.M., 1969. Classification and phylogeny of Cenozoic Trissocyclidae (Radiolaria) in the Pacific and Caribbean basins, Part II. *J. Paleontol.,* 43(2):322–339.

Goll, R.M., 1972. Leg 9 synthesis, Radiolaria. *In* Hays, J.D., et al., *Init. Repts. DSDP,* 9: Washington (U.S. Govt. Printing Office), 947–1058.

Goll, R.M., 1979. The Neogene evolution of *Zygocircus, Neosemantis* and *Callimitra:* their bearing on nassellarian classification. A revision of the Plagiacanthoidea. *Micropaleontology,* 25(4):365–396.

Haeckel, E., 1887. Report on the Radiolaria collected by H.M.S. *Challenger* during the years 1873–1876. *Rep. Sci. Results Voy. H.M.S. Challenger, 1873–1876, Zool.,* 18:1–1803.

Holdsworth, B.K., 1975. Cenozoic Radiolaria biostratigraphy: Leg 30: tropical and equatorial Pacific. *In* Andrews, J.E., Packham, G., et al., *Init. Repts. DSDP,* 30: Washington (U.S. Govt. Printing Office), 499–537.

Johnson, D.A., 1974. Radiolaria from the eastern Indian Ocean, DSDP Leg 22. *In* von der Borch, C.C., Sclater, J.G., et al., *Init. Repts. DSDP,* 22: Washington (U.S. Govt. Printing Office), 521–575.

Johnson, D.A., and Nigrini, C.A., 1985. Synchronous and time-transgressive Neogene radiolarian datum levels in the equatorial Indian and Pacific Oceans. *Mar. Micropaleontol.,* 9(6):489–523.

Kling, S.A., 1971. Radiolaria: Leg 6 of the Deep Sea Drilling Project. *In* Fischer, A.G., Heezen, B.C., et al., *Init. Repts. DSDP,* 6: Washington (U.S. Govt. Printing Office), 1069–1117.

Kozlova, G.E., and Gorbovets, A.N., 1966. Radiolyarii verkhnemelovykh i verkhneeotsenovykh otlozhenii Zapadno-Sibirskoi Nizmennosti [Radiolaria of the Upper Cretaceous and upper Eocene of the west Siberian Lowland]. *Tr. Vses. Neft. Nauchno-Issled. Geologorazved. Inst. (VNIGRI) [Proc. All-Union Pet. Sci. Res. Inst. Geol. Surv. (VNIGRI)],* 248:1–159.

Krasheninnikov, V.A., 1960. Nektorye Radiolyarii Nizhnego i Srednego Eotsena Zapadnogo Predkavkazya [Some radiolarians of the lower and middle Eocene of the western Caucasus]. *Min. Geol. Okhr. Nedr SSSR, Vses. Nauchno-Issled. Geol. Neft. Inst.,* 16:271–308.

Lanci, L., Parés, J.M., Channell, J.E.T., and Kent, D.V., 2004. Miocene magnetostratigraphy from equatorial Pacific sediments (ODP Site 1218, Leg 199). *Earth Planet. Sci. Lett.,* 226(1–2):207–224.

Lanci, L., Parés, J.M., Channell, J.E.T., and Kent, D.V., in press. Oligocene magnetostratigraphy from equatorial Pacific sediments (ODP Sites 1218 and 1219, Leg 199). *Earth Planet. Sci. Lett.*

Ling, H.Y., 1975. Radiolaria: Leg 31 of the Deep Sea Drilling Project. *In* Karig, D.E., Ingle, J.C., Jr., et al., *Init. Repts. DSDP,* 31: Washington (U.S. Govt. Printing Office), 703–761.

Lyle, M., Wilson, P.A., Janecek, T.R., et al., 2002. *Proc. ODP, Init. Repts.,* 199 [CD-ROM]. Available from: Ocean Drilling Program, Texas A&M University, College Station TX 77845-9547, USA.

Mato, C.Y., and Theyer, F., 1980. *Lychnocanoma bandyca* n. sp., a new stratigraphically important late Eocene radiolarian. *In* Sliter, W.V. (Ed.), *Studies in Marine Micropaleontology and Paleoecology: A Memorial Volume to Orville L. Bandy.* Spec. Publ. Cushman Found. Foram. Res., 19:225–229.

Maurrasse, F., and Glass, B.P., 1976. Radiolarian stratigraphy and North American microtektites in Caribbean RC9-58: implications concerning late Eocene radiolarian chronology and the age of the Eocene–Oligocene boundary. *Trans. 7th Caribbean Geol. Conf.,* Guadeloupe, 1974:205–212.

Moore, T.C., 1968. Deep-sea sedimentation and Cenozoic stratigraphy in the central equatorial Pacific [Ph.D. dissert.]. Univ. California, San Diego.

Moore, T.C., 1971. Radiolaria. *In* Tracey, J.R. et al. (Eds.), *Init. Repts. DSDP,* 8: Washington (U.S. Govt. Printing Office), 727–775.

Moore, T.C., 1972. Mid-Tertiary evolution of the radiolarian genus *Calocycletta*. *Micropaleontology,* 18(2):144–152.

Moore, T.C., Backman, J., Raffi, I., Nigrini, C., Sanfilippo, A., Pälike, H., and Lyle, M., 2004. The Paleogene tropical Pacific: clues to circulation, productivity and plate motion. *Paleoceanography,* 19. doi:10.1029/2003PA000998

Moore, T.C., Pisias, N.G., and Shackleton, N.J., 1993. Paleoceanography and the diachrony of radiolarian events in the eastern equatorial Pacific. *Paleoceanography,* 8(5):567–586.

Moore, T.C., Jr., Rea, D.K., Lyle, M., and Liberty, L.M., 2002. Equatorial ocean circulation in an extreme warm climate. *Paleoceanography,* 17(1). doi:10.1029/2000PA000566

Nakaseko, K., 1963. Neogene Cyrtoidea (Radiolaria) from the Isozaki Formation in Ibaraki Prefecture, Japan. *Sci. Rep., Coll. Gen. Educ., Osaka Univ.,* 12:165–198.

Nigrini, C., 1967. Radiolaria in pelagic sediments from the Indian and Atlantic Oceans. *Bull. Scripps Inst. Oceanogr.,* 11:1–125.

Nigrini, C., 1974. Cenozoic Radiolaria from the Arabian Sea, DSDP Leg 23. *In* Davies, T.A., Luyendyk, B.P., et al., *Init. Repts. DSDP,* 26: Washington (U.S. Govt. Printing Office), 1051–1121.

Nigrini, C., 1977. Tropical Cenozoic Artostrobiidae (Radiolaria). *Micropaleontology,* 23:241–269.

Nigrini, C., and Caulet, J.P., 1992. Late Neogene radiolarian assemblages characteristic of Indo-Pacific areas of upwelling. *Micropaleontology,* 38(2):139–164.

Nishimura, A., 1992. Paleocene radiolarian biostratigraphy in the northwest Atlantic at Site 384, Leg 43, of the Deep Sea Drilling Project. *Micropaleontology,* 38(4):317–362.

Norris, R.D., Klaus, A., and Kroon, D., 2001. Mid-Eocene deep water, the Late Palaeocene Thermal Maximum and continental slope mass wasting during the Cretaceous–Palaeogene impact. *In* Kroon, D., Norris, R.D., and Klaus, A. (Eds.), *Western North Atlantic Palaeogene and Cretaceous Palaeoceanography,* Spec. Publ.—Geol. Soc. London, 183:23–48.

O'Connor, B., 1994. Seven new radiolarian species from the Oligocene of New Zealand. *Micropaleontology,* 40(4):337–350.

O'Connor, B., 1997a. New Radiolaria from the Oligocene and early Miocene of Northland, New Zealand. *Micropaleontology,* 43(1):63–100.

O'Connor, B., 1997b. Lower Miocene Radiolaria from Te Kopua Point, Kaipara Harbour, New Zealand. *Micropaleontology,* 43(2):101–128.

O'Connor, B., 1999. Radiolaria from the late Eocene Oamaru diatomite, South Island, New Zealand. *Micropaleontology,* 45(1):1–55.

Pälike, H., Moore, T., Backman, J., Raffi, I., Lanci, L., Parés, J.M., and Janecek, T., 2005. Integrated stratigraphic correlation and improved composite depth scales for ODP Sites 1218 and 1219. *In* Wilson, P.A., Lyle, M., and Firth, J.V. (Eds.), *Proc. ODP, Sci. Results,* 199 [Online]. Available from World Wide Web: <http://www-odp.tamu.edu/publications/199_SR/213/213.htm>.

Parés, J.M., and Lanci, L., 2004. A complete middle Eocene–early Miocene magnetic polarity stratigraphy in equatorial Pacific sediments (ODP Site 1220). *In* Channell, J.E.T., Kent, D.V., Lowrie, W., and Meert, J. (Eds.), *Timescales of the Paleomagnetic Field.* Geophys. Monogr., 145:131–140.

Petrushevskaya, M.G., 1965. Osobennosti i konstruktsii skeleta radiolyarii Botryoidae otr. (Nassellaria). (Peculiarities of the construction of the skeleton of radiolarians Botryoidae [Order Nassellaria].) *Tr. Zool. Inst., Akad. Nauk SSSR,* 35:79–118.

Petrushevskaya, M.G., and Kozlova, G.E., 1972. Radiolaria: Leg 14, Deep Sea Drilling Project. *In* Hayes, D.E., Pimm, A.C., et al., *Init. Repts. DSDP,* 14: Washington (U.S. Govt. Printing Office), 495–648.

Riedel, W.R., 1953. Mesozoic and late Tertiary Radiolaria of Rotti. *J. Paleontol.,* 27(6):805–813.

Riedel, W.R., 1954. The age of the sediment collected at Challenger (1895) Station 225 and the distribution of *Ethmodiscus rex* (Rattray). *Deep-Sea Res., Part A,* 1:170–175.

Riedel, W.R., 1957. Radiolaria: a preliminary stratigraphy. *In* Petterson, H. (Ed.), *Rep. Swed. Deep-Sea Exped., 1947–1948,* 6(3):59–96.

Riedel, W.R., 1959. Oligocene and lower Miocene Radiolaria in tropical Pacific sediments. *Micropaleontology,* 5(3):285–302.

Riedel, W.R., and Funnell, B.M., 1964. Tertiary sediment cores and microfossils from the Pacific Ocean floor. *Q. J. Geol. Soc. London,* 120:305–368.

Riedel, W.R., and Sanfilippo, A., 1970. Radiolaria, Leg 4, Deep Sea Drilling Project. *In* Bader, R.G., Gerard, R.D., et al., *Init. Repts. DSDP,* 4: Washington (U.S. Govt. Printing Office), 503–575.

Riedel, W.R., and Sanfilippo, A., 1971. Cenozoic Radiolaria from the western tropical Pacific, Leg 7. *In* Winterer, E.L., Riedel, W.R., et al., *Init. Repts. DSDP,* 7 (Pt. 2): Washington (U.S. Govt. Printing Office), 1529–1672.

Riedel, W.R., and Sanfilippo, A., 1973. Cenozoic Radiolaria from the Caribbean, Deep Sea Drilling Project, Leg 15. *In* Edgar, N.T., Saunders, J.B., et al., *Init. Repts. DSDP,* 15: Washington (U.S. Govt. Printing Office), 705–751.

Riedel, W.R., and Sanfilippo, A., 1978. Stratigraphy and evolution of tropical Cenozoic radiolarians. *Micropaleontology,* 24(1):61–96.

Riedel, W.R., and Sanfilippo, A., 1986. Morphological characters for a natural classification of Cenozoic Radiolaria, reflecting phylogenies. *Mar. Micropaleontol.,* 11:151–170.

Sanfilippo, A., 1990. Origin of the subgenera *Cyclampterium, Paralampterium* and *Sciadiopeplus* from *Lophocyrtis* (*Lophocyrtis*) (Radiolaria, Theoperidae). *Mar. Micropaleontol.,* 15(3–4):287–312.

Sanfilippo, A., and Blome, C.D., 2001. Biostratigraphic implications of mid-latitude Paleocene–Eocene radiolarian faunas from Hole 1051A, Ocean Drilling Program Leg 171B, Blake Nose, western North Atlantic. *In* Kroon, D., Norris, R.D., and Klaus, A. (Eds.), *Western North Atlantic Palaeogene and Cretaceous Palaeoceanography.* Spec. Publ.—Geol. Soc. London, 183:l85–224.

Sanfilippo, A., Burckle, L.H., Martini, E., and Riedel, W.R., 1973. Radiolarians, diatoms, silicoflagellates and calcareous nannofossils in the Mediterranean Neogene. *Micropaleontology,* 19(2):209–234.

Sanfilippo, A., and Nigrini, C., 1995. Radiolarian stratigraphy across the Oligocene/Miocene transition. *Mar. Micropaleontology,* 24(3–4):239–285.

Sanfilippo, A., and Nigrini, C., 1998. Code numbers for Cenozoic low latitude radiolarian biostratigraphic zones and GPTS conversion tables. *Mar. Micropaleontol.,* 33:109–156.

Sanfilippo, A., and Riedel, W.R., 1970. Post-Eocene "closed" theoperid radiolarians. *Micropaleontology,* 16(4):446–462.

Sanfilippo, A., and Riedel, W.R., 1973. Cenozoic Radiolaria (exclusive of theoperids, artostrobiids and amphipyndacids) from the Gulf of Mexico, Deep Sea Drilling Project Leg 10. *In* Worzel, J.L., Bryant, W., et al., *Init. Repts. DSDP,* 10: Washington (U.S. Govt. Printing Office), 475–611.

Sanfilippo, A., and Riedel, W.R., 1974. Radiolaria from the west-central Indian Ocean and Gulf of Aden, DSDP Leg 24. *In* Fisher, R.L., Bunce, E.T., et al., *Init. Repts. DSDP,* 24: Washington (U.S. Govt. Printing Office), 997–1035.

Sanfilippo, A., and Riedel, W.R., 1980. A revised generic and suprageneric classification of the Artiscins (Radiolaria). *J. Paleontol.,* 54(5):1008–1011.

Sanfilippo, A., and Riedel, W.R., 1982. Revision of the radiolarian genera *Theocotyle, Theocotylissa,* and *Thyrsocyrtis*. *Micropaleontology,* 28(2):170–188.

Sanfilippo, A., and Riedel, W.R., 1992. The origin and evolution of Pterocorythidae (Radiolaria): a Cenozoic phylogenetic study. *Micropaleontology,* 38(1):1–36.

Sanfilippo, A., Westberg-Smith, M.J., and Riedel, W.R., 1985. Cenozoic Radiolaria. *In* Bolli, H.M., Saunders, J.B., and Perch-Nielsen, K. (Eds.), *Plankton Stratigraphy:* Cambridge (Cambridge Univ. Press), 631–712.

Saunders, J.B., Bernoulli, D., Müller-Merz, E., Oberhänsli, H., Perch-Nielsen, K., Riedel, W.R., Sanfilippo, A., and Torrini, R., Jr., 1984. Stratigraphy of the late middle Eocene to early Oligocene in the Bath Cliff section Barbados, West Indies. *Micropaleontology,* 30(4):390–425.

Shackleton, N.J., Crowhurst, S., Hagelberg, T., Pisias, N.G., and Schneider, D.A., 1995. A new late Neogene time scale: application to Leg 138 sites. *In* Pisias, N.G., Mayer, L.A., Janecek, T.R., Palmer-Julson, A., and van Andel, T.H. (Eds.), *Proc. ODP, Sci. Results,* 138: College Station, TX (Ocean Drilling Program), 73–101.

Shackleton, N.J., Crowhurst, S.J., Weedon, G.P., and Laskar, J., 1999. Astronomical calibration of Oligocene–Miocene time. *Philos. Trans. R. Soc. London, Ser. A,* 357:1907–1929.

Shipboard Scientific Party, 2002a. Explanatory notes. *In* Lyle, M., Wilson, P.A., Janecek, T.R., et al., *Proc. ODP, Init. Repts.,* 199, 1–70 [CD-ROM]. Available from: Ocean Drilling Program, Texas A&M University, College Station TX 77845-9547, USA.

Shipboard Scientific Party, 2002b. Leg 199 summary. *In* Lyle, M., Wilson, P.A., Janecek, T.R., et al., *Proc. ODP, Init. Repts.,* 199: College Station TX (Ocean Drilling Program), 1–87.

Shipboard Scientific Party, 2002c. Site 1219. *In* Lyle, M., Wilson, P.A., Janecek, T.R., et al., *Proc. ODP, Init. Repts.,* 199, 1–128 [CD-ROM]. Available from: Ocean Drilling Program, Texas A&M University, College Station TX 77845-9547, USA.

Sutton, H.J., 1896. Radiolaria: a new genus from Barbados. *Am. Mon. Microsc. J.,* 17:61–62.

Vinassa de Regny, P.E., 1900. Radiolari Miocenici Italiani. *Mem. R. Acad. Sci. Inst. Bologna, Ser. 5,* 8:227–257.

Wade, B.S., and Pälike, H., 2004. Oligocene climate dynamics: equatorial Pacific stable isotope measurements in an astronomical template. *Paleoceanography,* 19(4). doi:10.1029/2004PA001042

Wetzel, O., 1935. Die Mikropalaeontologie des Heiligenhafener Kieseltones (Ober-Eozän). *Niedersaechs. Geol. Verein, Jahresbericht,* 27:41–75.

APPENDIX

Taxonomic List

The shore-based investigation was divided among the three authors. Dr. T.C. Moore examined the Neogene sections, Dr. C. Nigrini examined the Oligocene, and Dr. A. Sanfilippo examined the Eocene. For this reason, it is suggested that citations of the new taxa described herein be quoted in the following manner:

Calocycletta (Calocycletta) anekathen Sanfilippo and Nigrini n. sp.
Dorcadospyris anastasis Sanfilippo n. sp.
Dorcadospyris copelata Sanfilippo n. sp.
Dorcadospyris cyclacantha Moore n. sp.
Dorcadospyris ombros Sanfilippo n. sp.
Dorcadospyris scambos Moore and Nigrini n. sp.
Eucyrtidium mitodes Nigrini n. sp.
Theocyrtis careotuberosa Nigrini and Sanfilippo n. sp.
Theocyrtis perpumila Sanfilippo n. sp.
Theocyrtis perysinos Nigrini and Sanfilippo n. sp.
Theocyrtis setanios Nigrini and Sanfilippo n. sp.
Thyrsocyrtis (Pentalacorys) orthotenes Sanfilippo n. sp.

Type specimens will be deposited in the U.S. National Museum, Washington, D.C.

Specimen illustrations are shown in Plates **P1, P2, P3, P4, P5,** and **P6.**

Acrobotrys disolenia Haeckel
(Pl. **P6,** fig. 14)

Acrobotrys disolenia Haeckel, 1887, p. 1114, pl. 96, fig. 10

Acrobotrys sp. aff. *A. disolenia* Haeckel, Petrushevskaya and Kozlova, 1972, p. 554, pl. 39, fig. 3 only [non fig. 9]

?*Phormobotrys cannothalamia* Haeckel, 1887, p. 1125, pl. 96, fig. 25

Remarks: Although Haeckel illustrates and describes *A. disolenia* with an open abdomen, we found specimens with both open and closed abdomens and do not think that this difference constitutes a generic distinction. We did not, however, observe the caplike structure or "abdomen" shown in Haeckel's illustration of *Phormobotrys cannothalamia* (1887, pl. 96, fig. 25).

The species is consistently present in Zones RP21 and RP22 in material from Sites 1218 and 1219. Below and in the lower part of its range (Tables **T1, T2**) we observed a similar form in which the antecephalic lobe is prolonged but never becomes an open tube (Pl. **P6,** fig. 15). These forms are tabulated as "cf" in the *A. disolenia* column of our range charts.

Acrocubus octopylus Haeckel
(Pl. **P1,** fig. 9)

Acrocubus octopylus Haeckel, 1887, p. 993, pl. 82, fig. 9; Goll, 1972, p. 961, pl. 37, figs. 1–3

Remarks: This relatively large, robust form is distinctive and preserves well. In Leg 199 material it has a discontinuous range. It first occurs for a very short interval at the base of Zone RP22 at both Sites 1218 and 1219. It was found in a single sample from Site 1220 at the base of Zone RP22. It then recurs within Zone RN4 and continues well into Zone RN5 before apparently becoming extinct. In its upper range it was also found at both Sites 1218 and 1219, as well as in nearby piston cores EW9709-7P and EW9709-12P. In Goll's (1972) DSDP Leg 9 report on sites in the equatorial Pacific, *A. octopylus* was found from the base

P1. *Zealithapium, Didymocyrtis, Lithocyclia, Acrocubus, Dorcadospyris,* p. 71.

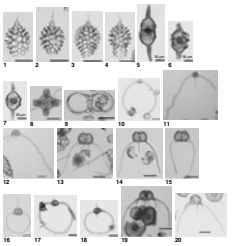

P2. *Dorcadospyris,* p. 72.

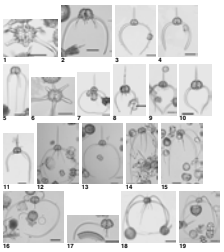

P3. *Dorcadospyris, Liriospyris, Tristylospyris, Zygocircus, Anthocyrtoma, Artophormis,* p. 73.

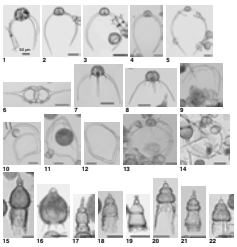

P4. *Artophormis, Eucyrtidium, Lamptonium, Lychnocanoma, Pterocodon, Eusyringium, Lychnocanoma, Rhopalocanium, Theocorys,* p. 74.

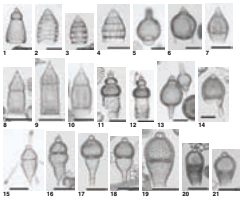

P5. *Theocotylissa, Pteropilium, Thyrsocyrtis, Calocycletta, Podocyrtis, Theocyrtis,* p. 75.

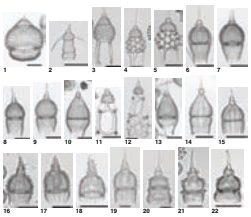

of the *Calocycletta costata* Zone (RN4) to the lower part of what he referred to as the *Cannartus laticonus* Zone. Given revisions in the radiolarian zonation and the lower resolution of rotary cored sites, this range is consistent with the upper part of the *A. octopylus* range noted in the Leg 199 material. Goll (1972) did not report *A. octopylus* from lower in the section, although if encountered its occurrence may have been mistaken for downhole contamination.

Amphicraspedum murrayanum Haeckel

Amphicraspedum murrayanum Haeckel, 1887, p. 523, pl. 44, fig. 10; Sanfilippo and Riedel, 1973, p. 524, pl. 10, figs. 3–6; pl. 28, fig. 1

Anthocyrtoma spp.

(Pl. **P3,** figs. 15, 16)

See genus *Anthocyrtoma* in Riedel and Sanfilippo, 1970, p. 524, pl. 6, figs. 2–4

Remarks: This relatively large two- to three-segmented form with inflated thorax and a rather constricted mouth is very distinctive in middle Eocene sediments from Leg 199. Individuals occurring early in the stratigraphic range of this species (Zones RP8–RP12) are smaller—(length of cephalothorax = 190–238 µm; maximum thoracic breadth = 170–202 µm), less spiny, and do not have a hyaline helmetlike covering on the cephalis. Later forms (Zone RP16) are larger—(length of cephalothorax = 222–283 µm; maximum thoracic breadth = 174–246 µm), commonly with a spiny surface and long spines extending distally from the peristome. In well-preserved specimens a thin-walled cylindrical abdomen is connected to the distal spines. The abdominal pores are large and irregular in size and arrangement.

Measurements (based on 30 specimens from Cores 199-1218A-26X and 28X; 199-1219A-19H, 21H, and 24H; 199-1220A-11H; and 199-1220B-16X):

Maximum length of cephalothorax (excluding horn and distal spines) = 190–283 µm (usually 210 µm)
Length of cephalis (including helmet and spines) = 44–109 µm
Length of cylindrical abdomen = 80–133 µm
Length of distal spines = 40–73 µm
Breadth of thorax = 162–246 µm

Artophormis barbadensis (Ehrenberg)

(Pl. **P3,** figs. 17–19)

Calocyclas barbadensis Ehrenberg, 1873, p. 217; 1875, pl. 18, fig. 8

Artophormis barbadensis (Ehrenberg), Haeckel, 1887, p. 1459; Riedel and Sanfilippo, 1970, p. 532, pl. 13, fig. 5

Remarks: The forms found in Leg 199 material commonly have well-developed latticed "bushy" horns, the third segment with large, subcircular pores irregular in size and arrangement, and the long fourth segment with irregular latticework and longitudinal ribs. A similar, very rare form with very small pores on all four segments (Pl. **P3,** fig. 19) is occasionally present throughout the range of *A. barbadensis* and is included in the concept.

Artophormis dominasinensis (Ehrenberg)

(Pl. **P4,** fig. 1)

Podocyrtis dominasinensis Ehrenberg, 1873, p. 250; 1875, pl. 14, fig. 4

Artophormis dominasinensis (Ehrenberg), Riedel and Sanfilippo, 1970, p. 532; 1971, p. 1592, pl. 6, fig. 6

P6. *Theocyrtis, Spirocyrtis, Dictyoprora, Acrobotrys, Botryocella, Botryopyle, Centrobotrys,* p. 76.

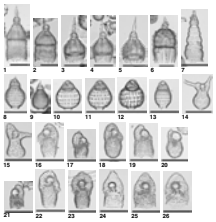

Artophormis gracilis Riedel
(Pl. P3, figs. 20–22)

Artophormis gracilis Riedel, 1959, p. 300, pl. 2, figs. 12, 13; Riedel and Sanfilippo, 1970, p. 532, pl. 13, fig. 6; 1971, pl. 3B, figs. 5–7; pl. 6, fig. 7; Sanfilippo and Nigrini, 1995, p. 272, pl. I, figs. 1–5

?*Artophormis fluminafauces* O'Connor, 1999, p. 20, pl. 3, figs. 12–16b; pl. 6, figs. 24a–27

Remarks: In the early part of its stratigraphic range, Zones RP18–RP19, *A. gracilis* is accompanied by a similar form, herein included, in which the thorax is subspherical and the third segment inflated annular with larger pores. The abdomen in these forms is usually only slightly wider than the thorax. We also allowed considerable variation with regard to pore size and development of the fourth segment and may well have included forms described by O'Connor (1999) as *Artophormis fluminafauces* in our tabulation.

Botryocella sp. group
(Pl. P6, figs. 16–18)

Botryopyle dictyocephalus Haeckel, 1887, p. 1113, pl. 96, fig. 6

Botryopyle dictyocephalus Haeckel gr., Riedel and Sanfilippo, 1971, p. 1602, pl. 1J, figs. 21–26; pl. 2J, figs. 16–18; pl. 3F, figs. 9–12

Remarks: We included in this species group forms that were previously referred to as *Botryopyle dictyocephalus* group. O'Connor (1999) made a sound argument for placing at least some of these forms in the genus *Botryocella,* and we are following his advice. However, we feel that there is sufficient variation in the forms we tabulated to consider our forms as an unnamed species group. For this reason we are also reluctant to place our forms in his species *Botryocella pauciperforata*.

Measurements (based on 30 specimens from Cores 199-1218A-24X and 25X; 199-1219A-18H; and 199-1220A-9H and 10H):

Total length = 88–166 µm
Length of terminally closed specimens = 129–162 µm
Breadth of antecephalic, eucephalic, and postcephalic lobes = 65–93 µm
Breadth of thorax = 56–77 µm

Botryopyle sp. A
(Pl. P6, figs. 19–21)

Botryopyle sp. A. Petrushevskaya, 1965, p. 90, fig. 6, III

Remarks: We included this species because it is found in our earliest samples (Zone RP7 at Site 1220). It may be related to the upper Maastrichtian form *Lithobotrys geminata* illustrated by Foreman (1968, text-fig. 1, fig. 11a–11c).

Measurements (based on 25 specimens from Cores 199-1218A-26X and 29X; 199-1219A-20H, 21H, and 24H; and 199-1220C-14X):

Total length = 101–141 µm
Length of closed forms = 81–141 µm
Length of horn = 20–49 µm
Breadth of thorax = 52–78 µm

Buryella clinata Foreman

Buryella clinata Foreman, 1973, p. 433, pl. 8, figs. 1–3; pl. 9, fig. 19

Buryella tetradica Foreman sensu stricto

Buryella tetradica Foreman, 1973, p. 433, pl. 8, figs. 4, 5; pl. 9, figs. 13, 14; Sanfilippo and Blome, 2001, p. 210

Calocyclas bandyca (Mato and Theyer)

Lychnocanoma bandyca Mato and Theyer, 1980, p. 225, pl. 1, figs. 1–6

Calocyclas bandyca (Mato and Theyer) Sanfilippo and Riedel in Saunders et al., 1985, p. 411, pl. 5, figs. 1, 5, 6

Calocyclas hispida (Ehrenberg)

Anthocyrtis hispida Ehrenberg, 1873, p. 216; 1875, pl. 8, fig. 2

Calocyclas hispida (Ehrenberg), Foreman, 1973, p. 434, pl. 1, figs. 12-15; pl. 9, fig. 18

Calocyclas turris Ehrenberg

Calocyclas turris Ehrenberg, 1873, p. 218; 1875, pl. 18, fig. 7; Foreman, 1973, p. 434

Calocycletta (Calocycletta) anekathen Sanfilippo and Nigrini n. sp.

(Pl. **P5,** figs. 7–9)

Theocyrtis tuberosa Riedel, Moore, 1971, p. 743, pl. 5, fig. 5 only (part)

Calocycletta virginis Haeckel sensu stricto in Petrushevskaya and Kozlova, 1972, p. 544, pl. 35, figs. 8–10

Type material: Holotype (Pl. **P5,** fig. 9) from Sample 199-1219A-17H-5, 32–34 cm, in the upper Eocene Zone RP19.

Description: Three-segmented pterocorythid with an ovate, sparsely pored cephalis, bearing a prominent, generally conical apical horn. Except for the earliest forms, the lateral lobes of the cephalis are situated directly below the large unpaired lobe and do not form distinct protrusions in profile. Early forms tend to have a short, weakly bladed horn, whereas later forms may have a longer, conical horn that is only bladed or furrowed near the base. Thorax is inflated hemispherical to inflated campanulate, rather thick walled, with hexagonally arranged circular pores tending toward longitudinal alignment. Lumbar stricture is distinct. The subcylindrical abdomen tapers distally and terminates in an undifferentiated margin. The subcircular abdominal pores are somewhat irregular in size and arrangement in early forms, becoming more regular in size and longitudinally arranged in later forms with a tendency toward having raised ridges separating the longitudinal rows of pores.

Measurements (based on 40 specimens from Cores 199-1218A-24X and 25X; 199-1219A-17H and 18H; and 199-1220A-8H and 9H):

Total length (excluding horn) = 186–311 µm
Length of cephalothorax = 153–190 µm
Length of horn = 40–109 µm
Maximum breadth = 129–174 µm

Etymology: The species name is the female form of the Greek adjective *anekathen,* meaning from the beginning.

Distinguishing characteristics: *Calocycletta (Calocycletta) anekathen* n. sp. is very similar to *Calocycletta (Calocycletta) robusta* but is stratigraphically separated from it by ~8 m.y., and for that reason we have chosen to make it a distinct species. It differs from *C. (C.) robusta* by having a less rough surface on the thorax, but even that feature is not always easily recognizable.

It is distinguished from *C. (C.) parva* by its larger size (*parva:* length of cephalis = 34–43 µm, thorax = 58–82 µm, abdomen = 24–48 µm; maximum breadth = 86–115 µm), from *C. (C.) virginis* by not having an abdomen terminating in 11–16 parallel lamellar feet, from *C. (Calocyclissima) costata* by not having longitudinal ribs between rows of thoracic pores, and from *C. (Calocyclopsis) serrata* by not having a short tapering abdomen terminating in shovel-shaped feet.

Variability: Early forms tend to have a broader-based cephalis, whereas in later forms the paired lobes are directly below the unpaired lobe. Later forms have a clear zone between the base of the horn and the pored part of the cephalis. Another variable character is the tendency toward longitudinal alignment of the abdominal pores in later forms.

Range: This species is consistently present at Sites 1218 and 1219 from the RP17/RP18 zonal boundary to the RP19/RP20 zonal boundary. Its lower limit at Site 1220 is somewhat higher, probably due to dissolution effects. It is possible that the 8-m.y. gap between the stratigaphic range of *C. (C.) anekathen* and *C. (C.) robusta* is a result of a very sparse population in Zones RP20 and most of Zone RP21 due to paleoenvironmental conditions or to dissolution.

Phylogeny: The phylogenetic relationship between *C. (C.) anekathen* n. sp. and the earliest member of the *Calocycletta (Calocycletta*) lineage, *C. (C.) parva*, is not understood. In the Leg 199 material there is an 8-m.y. time interval in the early Oligocene (Zone RP20 and most of Zone RP21) separating the last occurrence of *C. (C.) anekathen* and the first occurrence of *C. (C.) parva,* previously thought to be the origin of the genus near the middle of Zone RP21 (Moore, 1972; Sanfilippo and Riedel, 1992). Sanfilippo and Riedel (1992) noted very sporadic occurrences of individuals with a more cylindrical than bladed horn in the latest Eocene/early Oligocene but did not treat them as members of the genus *Calocycletta*. A possible explanation for the absence of *C. (C.) anekathen* in previous DSDP/ODP sequences may be that the short stratigraphic interval during which common *C. (C.) anekathen* is present in the Leg 199 material was not recovered or sampled during earlier legs, and thus the individuals observed by Sanfilippo and Riedel (1992) indeed are *C. (C.) anekathen*. The origin of the genus *Calocycletta* needs further study.

Remarks: Examination of a duplicate set of slides, deposited in SIO Geological Collections, from DSDP Site 140 prepared at the same time as those used by Petrushevskaya and Kozlova for their DSDP Leg 14 contribution (1972), suggests that the forms illustrated by Petrushevskaya and Kozlova (1972, pl. 35, figs. 8–10) are identical to the form herein described as *C. (C.) anekathen* n. sp. These specimens were probably obtained from Sample 14-140A-2-CC rather than 14-140-2-CC as indicated in the plate caption. Reexamination (by A.S.) of the slides shows that the radiolarians in DSDP Hole 140A Core 2 are from the latest Eocene Zone RP19, and radiolarians from Sample 14-140-2-CC early Miocene Zone RN4, while those from Samples 14-140-3-2; 3-3; 3-CC; and 4-CC are from the middle to late Eocene and those from Sample 14-140-5-CC are from the early Miocene Zone RN3. It is clear from a footnote to the "Explanation of Plates" that Petrushevskaya and Kozlova (1972, p. 557) identified the sample containing these specimens as being of Eocene age despite it being labeled 140-2CC, which they knew to be derived from a Miocene interval.

Calocycletta (Calocycletta) robusta Moore

(Pl. **P5,** fig. 6)

Calocycletta (Calocycletta) robusta Moore, 1971, p. 743, p. 10, figs. 5, 6; Sanfilippo and Riedel, 1992, pp. 28, 36; Sanfilippo and Nigrini, 1995, p. 272, pl. II, figs. 2, 3

Calocycletta (Calocycletta) virginis Haeckel

Calocyclas (Calocycletta) virginis Haeckel, 1887, p. 1381, pl. 74, fig. 4; Riedel, 1959, p. 295, pl. 2, fig. 8

Calocycletta virginis Haeckel, Riedel and Sanfilippo, 1970, p. 535, pl. 14, fig. 10

Calocycletta (Calocycletta) virginis Haeckel, Sanfilippo and Riedel, 1992, pp. 28, 36

***Calocycletta (Calocyclior) caepa* Moore**

Calocycletta caepa Moore, 1972, p. 150, pl. 2, figs. 4–7

Calocycletta (Calocyclior) caepa Moore, Sanfilippo and Riedel, 1992, p. 31, pl. 2, fig. 11

***Calocycletta (Calocyclissima) costata* (Riedel)**

Calocyclas virginis Haeckel, Riedel, 1957, p. 90, pl. 4, fig. 5 (*partim*.)

Calocyclas costata Riedel, 1959, p. 296, pl. 2, fig. 9

Calocycletta costata (Riedel), Riedel and Sanfilippo, 1970, p. 535, pl. 14, fig. 12; Sanfilippo et al., 1985, p. 691. fig. 28.3a, 28.3b

Calocycletta (Calocyclissima) costata (Riedel), Sanfilippo and Riedel, 1992, pp. 30, 36

***Calocycletta (Calocyclopsis) serrata* Moore**

Calocycletta cf. *viginis* Haeckel, Riedel and Sanfilippo, 1970, p. 568, pl. 14, fig. 11

Calocycletta serrata Moore, 1972, p. 148, pl. 2, figs. 2, 3

Calocycletta (Calocyclopsis) serrata Moore, Sanfilippo and Riedel, 1992, p. 30, pl. 2, fig. 10

***Calocycloma ampulla* (Ehrenberg)**

Eucyrtidium ampulla Ehrenberg 1854, pl. 36, fig. 15a–15c; 1873, p. 22.

Calocycloma ampulla (Ehrenberg), Foreman 1973, p. 434, pl. 1, figs. 1–5; pl. 9, fig. 20

***Calocycloma castum* (Haeckel)**

Calocyclas casta Haeckel, 1887, p. 1384, pl. 73, fig. 10

Calocycloma castum (Haeckel), Foreman, 1973, p. 434, pl. 1, figs. 7, 9, 10

Remarks: The presence of a form questionably assigned to *C. castum* was recorded in Hole 1220A from near the top of Zone RP14 through most of Zone RP16. This form is similar in all respects to *C. castum* except that the distinct change in contour between the conical upper part of the thorax and the inflated part is not always as obvious as in forms examined in the early part of the section (Zones RP7–RP11).

***Carpocanopsis bramlettei* Riedel and Sanfilippo**

Cycladophora favosa Haeckel in Riedel, 1954, pl. 1, fig. 3 (non fig. 2)

Carpocanopsis bramlettei Riedel and Sanfilippo, 1971, p. 1597, pl. 2G, figs. 8–14; pl. 8, fig. 7

***Carpocanopsis cingulata* Riedel and Sanfilippo**

Carpocanopsis cingulatum Riedel and Sanfilippo, 1971, p. 1597, pl. 2G, figs. 17–21; pl. 8, fig. 8

Carpocanopsis cingulata Riedel and Sanfilippo, Sanfilippo and Riedel, 1973, p. 531

***Carpocanopsis cristata* (Carnevale)**

? *Sethocorys cristata* Carnevale, 1908, p. 31, pl. 4, fig. 18

? *Sethocorys cristata* var. a Carnevale, 1908, p. 32, pl. 4, fig. 19

Carpocanopsis cristatum (Carnevale)?, Riedel and Sanfilippo, 1971, p. 1597, pl. 1G, fig. 16; pl. 2G, figs. 1–7

Carpocanopsis cristata (Carnevale)?, Sanfilippo and Riedel, 1973, p. 531

Remarks: This species is used in a restricted sense herein. As in Johnson and Nigrini (1985), only specimens resembling those figured by Riedel and Sanfilippo, 1971, pl. lG, fig. 16 and pl. 2G, fig. 1 are included.

Centrobotrys gravida Moore

Centrobotrys gravida Moore, 1971, p. 744, pl. 5, fig. 8

Centrobotrys petrushevskayae Sanfilippo and Riedel

(Pl. P6, figs. 22, 23)

Centrobotrys (?) sp. A Riedel and Sanfilippo, 1971, p. 1602, pl. 3F, figs. 15, 16

Centrobotrys petrushevskayae Sanfilippo and Riedel, 1973, p. 532, pl. 36, figs. 12, 13

Centrobotrys thermophila Petrushevskaya

(Pl. P6, figs. 24–26)

Centrobotrys thermophila Petrushevskaya, 1965, p. 115, text-fig. 20; Nigrini, 1967, p. 49, text-fig. 26, pl. 5, fig. 7

Remarks: At two of the studied sites (1218 and 1219) we observed an early form of *C. thermophila* that is similar to the typical form with the merged ante- and post-cephalic lobes apically pointed and no distinct change in contour between the cephalis and thorax. However, these forms have more numerous and larger pores than typical forms and are less hyaline. They first occur in Zone RP20 together with *C. petrushevskayae*. Both species are sparsely represented in the upper part of Zone RP21, but are found again in Zone RP22 with *C. thermophila* being more prevalent than *C. petrushevskayae*. Herein we include both forms of *C. thermophila* in our tabulation, but are not sufficiently confident of the relationship between them and *C. petrushevskayae* to include them in our list of stratigraphically useful radiolarian events (Table T6).

Cryptocarpium azyx (Sanfilippo and Riedel)

Carpocanistrum azyx Sanfilippo and Riedel, 1973, p. 530, pl. 35, fig. 9

Cryptocarpium azyx (Sanfilippo and Riedel), Sanfilippo and Riedel, 1992, p. 6, pl. 2, fig. 21

Cryptocarpium ornatum (Ehrenberg)

Cryptoprora ornata Ehrenberg, 1873, p. 222; 1875, pl. 5, fig. 8; Sanfilippo et al., 1985, p. 693, fig. 27.2a, 27.2b

Cryptocarpium ornatum (Ehrenberg), Sanfilippo and Riedel, 1992, pp. 6, 36, pl. 2, figs. 18–20

Cyrtocapsella cornuta Haeckel

Cyrtocapsa (Cyrtocapsella) cornuta Haeckel, 1887, p. 1513, pl. 78, fig. 9

Cyrtocapsella cornuta Haeckel, Sanfilippo and Riedel, 1970, p. 453, pl. 1, figs. 19, 20

Cyrtocapsella japonica (Nakaseko)

Eusyringium japonicum Nakaseko, 1963, p. 193, text-figs. 20, 21, pl. 4, figs. 1–3

Cyrtocapsella japonica (Nakaseko), Sanfilippo and Riedel, 1970, p. 452, pl. 1, figs. 13–15 (with synonymy)

Cyrtocapsella tetrapera Haeckel

Cyrtocapsa (Cyrtocapsella) tetrapera Haeckel, 1887, p. 1512, pl. 78, fig. 5

Cyrtocapsella tetrapera Haeckel, Sanfilippo and Riedel, 1970, p. 453, pl. 1, figs. 16–18; Sanfilippo et al., 1985, p. 670, fig. 16.1a, 16.1b; Sanfilippo and Nigrini, 1995, p. 275

Dendrospyris fragoides Sanfilippo and Riedel

Dendrospyris fragoides Sanfilippo and Riedel, 1973, p. 526, pl. 15, figs. 8–13; pl. 31, figs. 13, 14

Diartus hughesi (Campbell and Clark)

Ommatocampe hughesi Campbell and Clark, 1944, p. 23, pl. 3, fig. 12

Ommatartus hughesi (Campbell and Clark), Riedel and Sanfilippo, 1970, p. 521

Diartus hughesi (Campbell and Clark), Sanfilippo and Riedel, 1980, p. 1010

Diartus petterssoni (Riedel and Sanfilippo)

Cannartus (?) *petterssoni* conditional manuscript name proposed in Riedel and Funnell, 1964, p. 310; Riedel and Sanfilippo, 1970, p. 520, pl. 14, fig. 3

Diartus petterssoni (Riedel and Sanfilippo), Sanfilippo and Riedel, 1980, p. 1010

Dictyophimus craticula Ehrenberg

Dictyophimus craticula Ehrenberg 1873, p. 223; 1875, pl. 5, figs. 4, 5; Sanfilippo and Riedel 1973, p. 529, pl. 19, fig. 1; pl. 33, fig. 11

Dictyoprora armadillo (Ehrenberg) group
(Pl. **P6,** fig. 9)

Eucyrtidium armadillo Ehrenberg, 1873, p. 225; 1875, p. 70, pl. 9, fig. 10

Theocampe armadillo (Ehrenberg) group, Riedel and Sanfilippo, 1971, p. 1601, pl. 3E, figs. 3–5 (*partim*.)

Dictyoprora armadillo (Ehrenberg), Nigrini, 1977, p. 250, pl. 4, fig. 4

Remarks: In the Leg 199 material *Dictyoprora armadillo* is somewhat smaller in size than reported by Nigrini (1977) and due to poor preservation often lacks the well-developed three-bladed horn and the downwardly directed arches framing the distal pores.

The last occurrence of this species is consistently recognized at the Eocene/Oligocene boundary (RP19/RP20). The first occurrence, however, is more difficult to recognize. At Site 1218 it is within Zone RP15, at Site 1219 just below the RP15/RP16 zonal boundary, and at Site 1220 at the RP15/RP16 zonal boundary. In the early part of its stratigraphic range, when the abdomen has not yet reached its characteristic bulbous shape, it is difficult to distinguish this species from other members of the genus, in particular *Dictyoprora* cf. *ovata* (Pl. **P6,** fig. 8). As a distinguishing characteristic we counted the number of transverse rows of circular pores on the abdomen and include only individuals with 10–15 pore rows.

Measurements (based on 30 specimens from Cores 199-1218A-25X and 27X; 199-1219A-18H, 19H, and 20H; and 199-1220A-8H):

Total length (excluding horn) = 141–170 µm
Length of cephalothorax = 36–44 µm
Breadth = 76–105 µm

There are 10–15 transverse rows of pores on the abdomen.

Dictyoprora mongolfieri **(Ehrenberg)**

Eucyrtidium mongolfieri Ehrenberg, 1854, pl. 36, fig. 18, B lower; 1873, p. 230

Dictyoprora mongolfieri (Ehrenberg), Nigrini, 1977, p. 250, pl. 4, fig. 7

Dictyoprora pirum **(Ehrenberg) sensu stricto**
(Pl. **P6,** figs. 10, 11)

Eucyrtidium pirum Ehrenberg, 1873, p. 232; 1875, pl. 10, fig. 14

Dictyoprora pirum (Ehrenberg), Nigrini, 1977, p. 251, pl. 4, fig. 8

[*non*]-*Dictyoprora pirum* (Ehrenberg) var. A, Sanfilippo and Blome, 2001, p. 211, fig. 8c

Remarks: Prior to the earliest occurrence of *D. pirum* and co-occurring with it during the early part of its stratigraphic range are two very similar forms. One is almost identical to *D. pirum* in all respects except for the presence of longitudinal ridges separating single rows of pores on the abdomen or pores framed by downwardly directed arches (Pl. **P6,** fig. 12), and the other by not having an inflated abdomen (Pl. **P6,** fig. 13). We exclude these forms and restrict the concept of *D. pirum* to include only forms with a smooth hyaline very inflated (normal view) and laterally compressed abdomen.

Didymocyrtis bassanii **(Carnevale)**
(Pl. **P1,** fig. 5)

Cannartidium bassanii Carnevale, 1908, p. 21, pl. 3, fig. 12

Cannartus sp., Riedel and Sanfilippo, 1971, p. 1587, pl. 2B, figs. 9, 10

Cannartus bassanii (Carnevale), Sanfilippo et al., 1973, p. 222, pl. 1, figs. 1–3

Didymocyrtis bassanii (Carnevale), Sanfilippo and Riedel, 1980, p. 1010

Remarks: In Leg 199 material this form first occurs in the upper part of Zone RP22 where it co-occurs with relatively common *D. prismatica* and *D. tubaria*. Note that the medullary shells of *D. bassanii* appear to be spherical. It has a rather rough, equatorially constricted cortical shell and tapering spongy columns, but is otherwise unornamented with plicae or protuberances. It is most common in Zones RN1 and RN2 and disappears within Zone RN5. Its last occurrence is not well defined, as its shell gradually becomes more delicate in the upper part of its range where it probably gives rise to a more elongated and delicate variation. Preservation may play a significant role in its absence in this material. Within Zone RN2 some specimens begin to display plicae or thickenings on the bulged upper and lower parts of the cortical shell that are similar to those of *D. violina*.

Didymocyrtis laticonus **(Riedel)**

Cannartus laticonus Riedel, 1959, p. 291, pl. 1, fig. 5

Didymocyrtis laticonus (Riedel), Sanfilippo and Riedel, 1980, p. 1010

Didymocyrtis mammifera **(Haeckel)**

Cannartidium mammiferum Haeckel, 1887, p. 375, pl. 39, fig. 16

Cannartus mammiferus (Haeckel), Riedel, 1959, p. 291, pl. 1, fig. 4

Cannartus mammifer (Haeckel), Sanfilippo et al., 1973, p. 216, pl. 1, fig. 7

Didymocyrtis mammifera (Haeckel), Sanfilippo and Riedel, 1980, p. 1010

***Didymocyrtis prismatica* (Haeckel)**

Pipettella prismatica Haeckel, 1887, p. 305, pl. 39, fig. 6; Riedel, 1959, p. 287, pl. 1, fig. 1

Pipettella tuba Haeckel, 1887, p. 337, pl. 39, fig. 7

Cannartus prismaticus (Haeckel), Riedel and Sanfilippo, 1970, pl. 15, fig. 1

Didymocyrtis prismatica (Haeckel), Sanfilippo and Riedel, 1980, p. 1010; Sanfilippo and Nigrini, 1995, p. 275

***Didymocyrtis tubaria* (Haeckel)**
(Pl. **P1,** figs. 6, 7)

Pipettaria tubaria Haeckel, 1887, p. 339, pl. 39, fig. 15

Cannartus tubarius (Haeckel), Riedel, 1959, p. 289, pl. 1, fig. 2

Didymocyrtis tubaria (Haeckel), Sanfilippo and Riedel, 1980, p. 1010

Remarks: This species first occurs in the upper part of Zone RP21 where it is very rare, with an irregularly shaped cortical shell and often very delicate spongy columns (Pl. **P1,** fig. 6). It becomes somewhat more abundant in Zone RP22, but then virtually disappears in the lowermost part of Zone RN1. It recurs in the upper part of Zone RN2 and continues through Zone RN4 (Pl. **P1,** fig. 7), becoming very rare before extinction in lowermost Zone RN5.

***Didymocyrtis violina* (Haeckel)**

Cannartus violina Haeckel, 1887, p. 358, pl. 39, fig. 10; Riedel, 1959, p. 290, pl. 1, fig. 3 (with synonymy)

Didymocyrtis violina (Haeckel), Sanfilippo and Riedel, 1980, p. 1010

***Diploplegma somphum* Sanfilippo and Riedel**

Diploplegma somphum Sanfilippo and Riedel, 1973, p. 491, pl. 4, fig. 5; pl. 23, figs. 7, 8

***Dorcadospyris alata* (Riedel)**
(Pl. **P1,** fig. 10)

Brachiospyris alata Riedel, 1959, p. 293, pl. 1, figs. 11, 12

Dorcadospyris alata (Riedel), Riedel and Sanfilippo, 1970, p. 523, pl. 14, fig. 5

***Dorcadospyris anastasis* Sanfilippo n. sp.**
(Pl. **P1,** figs. 11, 12)

Type material: Holotype (Pl. **P1,** fig. 12) from Sample 199-1218A-26X-6, 45–47 cm, in the upper middle Eocene Zone RP16.

Description: Small, bilobed cephalis with thick-walled, latticed shell with slight external sagittal stricture and with circular to subcircular pores irregularly or hexagonally arranged. Two robust, very long primary feet extend laterally from the basal ring, curving gently downward. The entire length of these feet was not observed in the Leg 199 material. The feet are circular in cross section, and some distance away from the shell they are wavy. Remnants of six to twelve short, cylindrical secondary feet, circular in cross section, were observed.

Measurements (based on 30 specimens from Cores 199-1218A-26X and 27X; 199-1219A-20H; and 199-1220A-10H):

Length of shell = 60–81 µm (usually 68 µm)
Length of primary feet (never observed complete) = 255–1030 µm
Breadth of shell = 76–93 µm

Etymology: The species name is from the Greek noun (f) *anastasis,* meaning a stretching out or extension, and refers to the extraordinarily long feet on this species.

Distinguishing characteristics: *Dorcadospyris anastasis* n. sp. differs from all other species of the genus *Dorcadospyris* by the two extremely long, wavy primary feet.

Variability: The morphology of this species is rather constant over its short stratigraphic range. The only variable character is the length and robustness of the primary feet.

Range: This species occurs in moderate abundance and has a very short stratigraphic range in the upper middle Eocene Zone RP16.

Phylogeny: Unknown.

***Dorcadospyris ateuchus* (Ehrenberg)**
(Pl. **P1,** figs. 13–15)

Ceratospyris ateuchus Ehrenberg, 1873, pl. 218; 1875, pl. 21, fig. 4D

Cantharospyris ateuchus (Ehrenberg), Haeckel, 1887, p. 1051; Riedel, 1959, p. 294, pl. 22, figs. 3, 4

Dorcadospyris ateuchus (Ehrenberg), Riedel and Sanfilippo, 1970, p. 523, pl. 15, fig. 4; Sanfilippo and Nigrini, 1995, p. 275, pl. III, figs. 2–4

***Dorcadospyris circulus* (Haeckel) Moore**
(Pl. **P1,** fig. 16)

Gamospyris circulus Haeckel, 1887, p. 1042, pl. 83, fig. 19

Dorcadospyris circulus (Haeckel), Moore, 1971, p. 739, pl. 8, figs. 3–5

Remarks: We also observed forms similar to that described by O'Connor (1994) as *Dorcadospyris mahurangi*, but do not include them in our species concept because we are uncertain of their relationship to *D. circulus*. Although we find, as O'Connor suggests, forms in which the feet cross but are not joined, we also observed forms in which the crossed feet do join and extensions of the feet project from the resulting circular ring. We include forms with both robust and thin feet.

***Dorcadospyris copelata* Sanfilippo n. sp.**
(Pl. **P1,** figs. 19, 20; pl. **P2,** figs. 1, 2)

Type material: Holotype (Pl. **P1,** fig. 19) from Sample 199-1219A-17H-CC, in the upper Eocene Zone RP19.

Description: Bilobed cephalis with thick-walled latticed chambers bearing three strong cylindrical primary feet alternating in placement with three short, broad secondary feet. Primary feet vary from slightly divergent with most of the curvature proximally and almost straight distally, to semicircularly curved. Secondary feet are shorter, broad lamellar (paddle-shaped) with up-turned edges or occasionally fringed or pleated laterally, and widest distally.

Measurements (based on 40 specimens from Cores 199-1218A-18X and 25X; 199-1219A-17H through 19H; and 199-1220A-8H):
Length of shell = 81–97 µm
Length of primary feet = 202–404 µm
Length of tabular feet = 52–190 µm
Breadth of shell = 101–133 µm

Etymology: The species name is from the Greek adjective *kopelatos,* meaning like an oar.

Distinguishing characteristics: This species is similar to *Tristylospyris triceros* but differs from it by having three strongly developed broadly lamellar feet alternating with the three strong cylindrical primary feet.

Variability: The shape of the primary feet varies from slightly divergent to semicircularly curved, and the broad lamellar secondary feet show considerable variability in length and breadth.

Range: *Dorcadospyris copelata* n. sp. occurs in moderate to common abundance in the latest middle Eocene through the late Eocene, uppermost Zone RP16 through Zone RP19. Its last occurrence is at the RP19/RP20 zonal boundary.

Phylogeny: *D. copelata* n. sp. appears to be an offshoot from *Tristylospyris triceros* or a variant. The first occurrence of *D. copelata* is slightly later than the first occurrence of *T. triceros*, and the two species co-occur through the early part of the range of *T. triceros*.

Dorcadospyris cyclacantha **Moore n. sp.**

(Pl. **P1,** figs. 17, 18)

Dorcadospyris sp., Moore, 1968, pl. V, fig. 3a, 3b

Type material: Holotype (Pl. **P1,** fig. 18) from Sample 199-1219A-6H-7, 45–47 cm, in the upper Oligocene Zone RP22.

Description: The bilobed, latticed cephalis has two smoothly joined primary basal lateral feet and no apparent secondary feet. The shell usually bears a smoothly tapering conical apical horn. The "circle" formed by the joined feet is often somewhat flattened (Pl. **P1,** fig. 18) and has 15–30 conical spines of varying length, irregularly spaced along its convex side (Pl. **P1,** fig. 17).

Measurements (based on 15 specimens):

Lateral diameter of the circle formed by the primary feet = 419–539 µm (mean = 390 ± 54 µm)
Width of cephalis = 86–101 µm (mean = 96 ± 4 µm)
Ratio of circle width to cephalis width = 3.43–5.39 (mean = 4.04 ± 0.51)
Apical horn (when present) maximum measured length = 160 µm

Etymology: The specific name of this species is derived form a combination of the Greek nouns *kyklos* (m), meaning circle, and *acantha* (f), meaning thorn.

Distinguishing characteristics: This species is distinguished from *D. circulus* by the numerous conical spines along the convex side of the primary feet. It is distinguished from *D. spinosa* by having only two joined primary feet and no secondary feet and by the common presence of an apical horn. It is distinguished from *D. alata* by having an apical horn and joined primary basal feet.

Variability: This relatively short lived species varies in the number and size of short conical spines and in their distribution around the joined primary feet. The joined feet rarely make a perfect circle, but are usually smoothly joined.

Range: *Dorcadospyris cyclacantha* n. sp. occurs briefly in upper part of Zone RP22 within the upper range of *D. riedeli* and above the last occurrence of *D. papilio*. Its first occurrence is just preceded by the brief recurrence of a very rare form that is consistent with the description of *D. circulus*.

Phylogeny: *D. cyclacantha* appears to be an offshoot of *D. circulus*.

Dorcadospyris dentata **Haeckel**

(Pl. **P2,** fig. 3)

Dorcadospyris dentata Haeckel, 1887, p. 1040, pl. 85, fig. 6; Riedel, 1957, p. 79, pl. 1, fig. 4; Holdsworth, 1975, p. 528

Dorcadospyris decussata Haeckel, 1887, p. 1041, pl. 85, fig. 7

Dorcadospyris forcipata (Haeckel)

(Pl. P2, fig. 4)

Dipodospyris forcipata Haeckel, 1887, p. 1037, pl. 85, fig. 1; Riedel, 1957, p. 79, pl. 1, fig. 3

Dorcadospyris forcipata (Haeckel), Riedel and Sanfilippo, 1970, p. 523, pl. 15, fig. 7; Sanfilippo et al., 1985, p. 663, fig. 10.5a, 10.5b; Sanfilippo and Nigrini, 1995, p. 276

Remarks: This species is distinguished from *D. praeforcipata* by the lack of secondary feet. It first occurs in the uppermost part of Zone RN2 and disappears in the uppermost part of Zone RN5. Although always rare or very rare, it is most common in Zone RN3, where well over 100 specimens were often found per slide.

Dorcadospyris ombros Sanfilippo n. sp.

(Pl. P2, figs. 5, 6)

Type material: Holotype (Pl. P2, fig. 5) from Sample 199-1218A-25X-6, 42–44 cm, in the upper middle Eocene Zone RP16.

Description: Thick-walled, bilobed shell with slight external sagittal stricture and circular to subcircular pores irregular in size and distribution. No apical horn. Occasionally the surface, especially the apical part of the shell, bears several small spines. Five to six long, cylindrical feet, similar in length and thickness, diverge at an angle of <180° and then curve gently to extend straight downward. The distal part of the feet taper gently and occasionally broaden and/or fork at their termination. The distalmost parts of the feet are often turned sharply outward. Early forms tend to have a longer (in the apical direction) shell and shorter feet, whereas later forms have a more compressed shell and longer, more slender feet.

Measurements (based on 45 specimens from Cores 199-1218A-24X through 29X; 199-1219A-18H; 199-1220A-8H and 9H; and 199-1220B-8H):

Length of shell = 60–85 µm (usually 68 µm)
Length of feet = 202–364 µm (some forms have shorter feet = 121–182 µm)
Breadth of shell = 68–101 µm (usually 85 µm)

Etymology: This species name is derived from the Greek noun *ombros,* meaning rainfall.

Distinguishing characteristics: *Dorcadospyris ombros* n. sp. is distinguished from other members of the *Dorcadospyris* genus by having five to six long, cylindrical feet that are similar in length and thickness and diverge at an angle of <180°, curving gently, extending straight downward and with upturned terminations.

Variability: The length of the primary feet is quite variable, later forms tend to have longer feet than earlier ones, and the number of feet varies from five to six. In the uppermost material from Zone RP19 up to the top of Zone RP20 the form occurs sporadically and may exhibit unusually long feet (up to 515 µm). In addition, we also observed similar forms that differ mostly in that they possess and apical horn. It is possible that these are more closely related to *D. praeforcipata* but have exceptionally long secondary feet.

Range: This species occurs in rare abundance at all three sites that we examined from the middle Eocene through the late Eocene, uppermost Zone RP14 to the middle of Zone RP19. At all three sites we found a brief discontinuity in the stratigraphic range of *D. ombros* in the lower part of Zone RP16. It is interesting to note that this early gap corresponds to the stratigraphic range of *D. anastasis*.

Phylogeny: Unknown

Dorcadospyris papilio **(Riedel)**
(Pl. **P2,** fig. 7)

Hexaspyris papilio Riedel, 1959, p. 294, pl. 2, figs. 1, 2

Dorcadospyris papilio (Riedel), Riedel and Sanfilippo, 1970, p. 523, pl. 15, fig. 5; Sanfilippo and Nigrini, 1995, p. 278, pl. III, fig. 1

Remarks: This species is very rare to rare in the uppermost part of Zone RP21 through the lower half of Zone RP22. In the lowermost part of its range this species is transitional with forms of *D. praeforcipata* having widely arched primary feet that are separated by something less than the 180° required by the definition of *D. papilio*. The rare variant form of this species noted by Moore (1971, p. 739, pl. 8, fig. 9), having a small shell, arching primary feet, and two tabular feet that branch distally, is found with these transitional *D. praeforcipata* > *D. papilio* forms in uppermost Zone RP21.

Dorcadospyris praeforcipata **Moore**
(Pl. **P2,** figs. 8–13)

Dorcadospyris praeforcipata Moore, 1971, p. 738, pl. 9, figs. 4–7

Remarks: In the original description of this species, Moore (1971) distinguished it from *D. forcipata* primarily by the presence of four to six secondary feet but noted that there was considerable variation in the morphology of *D. praeforcipata*. Some of the smaller, earlier forms might have recurved ends on the primary feet, as well as having relatively short primary and secondary feet (Moore, 1971, p.738, pl. 9, figs. 6, 7). In Leg 199 material, the more diminutive form is found only in the lower part of its range (Pl. **P2,** figs. 8–10), whereas a somewhat larger form is typical of the upper part of its range (Pl. **P2,** fig. 11). In some of the earlier forms stubs of the broken secondary feet are clearly visible (e.g, Pl. **P2,** fig. 8). In others the secondary feet may actually form a more delicate mesh (Pl. **P2,** fig. 9), which is rarely preserved except for a ragged fringe appearing at the base of the cephalis (Pl. **P2,** fig. 10). In moderate to poorly preserved material the more delicate secondary feet may be largely missing except for these remnant "stubs" or a ragged fringe along the basal ring between the primary feet; thus, taken without stratigraphic context, this species may be difficult to distinguish from *D. forcipata*. The species first occurs in the upper part of Zone RP21. In Leg 199 material it is extremely rare or absent in the middle part of Zone RP22 and then returns to its more usual abundance of 2–30 specimens per slide in the upper part of Zone RP22, just after the disappearance of *D. riedeli*. In Leg 199 material *D. praeforcipata* disappears in the middle part of Zone RN2, within the range of *D. simplex* (as defined here) and before the first occurrence of *D. forcipata*. The fairly large variation in the abundance of this species (0–60 specimens/slide) and its disjunct occurrence in Leg 199 material suggest that either the true stratigraphic range of this species is not represented in this material or that the form requires further taxonomic refinement.

Dorcadospyris pseudopapilio **Moore**
(Pl. **P2,** figs. 16, 17)

Dorcadospyris pseudopapilio Moore, 1971, p. 738, pl. 6, figs. 7, 8

Dorcadospyris quadripes **Moore**
(Pl. **P2,** figs. 14, 15)

Dorcadospyris quadripes Moore, 1971, p. 738, pl. 7, figs. 3–5

Remarks: In contrast to the original description of this species, at least some of the *D. quadripes* specimens in Leg 199 material have a broadly arching (>180°) pair of primary feet that arise from the apical part of the cortical shell rather than from the base of the shell (as described by Moore, 1971, p. 738). In this way these forms of *D. quadripes* are similar to *D. riedeli*. However, there are several features that distinguish the two species. In *D. riedeli* the broadly arching

pair of feet always arise from the apical part of the cortical shell and the secondary pair of feet extend from the basal ring at nearly 180° and curve to form a circle or ellipse (sometimes crossing, but usually not joined). *D. riedeli* never has more than four primary feet, whereas *D. quadripes* may have six to eight. The primary feet of *D. quadripes* that are not broadly arching extend from the basal ring at an angle distinctly <180°. They tend to diverge distally and recurve only slightly. The stratigraphic ranges of the two species are different, with *D. quadripes* occurring in Zone RP20 and *D. riedeli* occurring most abundantly, but not exclusively, in the upper part of Zone RP22.

***Dorcadospyris riedeli* Moore**
(Pl. **P2,** figs. 18, 19)

Dorcadospyris riedeli Moore, 1971, p. 739, pl. 9, figs. 1–3

Remarks: See remarks under *Dorcadospyris quadripes*. *D. riedeli* is most abundant in the upper part of Zone RP22; however, rare specimens occur sporadically in Zone RP21 and in Zone RP20. Although part of the cephalis and primary legs are obscured in the illustrated specimen (Pl. **P2,** fig. 18) from the middle part of Zone RP22 and the upper part of the range of *D. riedeli*, many of the distinguishing features of this species can be seen: the high arching pair of primary legs arising from the back side of the cephalis, the other pair of secondary legs diverge widely and curve to form a circle, the small apical horn, and several prominent secondary feet. *D. riedeli* may actually arise from *D. quadripes* in the upper part of Zone RP20.

***Dorcadospyris scambos* Moore and Nigrini n. sp.**
(Pl. **P3,** figs. 1–4)

Brachiospyris simplex Riedel, Goll, 1972, pl. 42, figs. 2, 3

Dorcadospyris sp. cf. *D. ateuchus* Sanfilippo and Nigrini, 1995, pl. 3, fig. 3

Type material: Holotype (Pl. **P3,** fig. 1) from Sample 199-1219B-6H-3, 45–47 cm, from the uppermost part of the upper Oligocene Zone RP21.

Description: Cephalis bilobed, thick-walled lattice shell with slight external sagittal stricture and circular to subcircular pores irregular in size and distribution. In some specimens a small apical horn is present. The primary feet are cylindrical, robust, and convexly curved. The length of the primary feet is quite variable. Two to six secondary feet are commonly present. A very small apical horn is present in about one-quarter of the specimens measured. The specimen illustrated in Plate **P3,** fig. 1, from the uppermost part of Zone RP21, represents one of the smaller forms of this species. It shows one broken secondary foot, but no apical horn, while secondary feet are seen in the larger variety of *D. scambos* (Pl. **P3,** fig. 2) from the lower part of Zone RN1. There are no secondary feet visible on the specimen from the lowermost part of Zone RN3 and in the upper part of the range of this species (Pl. **P3,** fig. 3).

Measurements (based on 31 specimens):
Length of primary feet = 272–615 µm (mean = 470 ± 103 µm);
Width of cephalis = 81–115 µm (mean = 94 ± 12 µm);
Ratio of leg length to cephalis width = 2.45–6.91 (mean = 5.05 ± 1.26).

Etymology: The specific name is derived from the Greek adjective *skambos,* meaning bowlegged.

Distinguishing characteristics: This species was figured by Goll (1972) and ascribed to *Brachiospyris simplex*. Sanfilippo and Nigrini (1995) figured and compared this form to *D. ateuchus*, but noted that its convex feet do not fit the description of *D. ateuchus*. *D. scambos* differs from *D. simplex* in having relatively short primary feet and by the presence of secondary feet and/or a small apical horn in some specimens. See "Remarks" under *D. simplex*. Plate **P3,** figs. 1–4 illustrate the approximate range of leg length and shell robustness observed in this species.

Variability: The length of the primary feet is highly variable, as is the presence of secondary feet. Both the apical horn and the secondary feet, when present, are thin and usually short.

Range: *D. scambos* n. sp. first occurs in Zone RP21. It commonly has abundances of 20–30 specimens per slide in Zone RP22 and occasionally exceeds 50 specimens per slide in lower Zone RN1. It is frequently found in samples up through Zone RN2 and is rare to very rare through Zone RN3. It becomes very rare in its upper range and its uppermost limit is difficult to define in the Leg 199 material because of the relatively poor preservation and frequent reworking of older material.

Phylogeny: The evolutionary relationship of *D. scambos* to other Dorcadospyrids is not clear; however, it probably arose from *D. ateuchus* and may give rise to *D. simplex*.

Dorcadospyris simplex (Riedel) sensu stricto
(Pl. P3, fig. 5)

Brachiospyris simplex Riedel, 1959, p. 293, pl. 1, fig. 10

Dorcadospyris simplex (Riedel), Riedel and Sanfilippo, 1970, p. 523, pl. 15, fig. 6; Moore, 1971, p. 740, pl. 10, figs. 3, 4

Remarks: In this study *D. simplex* is restricted to those forms that closely resemble figure 10 in Riedel (1959) and plate 10, figures 3 and 4 in Moore (1971) with very long, broadly arching feet nearly forming a circle, but not usually crossing or joined at their termination.

Measurements (based on 20 specimens in Leg 199 material):
Length of primary feet of *D. simplex* (as defined here) = 615–810 µm (mean = 702 ± 63 µm)
Width of cephalis = 74–88 µm (mean = 83 ± 4 µm)
Ratio of leg length to cephalis width = 7.41–9.99 (mean = 8.5 ± 0.77)

The stratigraphic range of *D. simplex* is confined to the middle part of Zone RN2.

Dorcadospyris spinosa Moore
(Pl. P3, figs. 13, 14)

Dorcadospyris spinosa Moore, 1971, p. 739, pl. 6, figs. 1, 2

Eucyrtidium diaphanes Sanfilippo and Riedel

Calocyclas coronata Carnevale, 1908, p. 33, pl. 4, fig. 24 (*non Eucyrtidium coronatum* Ehrenberg, 1873)

Eucyrtidium diaphanes Sanfilippo and Riedel, Sanfilippo et al., 1973, p. 221, pl. 5, figs. 12–14 (new name); Sanfilippo and Nigrini, 1995, p. 278, pl. I, figs. 6–11

Remarks: Sanfilippo and Riedel (in Sanfilippo et al., 1973) removed this species from *Calocyclas* because they did not consider it closely related to the type species of that genus (*Calocyclas turris* Ehrenberg) and transferred it to *Eucyrtidium*, not because of any conviction that it was closely related to the type species of that genus (*Lithocampe acuminata* Ehrenberg) but because they had used that name for a number of stichocyrtids of uncertain evolutionary relationships. The transfer of the species to *Eucyrtidium* resulted in Carnevale's specific name becoming a junior secondary homonym of *Eucyrtidium coronatum* Ehrenberg, 1873, and they therefore proposed the new specific name *diaphanes* to be used while the species is included in this genus.

O'Connor (1997b, p. 116), on the contrary, considered the distally closed, four segmented forms he encountered to resemble members assigned to the genus *Stichocorys*, and reinstated Carnevale's original specific name. We prefer to leave this species in the genus *Eucyrtidium* until its evolutionary relationship can be determined. O'Connor's (1997b, pl. 7, fig. 13) single-figured specimen of

"*Stichocorys coronata*" (equivalent to *E. diaphanes*) displays characteristics of both *E. diaphanes* and *E. plesiodiaphanes* (e.g., apical horn is a single spine, but the thoracic wall is thorny). His specimen is from the lower Miocene of New Zealand, whereas we recorded *E. diaphanes* in the tropical lower Miocene and *E. plesiodiaphanes* in the tropical Oligocene with a gap between their ranges. However, the relationship between ranges in middle and low latitudes may account for morphological and stratigraphic differences of this sort.

Eucyrtidium mitodes Nigrini n. sp.
(Pl. **P4,** figs. 2–4)

Type Material: Holotype (Pl. **P4,** fig. 3) from Sample 199-1219A-6H-3, 45–47 cm, in the lowermost Miocene Zone RN1.

Description: Multisegmented shell consisting of cephalis, thorax, and 3–6 post-thoracic segments widening distally and in some specimens becoming triangular in cross section. Cephalis is simple and spherical with a very short, three-bladed apical horn. Thorax is conical with subcircular pores aligned more or less longitudinally. Post-thoracic segments expand distally for two to four segments and then become subcylindrical: subcircular pores aligned longitudinally, much wider than intervening bars. Shell of early specimens is smooth. However, later specimens exhibit signs of dissolution and a somewhat rougher surface. In addition, longitudinal lines, not obviously connected to ribs of any kind, can be seen where the shell has been more resistant to dissolution. Termination is ragged.

Measurements (based on 20 specimens from Cores 199-1218A-10H, 12H, 13H, 14H, and 16H; and 199-1219A-6H, 8H, and 9H):
Maximum length (excluding horn) = 160–225 µm
Length of cephalothorax = 40–50 µm
Maximum breadth = 105–145 µm

Etymology: The species name is derived from the Greek adjective *mitodes,* meaning threadlike, and refers to the multiple dissolution-resistant lines between pore rows running the length of the shell in later specimens.

Distinguishing characteristics: This species is mostly easily recognized when it is partially dissolved, revealing longitudinal lines not connected to ribs of any kind.

Variability: In early forms the longitudinal lines are not readily apparent, but the general shell form is the same as that of later forms that do exhibit longitudinal lines. Early forms tend to have a somewhat larger thorax.

Range: *E. mitodes* n. sp. is present, but generally rare, at Sites 1218, 1219, and 1220 from the upper part of Zone RP20 to the lowermost part of Zone RN1.

Phylogeny: Unknown

Eucyrtidium plesiodiaphanes Sanfilippo
(Pl. **P4,** figs. 11, 12)

Eucyrtidium plesiodiaphanes Sanfilippo in Sanfilippo and Nigrini, 1995, p. 278, pl. 1, figs. 12–14, 16

Artophormis cf. *A. gracilis* in Moore, 1971, p. 742, pl. 5, fig. 12

Remarks: See remarks for *E. diaphanes*.

Eusyringium fistuligerum (Ehrenberg)
(Pl. **P4,** fig. 13)

Eucyrtidium fistuligerum Ehrenberg, 1873, p. 229; 1875, pl. 9, fig. 3

Eusyringium fistuligerum (Ehrenberg), Riedel and Sanfilippo, 1970, p. 527, pl. 8, figs. 8, 9; Sanfilippo and Blome, 2001, p. 212, fig. 9a–9d

Eusyringium lagena (Ehrenberg)

Lithopera lagena Ehrenberg, 1873, p. 241; 1875, pl. 3, fig. 4

Eusyringium lagena (Ehrenberg), Riedel and Sanfilippo, 1970, p. 527, pl. 8, figs. 5–7; Foreman, 1973, p. 436, pl. 11, figs. 4, 5; Sanfilippo et al., 1985, p. 672, fig. 17.2a–17.2c

Giraffospyris lata Goll

Giraffospyris lata Goll, 1969, p. 334, pl. 58, figs. 22, 24–26

Lamptonium fabaeforme chaunothorax Riedel and Sanfilippo

(Pl. **P4,** fig. 5)

Lamptonium (?) *fabaeforme* (?) *chaunothorax* Riedel and Sanfilippo, 1970, p. 524, pl. 5, figs. 8, 9

Remarks: Well-preserved specimens were observed with a massive layer of rough shell material extending upward from the cephalis to cover the base and the proximal part of the horn. The thorax is covered by numerous small spines. The abdomen is a short, inverted, delicate, porous caplike segment; pores are irregular in size and arrangement. This morphological feature has not been previously observed in this subspecies.

Lamptonium fabaeforme constrictum Riedel and Sanfilippo

Lamptonium (?) *fabaeforme* (?) *constrictum* Riedel and Sanfilippo, 1970, p. 523, pl. 5, fig. 7

Lamptonium fabaeforme fabaeforme (Krasheninnikov)

[?] *Cyrtocalpis fabaeformis* Krasheninnikov, 1960, p. 296, pl. 3, fig. 11

Lamptonium (?) *fabaeforme fabaeforme* (Krasheninnikov), Riedel and Sanfilippo, 1970, p. 523, pl. 5, fig. 6; Foreman, 1973, p. 436, pl. 6, figs. 6–9

Lamptonium pennatum Foreman

Lamptonium pennatum Foreman, 1973, p. 436, pl. 6, figs. 3–5; pl. 11, fig. 13

Remarks: Occasional very inflated forms were observed in which the abdomen is in the form of an inverted conical, porous thin-walled closed cap.

Lamptonium sanfilippoae Foreman

Lamptonium sanfilippoae Foreman, 1973, p. 436, pl. 6, figs. 15, 16; pl. 11, figs. 16, 17

Liriospyris longicornuta Goll

(Pl. **P3,** fig. 6)

Liriospyris longicornuta Goll, 1968, p. 1428, pl. 176, figs. 8, 10, 12; text-fig. 9

Liriospyris parkerae Riedel and Sanfilippo

Liriospyris parkerae Riedel and Sanfilippo, 1971, p. 1590, pl. 2C, fig. 15; pl. 5, fig. 4

Liriospyris stauropora (Haeckel)

Trissocyclus stauroporus Haeckel, 1887, p. 987, pl. 83, fig. 5

Liriospyris stauropora (Haeckel), Goll, 1968, p. 1431, pl. 175, figs. 1–3, 7; text-fig. 9; Riedel and Sanfilippo, 1971, pp. 1590, 1591, pl. 2C, figs. 16–19

***Lithochytris archaea* Riedel and Sanfilippo**

Lithochytris archaea Riedel and Sanfilippo 1970, p. 528, pl. 9, fig. 7; 1971, pl. 7, fig. 13; Foreman, 1973, p. 436, pl. 2, figs. 4, 5

***Lithochytris vespertilio* Ehrenberg**

Lithochytris vespertilio Ehrenberg, 1873, p. 239; 1875, pl. 4, fig. 10; Riedel and Sanfilippo, 1971, p. 528, pl. 9, figs. 8, 9

***Lithocyclia angusta* (Riedel)**

Trigonactura? *angusta* Riedel, 1959, p. 292, pl. 1, fig. 6

Lithocyclia angustum (Riedel), Riedel and Sanfilippo, 1970, p. 522, pl. 13, figs. 1, 2

Lithocyclia angusta (Riedel), Sanfilippo and Riedel, 1973, p. 523; Sanfilippo et al., 1985, p. 653, fig. 7.3a–7.3c

***Lithocyclia aristotelis* (Ehrenberg) group**

Astromma aristotelis Ehrenberg, 1847, p. 55, fig. 10

Lithocyclia aristotelis (Ehrenberg) group, Riedel and Sanfilippo, 1970, p. 522, pl. 3, figs. 1, 2

Remarks: We do not include herein the form illustrated by Sanfilippo et al. (1985, fig. 7, 2d), nor do we consider this form to be *L. crux*. The specimen illustrated on Pl. **P1,** fig. 8 is not included in the *L. aristotelis* group concept.

***Lithocyclia crux* Moore**

Lithocyclia crux Moore, 1971, p. 737, pl. 6, fig. 4

***Lithocyclia ocellus* Ehrenberg group**

Lithocyclia ocellus Ehrenberg, 1854, pl. 36, fig. 30; 1873, p. 240; Riedel and Sanfilippo, 1970, p. 522, pl. 5, figs. 1, 2

***Lithopera (Lithopera) neotera* Sanfilippo and Riedel**

Lithopera (Lithopera) neotera Sanfilippo and Riedel, 1970, p. 454, pl. 1, figs. 24–26, 28

***Lithopera (Lithopera) renzae* Sanfilippo and Riedel**

Lithopera (Lithopera) renzae Sanfilippo and Riedel, 1970, p. 454, pl. 1, figs. 21–23, 27

***Lophocyrtis biaurita* (Ehrenberg)**

Eucyrtidium biaurita Ehrenberg, 1873, p. 226; 1875, p. 70, pl. 10, figs. 7, 8

Lophocyrtis biaurita (Ehrenberg), Haeckel, 1887, p. 1411; Cita et al., 1970, p. 404, pl. 2, figs. I–K; Foreman, 1973, p. 442, pl. 8, figs. 23–26

***Lophocyrtis (Cyclampterium) hadra* Riedel and Sanfilippo**

Lophocyrtis hadra Riedel and Sanfilippo, 1986, p. 168, pl. 7, figs. 12–15

Lophocyrtis (Cyclampterium) hadra (Riedel and Sanfilippo), Sanfilippo, 1990, p. 304, pl. I, figs. 11, 12

Lophocyrtis (Cyclampterium) leptetrum **(Sanfilippo and Riedel)**

Cyclampterium? *leptetrum* Sanfilippo and Riedel, 1970, p. 456, pl. 2, figs. 11, 12; Riedel and Sanfilippo, 1978, p. 67, pl. 4, figs. 12, 13; Goll, 1972, p. 958, pl. 22, fig. 1

Lophocyrtis (Cyclampterium) leptetrum (Sanfilippo and Riedel), Sanfilippo, 1990, p. 306, pl. II, figs. 6–9

Lophocyrtis (Cyclampterium) milowi **(Riedel and Sanfilippo)**

Cyclampterium ? *milowi* Riedel and Sanfilippo, 1971, p. 1593, pl. 3B, fig. 3; pl. 7, figs. 8, 9; 1978, p. 67, pl. 4, fig. 14; Ling, 1975, p. 731, pl. 12, fig. 15

Lophocyrtis (Cyclampterium) milowi (Riedel and Sanfilippo), Sanfilippo, 1990, p. 306, pl. I, figs. 13–16; pl. II, figs. 1, 2

Lophocyrtis (Cyclampterium) pegetrum **(Sanfilippo and Riedel)**

Cyclampterium ? *pegetrum* Sanfilippo and Riedel, 1970, p. 456, pl. 2, figs. 8–10; Riedel and Sanfilippo, 1978, p. 68, pl. 4, fig. 16; Goll, 1972, p. 959, pl. 24, figs. 1–4; pl. 25, figs. 1–3

Lophocyrtis (Cyclampterium) pegetrum (Sanfilippo and Riedel), Sanfilippo, 1990, p. 307, pl. II, figs. 3–5

Lophocyrtis (Lophocyrtis) exitelus **Sanfilippo**

Lophocyrtis (Lophocyrtis) exitelus Sanfilippo, 1990, p. 300, pl. 1, figs. 1–4

Lophocyrtis (Lophocyrtis) jacchia **(Ehrenberg)**

Thyrsocyrtis jacchia Ehrenberg, 1873, p. 261; 1875, pl. 12, fig. 7

Lophocyrtis (?) *jacchia* (Ehrenberg), Riedel and Sanfilippo, 1970, p. 530; Riedel and Sanfilippo, 1971, p. 1594, pl. 3C, figs. 4, 5; pl. 7, fig. 16

Lophocyrtis (Lophocyrtis) jacchia (Ehrenberg), Sanfilippo, 1990, p. 302, pl. I, figs. 5–10; pl. III, fig. 6

Lophocyrtis (Sciadiopeplus) oberhaensliae **Sanfilippo**

Lophocyrtis (Sciadiopeplus) oberhaensliae Sanfilippo, 1990, p. 310, pl. II, figs. 10–14

Lychnocanoma amphitrite **Foreman**

Lychnocanoma amphitrite Foreman, 1973, p. 437, pl. 11, fig. 10

Remarks: Foreman (1973, p. 437) raised the subgenus *Lychnocanoma* to the generic level to include two-segmented theoperids with three feet, without accompanying ribs in the thorax, and without a large cephalis. That designation has been followed by a number of workers and is used herein. O'Connor (1997a, p. 77) argued for the reuse of *Lychnocanium* as the generic name for forms formerly placed in *Lychnocanoma*. For an in-depth discussion of *Lychnocanoma/Lychnocanium* see O'Connor (1999, p. 24), who raised questions regarding the validity of the presence of (externally visible) thoracic ribs and the disposition of the feet in all of the forms described by Haeckel (1887) under *Lychnocanium* and its various subgenera.

Lychnocanoma apodora **Sanfilippo**
(Pl. **P4,** fig. 14)

Lychnocanoma apodora Sanfilippo in Sanfilippo and Nigrini, 1995, p. 280, pl. 4, figs. 5–10

Remarks: See remarks for *Lychnocanoma amphitrite*.

Lychnocanoma auxilla Foreman

Lychnocanoma auxilla Foreman, 1973, p. 437, pl. 2, fig. 6; pl. 11, figs. 1, 2

Remarks: See remarks for *Lychnocanoma amphitrite*.

Lychnocanoma babylonis (Clark and Campbell) group

Dictyophimus babylonis Clark and Campbell, 1942, p. 67, pl. 9, figs. 32, 36

Lychnocanoma babylonis (Clark and Campbell) group, Foreman, 1973, p. 437, pl. 2, fig. 1

Remarks: See remarks for *Lychnocanoma amphitrite*.

Lychnocanoma elongata (Vinassa de Regny)

Tetrahedrina elongata Vinassa de Regny, 1900, p. 243, pl. 2, fig. 31

Lychnocanium bipes Riedel, 1959, p. 294, pl. 2, figs. 5, 6

Lychnocanoma elongata (Vinassa de Regny), Sanfilippo et al., 1973, p. 221, pl. 5, figs. 19, 20; Sanfilippo and Nigrini, 1995, p. 282, pl. IV, fig. 11

Remarks: See remarks for *Lychnocanoma amphitrite*. This species varies greatly in its abundance throughout its range, reaching peaks in abundance of >200 specimens per slide in Zones RP22, RN1, RN2, and RN4. The abundance of *L. elongata* is very low in the last 8 m.y. of its range, being absent in a few of the samples before reoccurring briefly.

Lychnocanoma pileus Nishimura

Lychnocanoma (?) *pileus* Nishimura, 1992, p. 344, pl. 6, figs. 7, 8; pl. 13, fig. 5

Remarks: See remarks for *Lychnocanoma amphitrite*.

Lychnocanoma turgidum (Ehrenberg)

(Pl. **P4,** fig. 6)

Lychnocanium turgidum Ehrenberg, 1873, p. 245; 1875, pl. 7, fig. 6

[?] *Lychnocanium pyriforme* Haeckel, 1887, p. 1225, pl. 61, fig. 11

Gen. et sp. indet, Riedel and Sanfilippo, 1970, pl. 8, fig. 10

Lithochytris (Lithochytroides) turgidulum (sic) (Ehrenberg), Petrushevskaya and Kozlova, 1972, p. 552, pl. 27, figs. 8, 9

Lithochytris sp. T, Petrushevskaya and Kozlova, 1972, p. 552, pl. 27, fig. 6

Sethochytris cavipodis O'Connor, 1999, p. 28, pl. 4, figs. 22–27; pl. 7, figs. 24a–27

Remarks: See remarks for *Lychnocanoma amphitrite*. O'Connor (1999) tentatively placed *Lithocytris turgidulum* (*sic*) Petrushevskaya and Kozlova (1972) in synonymy with his new species *Sethochytris cavipodes*. We, however, think that these species are one and the same. Therefore, the specific name *turgidum* takes priority. *Lychnocanoma turgidum* differs from *L. babylonis* group by being larger and more inflated, having shorter feet, and a small aperture no larger than the diameter of two thoracic pores.

Measurements (based on 30 specimens from Cores 199-1218A-24X, 26X, and 28X; 199-1219A-19H and 20H; and 199-1220A-11H):

Length (excluding horn and feet) = 182–255 µm
Length of horn = 8–44 µm
Length of feet when present = 20–101 µm
Maximum breadth of shell = 153–210 µm

***Lychnodictyum audax* Riedel**

Lychnodictyum audax Riedel, 1953, p. 810, pl. 85, fig. 9; Sanfilippo and Riedel, 1974, p. 1022, pl. 2, fig. 8

***Periphaena delta* Sanfilippo and Riedel**

Periphaena delta Sanfilippo and Riedel, 1973, p. 523, pl. 8, figs. 11, 12; pl. 27, figs. 6, 7

***Periphaena tripyramis triangula* (Sutton)**

Phacotriactus triangula Sutton, 1896, p. 61

Periphaena tripyramis triangula (Sutton), Riedel and Sanfilippo, 1970, p. 521, pl. 4, figs. 9, 10; Sanfilippo and Riedel, 1973, p. 523, pl. 9, figs. 7–9

***Phormocyrtis cubensis* (Riedel and Sanfilippo)**

Eucyrtidium cubense Riedel and Sanfilippo, 1971, p. 1594, pl. 7, figs. 10, 11

Phormocyrtis cubensis (Riedel and Sanfilippo), Foreman, 1973, p. 438, pl. 7, figs. 11, 12, 14

***Phormocyrtis striata exquisita* (Kozlova)**

Podocyrtis exquisita Kozlova in Kozlova and Gorbovets, 1966, p. 106, pl. 17, fig. 2

Phormocyrtis striata exquisita (Kozlova), Foreman, 1973, p. 438, pl. 7, figs. 1–4, 7, 8; pl. 12, fig. 5

***Phormocyrtis striata striata* Brandt**

Phormocyrtis striata Brandt in Wetzel, 1935, p. 55, pl. 9, fig. 12; Riedel and Sanfilippo, 1970, p. 532, pl. 10, fig. 7

Phormocyrtis striata striata Brandt, Foreman, 1973, p. 438, pl. 7, figs. 5, 6, 9

***Phormocyrtis turgida* (Krasheninnikov)**

Lithocampe turgida Krasheninnikov, 1960, p. 301, pl. 3, fig. 17

Phormocyrtis turgida (Krasheninnikov), Foreman, 1973, p. 438, pl. 7, fig. 10; pl. 12, fig. 6

***Podocyrtis (Lampterium) chalara* Riedel and Sanfilippo**

Podocyrtis (Lampterium) chalara Riedel and Sanfilippo, 1970, p. 535, pl. 12, figs. 2, 3; Riedel and Sanfilippo, 1978, p. 71, pl. 8, fig. 3; text-fig. 3

***Podocyrtis (Lampterium) fasciolata* (Nigrini)**

Podocyrtis (Podocyrtis) ampla fasciolata Nigrini, 1974, p. 1069, pl. 1K, figs. 1, 2; pl. 4, figs. 2, 3

Podocyrtis (Lampterium) fasciolata (Nigrini), Sanfilippo et al., 1985, p. 697, fig. 30.7

***Podocyrtis (Lampterium) goetheana* (Haeckel)**
(Pl. **P5,** figs. 11, 12)

Cycladophora goetheana Haeckel, 1887, p. 1376, pl. 65, fig. 5

Podocyrtis (Lampterium) goetheana (Haeckel), Riedel and Sanfilippo, 1970, p. 535

Remarks: In the investigated material this species exhibits great variation in the length and breadth of the abdomen and the presence or absence of one to three additional rows of pores distal to the elongated abdominal pores that are separated by long, straight bars.

***Podocyrtis (Lampterium) helenae* Nigrini**

Podocyrtis (Lampterium) helenae Nigrini, 1974, p. 1070, pl. lL, figs. 9–11; pl. 4, figs. 4, 5

***Podocyrtis (Lampterium) mitra* Ehrenberg**

Podocyrtis mitra Ehrenberg, 1854, pl. 36, fig. B20; 1873, p. 251; *non* Ehrenberg, 1875, pl. 15, fig. 4; Riedel and Sanfilippo, 1970, p. 534, pl. 11, figs. 5, 6; 1978, text-fig. 3; Sanfilippo et al., 1985, p. 698, fig. 30.10

***Podocyrtis (Lampterium) sinuosa* Ehrenberg**

Podocyrtis sinuosa Ehrenberg, 1873, p. 253; 1875, pl. 15, fig. 5; Riedel and Sanfilippo, 1970, p. 534, pl. 11, figs. 3, 4; 1978, text-fig. 3; Sanfilippo et al., 1985, p. 698, fig. 30.9

***Podocyrtis (Lampterium) trachodes* Riedel and Sanfilippo**

Podocyrtis (Lampterium) trachodes Riedel and Sanfilippo, 1970, p. 535, pl. 11, fig. 7; pl. 12, fig. 1; Sanfilippo et al., 1985, p. 699, fig. 30.14

***Podocyrtis (Podocyrtis) papalis* Ehrenberg**
(Pl. **P5,** fig. 13)

Podocyrtis papalis Ehrenberg, 1847, p. 55, fig. 2; Riedel and Sanfilippo, 1970, p. 533, pl. 11, fig. 1; Sanfilippo and Riedel, 1973, p. 531, pl. 20, figs. 11–14; pl. 36, figs. 2, 3

Remarks: Highly variable in size. Included are small squat forms and forms with very short abdomens (see illustration in Sanfilippo and Blome, 2001, fig. 10f). Also included are large forms occurring in Holes 1219A and 1220B during the evolutionary transition of *P. (Podocyrtoges) phyxis* to *P. (P.) ampla* at the RP12/RP13 zonal boundary near the top of the stratigraphic range of *P. (Podocyrtoges) diamesa*.

Measurements:
Total length, excluding horn, of large forms = 291–323 µm
Maximum breadth = 157–174 µm
(cf. *papalis* total length, excluding horn = 170 (rarely 150)–280 µm, maximum breadth = 95–140 µm)

***Podocyrtis (Podocyrtoges) ampla* Ehrenberg**

Podocyrtis (?) *ampla* Ehrenberg, 1873, p. 248; 1875, pl. 16, fig. 7

Podocyrtis (Podocyrtis) ampla Ehrenberg, Riedel and Sanfilippo, 1970, p. 533, pl. 12, figs. 7, 8

Podocyrtis (Podocyrtoges) ampla Ehrenberg, Sanfilippo and Riedel, 1992, p. 14, pl. 5, fig. 4

Remarks: *P. (P.) ampla* occurs commonly in all our samples from the lower boundary of Zone RP13 through most of Zone RP14 at Sites 1219 and 1220, the earliest sample from Site 1218 is above the last occurrence of *P. (P.) ampla*.

***Podocyrtis (Podocyrtoges) diamesa* Riedel and Sanfilippo**
(Pl. **P5,** fig. 10)

Podocyrtis (Podocyrtis) diamesa Riedel and Sanfilippo, 1970, p. 533 (*pars*), pl. 12, fig. 4, *non* figs. 5, 6; Sanfilippo and Riedel, 1973, p. 531, pl. 20, figs. 9, 10; pl. 35, figs. 10, 11

Podocyrtis (Podocyrtoges) diamesa Sanfilippo and Riedel, 1992, p. 14

***Podocyrtis (Podocyrtoges) phyxis* (Sanfilippo and Riedel)**

Podocyrtis (Podocyrtis) diamesa Riedel and Sanfilippo, 1970, p. 533, (*pars*), pl. 12, fig. 6

Podocyrtis (Podocyrtis) phyxis Sanfilippo and Riedel, 1973, p. 531

Podocyrtis (Podocyrtoges) phyxis (Sanfilippo and Riedel), Sanfilippo and Riedel, 1992, p. 14

***Podocyrtis (Podocyrtopsis) apeza* Sanfilippo and Riedel**

Podocyrtis (Podocyrtopsis) apeza Sanfilippo and Riedel, 1992, p. 14, pl. 3, figs. 13–15

***Pterocodon ampla* (Brandt)**

Theocyrtis ampla Brandt in Wetzel, 1935, p. 56, pl. 9, figs. 13–15

Pterocodon (?) *ampla* (Brandt), Foreman, 1973, p. 438, pl. 5, figs. 3–5

***Pterocodon anteclinata* Foreman**

Pterocodon (?) *anteclinata* Foreman, 1975, p. 621, pl. 9, figs. 32–34

***Pterocodon tenellus* Foreman**
(Pl. **P4,** figs. 7–10)

Pterocodon (?) *tenellus* Foreman, 1973, p. 439, pl. 5, fig. 7; pl. 12, fig. 4; Sanfilippo and Blome, 2001, p. 217, pl. 10, figs. e, j–n

Remarks: As noted by Sanfilippo and Blome (2001), this species is quite variable especially in its size and number of segments. In the distalmost part of the specimens illustrated on Plate **P4,** figs. 8, 9, two internal strictures separate additional postabdominal segments that are only one pore row in height.

***Pteropilium* sp. aff. *Pterocanium contiguum* (Ehrenberg)**
(Pl. **P5,** fig. 2)

?*Pterocanium contiguum* Ehrenberg, 1873, p. 255; 1875, pl. 17, fig. 7

Pteropilium? sp. aff. *Pterocanium contiguum* Petrushevskaya and Kozlova, 1972, pl. 29, figs. 8–10

Pteropilium sp. O'Connor, 1999, p. 36, pl. 9, fig. 39

***Rhopalocanium ornatum* Ehrenberg**
(Pl. **P4,** figs. 15, 16)

Rhopalocanium ornatum Ehrenberg, 1847, fig. 3; 1854, pl. 36, fig. 9; 1873, p. 256; 1875, pl. 17, fig. 8; Foreman, 1973, p. 439, pl. 2, figs. 8–10; pl. 12, fig. 3

Remarks: The forms encountered herein range from well developed with robust, long horns and feet to forms with atrophied feet and horns. Rare forms were seen with the inverted conical abdomen closed distally, lacking feet and with the horn reduced to a thickened hyaline structure completely enclosing the cephalis (Pl. **P4,** fig. 16).

***Sethochytris triconiscus* Haeckel**

[?] *Sethochytris triconiscus* Haeckel, 1887, p. 1239, pl. 57, fig. 13; Riedel and Sanfilippo, 1970, p. 528, pl. 9, figs. 5, 6; Sanfilippo et al., 1985, p. 680, fig. 22.1a–22.1d

***Spirocyrtis subtilis* Petrushevskaya**
(Pl. P6, fig. 7)

Spirocyrtis subtilis Petrushevskaya in Petrushevskaya and Kozlova, 1972, p. 540, pl. 24, figs. 22–24; Nigrini, 1977, p. 260, pl. 3, fig. 3

Spirocyrtis proboscis O'Connor, 1994, p. 341, pl. 2, figs. 1-4; pl. 3, figs. 13-16

Remarks: We are fairly certain that the form described by O'Connor (1994) as *S. proboscis* is synonymous with *S. subtilis*, but note that the upper limit of the species is younger in our material than that reported by O'Connor.

***Spongatractus balbis* Sanfilippo and Riedel**

Spongatractus balbis Sanfilippo and Riedel, 1973, p. 518, pl. 2, figs. 1–3; pl. 25, figs. 1, 2

Remarks: The presence of *S. balbis* and its evolutionary transition to *S. pachystylus* is difficult to document due to a combination of heavy development of the spongy meshwork on *S. balbis* and the effects of dissolution that make it difficult to distinguish the two taxa from each other.

***Spongatractus pachystylus* (Ehrenberg)**

Spongosphaera pachystyla Ehrenberg, 1873, p. 256; 1875, pl. 26, fig. 3

Spongatractus pachystylus (Ehrenberg), Sanfilippo and Riedel, 1973, p. 519, pl. 2, figs. 4–6; pl. 25, fig. 3

Remarks: See remarks for *S. balbis*.

***Stichocorys delmontensis* (Campbell and Clark)**

Eucyrtidium delmontense Campbell and Clark, 1944, p. 56, pl. 7, figs. 19, 20

Stichocorys delmontensis (Campbell and Clark), Sanfilippo and Riedel, 1970, p. 451, pl. 1, fig. 9 (with synonymy)

***Stichocorys wolffii* Haeckel**

Stichocorys wolffii Haeckel, 1887, p. 1479, pl. 80, fig. 10; Riedel, 1957, p. 92, pl. 4, figs. 6, 7

Stichocorys baerii Haeckel, 1887, p. 1479, pl. 80, fig. 8

Stichocorys mulleri Haeckel, 1887, p. 1480

***Theocorys anaclasta* Riedel and Sanfilippo**

Theocorys anaclasta Riedel and Sanfilippo, 1970, p. 530, pl. 10, figs. 2, 3; 1978, p. 76, pl. 1, figs. 6–8; Sanfilippo et al., 1985, p. 683, fig. 24.1a–24.1d

***Theocorys puriri* O'Connor**
(Pl. P4, figs. 17, 18)

Theocorys puriri O'Connor, 1997a, p. 88, pl. 4, figs. 5–8; pl. 10, figs. 5–8; pl. 11, fig. 7

Remarks: In an earlier publication (Sanfilippo and Nigrini, 1998) we included this form in our tabulation of *T. spongoconus* and illustrated it as such. Herein we separate it from *T. spongoconus* of Kling (1971). Although it is rare, it is such a distinctive and easily recognizable form that we think it may be stratigraphically useful.

***Theocorys spongoconus* Kling**
(Pl. P4, figs. 19–21)

Theocorys spongoconus Kling, 1971, p. 1087, pl. 5, fig. 6

Remarks: In our tabulation of this species we include forms with spongy abdomens, such as that illustrated by Kling, and forms with less spongy abdomens. The less spongy forms tend to be early in the range of the species, but may reflect dissolution rather than an evolutionary trend.

Theocotyle conica Foreman

Theocotyle (Theocotyle) cryptocephala (?) *conica* Foreman, 1973, p. 440, pl. 4, fig. 11; pl. 12, figs. 19, 20

Theocotyle conica Foreman, Sanfilippo and Riedel, 1982, p. 177, pl. 2, fig. 13

Theocotyle cryptocephala (Ehrenberg)

[?] *Eucyrtidium cryptocephalum* Ehrenberg, 1873, p. 227; 1875, pl. 11, fig. 11

Theocotyle cryptocephala (Ehrenberg), Sanfilippo and Riedel, 1982, p. 178, pl. 2, figs. 4–7

Theocotyle nigriniae Riedel and Sanfilippo

Theocotyle cryptocephala (?) *nigriniae* Riedel and Sanfilippo, 1970, p. 525, pl. 6, fig. 5 (*non* 6)

Theocotyle nigriniae Riedel and Sanfilippo, Sanfilippo and Riedel, 1982, p. 178, pl. 2, figs. 1–3

Theocotyle venezuelensis Riedel and Sanfilippo

Theocotyle venezuelensis Riedel and Sanfilippo, 1970, p. 525, pl. 6, figs. 9, 10; pl. 7, figs. 1, 2; Sanfilippo and Riedel, 1982, p. 179, pl. 2, figs. 8–12

Theocotylissa alpha Foreman

Theocotyle (Theocotylissa) alpha Foreman, 1973, p. 441, pl. 4, figs. 13–15 (*non* 14); pl. 12, fig. 16; Foreman, 1975, p. 621

Theocotylissa alpha Foreman, Sanfilippo and Riedel, 1982, p. 179, pl. 2, figs. 16, 17

Theocotylissa ficus (Ehrenberg)

(Pl. **P5,** fig. 1)

Eucyrtidium ficus Ehrenberg 1873, p. 228; 1875, pl. 11, fig. 19

Theocotylissa ficus (Ehrenberg), Sanfilippo and Riedel, 1982, p. 180, pl. 2, figs. 19, 20

Remarks: Near the top of the range of this species we observed rare specimens with a distinct lumbar stricture, large abdominal pores, and a fourth, inverted caplike segment covering the distal aperture. This segment has a thinner wall than the abdomen with subcircular pores that are irregular in size and arrangement. The first observed occurrence of *T. ficus* in Hole 1218A in Zone RP15 between Samples 199-1218A-27X-CC and 28X-2, 46–48 cm, is not the true bottom. In other locations the first evolutionary occurrence of this species is known to be in Zone RP8.

Theocotylissa fimbria Foreman

Theocotyle (Theocotylissa) (?) *fimbria* Foreman, 1973, p. 441, pl. 5, figs. 1, 2; pl. 12, fig. 21

Theocotylissa fimbria Foreman, Sanfilippo and Riedel, 1982, p. 181, pl. 12, fig. 18

Theocyrtis annosa **(Riedel)**
(Pl. **P5,** fig. 14)

Phormocyrtis annosa Riedel, 1959, p. 295, pl. 2, fig. 7

Calocycletta annosa (Riedel), Petrushevskaya and Kozlova, 1972, p. 544

Theocyrtis annosa (Riedel), Riedel and Sanfilippo, 1970, p. 535, pl. 15, fig. 9; Sanfilippo et al., 1985, p. 701, fig. 32.2a, 32.2b; Sanfilippo and Nigrini, 1995, p. 282, pl. IV, figs. 1–4

Theocyrtis careotuberosa **Nigrini and Sanfilippo n. sp.**
(Pl. **P5,** figs. 15–18)

Theocyrtis tuberosa Riedel, Riedel and Sanfilippo, 1970, pl. 13, figs. 9, 10

Theocyrtis sp. aff. *T. tuberosa* Riedel, Riedel and Sanfilippo, 1971, pl. 3D, figs. 16–18

Theocyrtis tuberosa Sanfilippo et al., 1985, figs. 32.1a, 32.1b; Saunders et al., 1985, pl. 5, fig. 10 (only)

Type material: Holotype (Pl. **P5,** fig. 15) from Sample 199-1219A-18H-6, 45–47 cm, in the upper Eocene Zone RP17.

Description: Three-segmented pterocorythid with a robust, generally smooth subspherical thorax and a cylindrical abdomen with an undifferentiated termination. The long porous cephalis, sometimes open apically, bears a broad-based three-bladed horn. The apical opening is often surrounded by one to three short spines. The closed cephalis appears to have a hyaline cap and a corona of short spines, or a single short spine opposite the apical spine. Thick-walled thorax with closely spaced circular pores arranged hexagonally with a tendency to longitudinal alignment. Plicae extend from the base of the horn to the collar region, giving the cephalis and the collar region a puckered look. These plicae, separating two to six rows of pores, progressively become more developed to cover the entire thorax and frequently extend onto the abdomen. Development of plicae across the lumbar stricture is a good distinguishing characteristic to separate this taxon from co-occurring *Calocycletta anekathen*. The lumbar stricture is not marked on the external contour. The abdomen is cylindrical in the lumbar region and tapers distally. The wall is somewhat thinner than that of the thorax, with subcircular pores arranged in longitudinal rows. For a discussion of the thoracic wall see discussion below for *T. tuberosa*.

Measurements (based on 40 specimens from Cores 199-1218A-25X; 199-1218C-18X, 199-1219A-17H and 19H; and 199-1220A-8H and 10H):
Maximum length (excluding horn) = 153–242 µm
Length of cephalothorax = 101–182 µm
Length of abdomen = 32–101 µm
Length of horn = 24–100 µm
Breadth of cephalis = 32–49 µm
Breadth of thorax = 101–158 µm
Breadth of abdomen = 93–150 µm

Etymology: The species name is taken from the Latin adjective *caritus,* meaning devoid of, referring to its lack of tubercules, in combination with *tuberosa*.

Distinguishing characteristics: This species is distinguished from its descendant *T. tuberosa* by not having a tuberculate surface on the thorax and from its ancestor *T. perpumila* by having a longer horn that is always three-bladed, a longer cephalis where the paired lobes are well separated from the top of the cephalis and are less pronouncedly marked on the external contour, and a tendency to have plicae on the abdomen and across the lumbar stricture.

Variability: There is considerable variability in the degree of ornamentation surrounding the base of the apical horn, and the cephalis may be open apically

or closed by a hyaline cap. In our material the abdomen is usually severely truncated.

Range: *T. careotuberosa* n. sp. is commonly present at Sites 1218, 1219, 1220 and has been found at other tropical localities of late Eocene and early Oligocene age (i.e., upper part of Zone RP16 into the early part of Zone RP20).

Phylogeny: *T. careotuberosa* is a member of the lineage leading from *T. perpumila* to *T. annosa*.

***Theocyrtis perpumila* Sanfilippo n. sp.**
(Pl. **P5,** figs. 19–22)

Theocyrtis sp. Sanfilippo and Riedel, 1992, pl. 1, fig. 23 (only); (see also same reference, pl. 1, figs. 20–22)

Type material: Holotype (Pl. **P5,** fig. 21) from Sample 199-1219A-21H-6, 45–47 cm, in the upper middle Eocene Zone RP15.

Description: Three-segmented pterocorythid with plicae and tubercles extending from the cephalis to the surface of the thorax and abdomen. The thick wall, especially in the early part of the range, appears transversely "puckered" rather than longitudinally tuberculate. The broad-based horn is bladed proximally and commonly conical distally. The cephalis is compressed longitudinally with a short eucephalic lobe and laterally placed paired lobes. Cephalis has numerous small subcircular pores commonly obscured by the thick plicate surface. Thorax is subhemispherical with circular to subcircular pores arranged hexagonally. The thoracic wall is thick, especially in the proximal part where a concentration of plicae and tubercles make the external contour appear angular. Abdomen has an undifferentiated termination, approximately cylindrical, thinner walled than the thorax, with subcircular to circular pores. Early in the range the pores are irregular in size and arrangement, while in later forms they are more regular in size tending to longitudinal alignment.

Measurements (based on 35 specimens from Cores 199-1218A-26X and 28X; 199-1219A-19H and 23H: 199-1220A-10H and 11H; and 199-1220B-9H):
Maximum length (excluding horn) = 133–242 µm
Length of cephalothorax = 93–137 µm (usually 129 µm)
Length of abdomen = 36–133 µm
Length of horn = 48–101 µm
Breadth of cephalis = 40–61 µm
Breadth of thorax = 101–141 µm
Breadth of abdomen = 93–137 µm

Etymology: The species name is taken from the Latin adjective *pumilus,* meaning dwarfish or little, in combination with *per,* meaning very.

Distinguishing characteristics: *Theocyrtis perpumila* n. sp. is distinguished from the ancestral *Albatrossidium* stock by developing plicae in the cephalic and collar region, and from *T. careotuberosa* by being compressed longitudinally, having a short cephalis with laterally placed paired lobes, and a less robust horn that is conical distally.

Variability: The most notable variation in this thick-walled, puckered form is the thickness of the wall and the degree of development of the tubercules that, to some extent, may depend on the state of preservation.

Range: This species is common in the middle middle Eocene through the early part of the late Eocene, ranging from lower Zone RP14 into Zone RP18.

Phylogeny: *T. perpumila* is the earliest member of the *Theocyrtis* lineage leading from *T. perpumila* to *T. annosa*.

Theocyrtis perysinos **Nigrini and Sanfilippo n. sp.**
(Pl. P6, figs. 1, 2)

Theocyrtis annosa (Riedel) in Sanfilippo and Nigrini, 1995, pl. IV, figs. 2, 3 (only); Moore, 1971, pl. 7, fig. 6 (only)

Type material: Holotype (Pl. P6, fig. 1) from Sample 199-1218A-17H-6, 45–47 cm, in the upper Oligocene Zone RP21.

Description: Large thin-walled three-segmented shell with a strong, three-bladed apical horn. Cephalis is trilobate with lateral lobes beneath the main cephalic lobe and covered with small subcircular pores. Thorax is inflated campanulate with subcircular pores aligned longitudinally. Very delicate, irregularly spaced, discontinuous plicae are present but not expressed on the external contour. There are no strong plicae as in *T. annosa*. Lumbar stricture is a gentle indentation. Abdomen is cylindrical with subcircular pores aligned more or less longitudinally, increasing in size distally. The abdomen is somewhat constricted halfway down its length, this being the level at which the pores change in size and where breakage occurs. Plicae are sometimes present on abdomen. Termination is ragged or with small, hyaline, triangular lamellar teeth irregularly placed along the margin.

Measurements (based on 20 specimens from Cores 199-1220A-5H and 6H; 199-1220B-2H; and 199-1219A-11H and 12H):
Maximum length (excluding horn) = 170–250 µm
Length of cephalothorax = 120–130 µm
Length of abdomen = 115–130 µm
Length of horn = 50–90 µm
Breadth of cephalis = 40–45 µm
Breadth of thorax = 120–130 µm
Breadth of abdomen = 115–130 µm

Etymology: The species name is taken from the Greek adjective *perysinos,* meaning of last year.

Distinguishing characteristics: This species is distinguished from *T. annosa* by its lack of externally prominent plicae on both the thorax and abdomen. It is distinguished from species of *Albatrossidium* by the presence of delicate plicae on both the thorax and the abdomen.

Variability: The abdomen is frequently broken off about midway down its length, but when complete shows some variation in the termination, from ragged to smooth with several small triangular teeth.

Range: *T. perysinos* n. sp. is rare in Oligocene material from Sites 1218, 1219, and 1220 and has a short range from the upper part of Zone RP20 to the lower part of Zone RP21.

Phylogeny: Possible ancestor of *Theocyrtis annosa.*

Theocyrtis setanios **Nigrini and Sanfilippo n. sp.**
(Pl. P6, figs. 3–5)

Calocycletta acanthocephala (Ehrenberg), Johnson, 1974, p. 550, pl. 6, fig. 3

Theocyrtis annosa (Riedel), Sanfilippo and Nigrini, 1995, pl. IV, fig. 4 (only)

Type material: Holotype (Pl. P6, fig. 4) from Sample 199-1218A-17H-2, 48–50 cm, in the upper Oligocene Zone RP21.

Description: Small three-segmented shell with a strong three-bladed apical horn. Cephalis is trilobate with lateral lobes beneath the main cephalic lobe and covered with small subcircular pores. Thorax is thick walled, smooth, inflated, and conical with subcircular pores aligned longitudinally. There is, at least, the appearance of plicae between the longitudinal pore rows. There is no indentation at lumbar stricture. The abdomen tapers distally and is less robust

than the thorax and thus is often truncated or missing. Abdominal pores are subcircular in longitudinal rows; termination is ragged.

Measurements (based on 20 specimens from Cores 199-1220A-5H and 6H; 199-1219A-12H and 13H; and 199-1218A-16X):

Maximum length (excluding horn) = 140–195 µm
Length of cephalothorax = 105–130 µm
Length of horn = 65–90 µm
Breadth of cephalis = 30–40 µm
Breadth of thorax = 105–130 µm
Breadth of abdomen = 90–120 µm

Etymology: The species name is taken from the Greek adjective *setanios,* meaning of this year.

Distinguishing characteristics: *Theocyrtis setanios* n. sp. is distinguished from *T. annosa* by not having distinct plicae that are expressed on the external contour and by its smaller size. It is distinguished from *T. perysinos* by its size and the marked difference in the thickness of the shell wall of the robust thick-walled thorax and the more delicate abdomen, and from *T. careotuberosa* by its simpler cephalic structure and lack of additional spines around the apical horn. The apical horn is well developed, usually one-third to one-half the length of the shell.

Variability: This species varies very little over its short stratigraphic range. Variation in the total length of the shell is determined almost entirely by the length of the abdomen, which is often missing. Rarely, the apical horn is short, being about the same length as the cephalis.

Range: Generally rare to moderately rare over a short range from the uppermost part of Zone RP20 to the lowermost part of Zone RP21.

Phylogeny: Probably part of the lineage between *T. tuberosa* and *T. annosa*, but details are unknown.

Remarks: It seems likely that this form is the same as that recorded by Holdsworth (1975, p. 532), but in order to be sure, it would be necessary to examine his material.

Theocyrtis tuberosa Riedel, emend. Sanfilippo et al.

(Pl. P6, fig. 6)

Theocyrtis tuberosa Riedel, 1959, p. 298, pl. 2, figs. 10, 11; Sanfilippo et al., 1985, p. 701, fig. 32.1a–32.1d

Remarks: Forms lacking pronounced tubercles on the thorax were excluded from the original species description (Riedel, 1959). Subsequently, Riedel and Sanfilippo (1970) included forms with less pronounced tubercules (p. 535, pl. 13, figs. 9, 10). In 1971, Riedel and Sanfilippo recognized that there was an evolutionary sequence between forms in which the thoracic wall is smooth or plicate (and occasionally slightly tuberose). They defined the evolutionary lower limit of *T. tuberosa* as the level at which tuberose specimens (pl. 3D, figs. 14, 15) predominate over those that are not tuberose (*Theocyrtis* sp. aff. *T. tuberosa,* pl. 3D, figs. 16–18). Sanfilippo et al. (1985) emended the definition of *T. tuberosa* to include the less tuberose forms and illustrated them as early *T. tuberosa* (fig. 32.1a, 32.1b), because of the difficulty of satisfactorily separating "pronounced" from less pronounced tubercles.

The quality of the Leg 199 material allowed us to recognize the evolutionary sequence between more (*T. tuberosa*) and less (*T. careotuberosa* n. sp.) pronounced tubercules. Although we recognize that there are some intermediate forms, we found it to be biostratigraphically useful to distinguish between the two forms.

Thyrsocyrtis (Pentalacorys) krooni Sanfilippo and Blome

Thyrsocyrtis tetracantha (Ehrenberg), Riedel and Sanfilippo, 1970, p. 527 (*partim*); Riedel and Sanfilippo, 1978, p. 81 (*partim*), pl. 10, fig. 9

Thyrsocyrtis (Pentalacorys) tetracantha (Ehrenberg), Sanfilippo and Riedel, 1982, p. 176 (in part), pl. 1, fig. 11; Sanfilippo et al., 1985, p. 690 (*partim*), fig. 26.8b

Thyrsocyrtis (Pentalacorys) krooni Sanfilippo and Blome, 2001, p. 207, fig. 7a–7e

Thyrsocyrtis (Pentalacorys) lochites Sanfilippo and Riedel

Thyrsocyrtis (Pentalacorys) lochites Sanfilippo and Riedel, 1982, p. 175, pl. 1, fig. 13; pl. 3, figs. 5–9

Remarks: Rare thick-walled forms with tubercles on the thorax and/or abdomen were observed in the early part of its range at the three investigated sites.

Thyrsocyrtis (Pentalacorys) orthotenes Sanfilippo n. sp.

(Pl. **P5,** figs. 3–5)

Thyrsocyrtis sp. Petrushevskaya and Kozlova, 1972, pl. 34, fig. 5

Type material: Holotype (Pl. **P5,** fig. 5) from Sample 199-1219A-19H-1, 45–47 cm, in the upper middle Eocene to upper Eocene Zone RP17.

Description: Three-segmented shell in which the large-pored abdomen forms the major part. Cephalis is subspherical, poreless or with a few small pores, bearing a cylindrical to elongate cylindroconical horn of variable length and thickness. Collar stricture distinct. Thorax is shorter than the abdomen, broadly conical to inflated conical, with small subcircular pores. Lumbar stricture is distinct. Abdomen is thick walled with 2–7 large subcircular pores longitudinally, with a rough and occasionally very thorny surface. Descending from a distinct peristome are three cylindrical straight feet of variable thickness with simple or ragged terminations, rarely forked.

Measurements (based on 40 specimens from Cores 199-1218A-25X and 27X; 199-1219A-18H, 20H, and 23H; 199-1220A-10H and 12H; and 199-1220B-10H and 11H):

Total length (excluding horn) = 263–424 µm
Length of cephalothorax = 68–105 µm
Length of abdomen = 109–182 µm
Length of horn (usually broken) = >133 µm
Maximum breadth of thorax = 85–117 µm
Breadth of abdomen = 145–194 µm
Number of abdominal pores (along its length) = 2–7
Number of pores on half the abdominal circumference = 3–11

Etymology: The species name is derived from the Greek adjective *orthotenes,* meaning stretched out straight.

Distinguishing characteristics: *Thyrsocyrtis (Pentalacorys) orthotenes* n. sp. is similar to *T. (P.) triacantha* and *T. (P.) tensa* and is distinguished from both by having straight feet.

Variability: Thorax varies from broadly conical to slightly inflated, decreasing in size in later forms. The number of pores on the thick-walled abdomen varies from 7–10 on a half circumference (in early forms) to 4–6 (in late forms), and the three cylindrical feet are variable in length and thickness.

Range: *T. (P.) orthotenes* has a longer stratigraphic range than previously noted for *T. (P.) tensa* and occurs in moderate abundance, occasionally outnumbering *T. (P.) triacantha* in the middle to late part of its range. At Sites 1219 and 1220 the last occurrence of *T. (P.) orthotenes* is just above the lower boundary of Zone RP17; at Site 1218 the upper limit of this species is somewhat higher in

the lower part of the Zone RP18, well below the last occurrence of *T. (P.) triacantha* in Zone RP20.

Phylogeny: The morphology of *T. (P.) orthotenes* is intermediate between *T. (P.) tensa* and *T. (P.) triacantha* if one considers the development of the three cylindrical feet from slightly curved with convexity inward (*tensa*) to curved with convexity outward (*triacantha*). Throughout its range in the middle Eocene, which is parallel with that of *T. (P.) triacantha*, it mimics the morphological variations of *T. (P.) triacantha*. The range of *orthotenes* is not consistent with the idea of it being the transitional form between *tensa* and *triacantha*. It is desirable, therefore, to erect a new species to document the various species that make up the *Thyrsocyrtis* lineage We consider *T. (P.) orthotenes* to be part of the evolutionary lineage of the subgenus *Pentalacorys* leading from *T. (P.) tensa* via *T. (P.) triacantha* to *T. (P.) tetracantha*. Both *triacantha* and *orthotenes* may have evolved from *tensa* or *orthotenes* could simply be an offshoot of *triacantha*.

Thyrsocyrtis (Pentalacorys) tensa Foreman, emend. herein Sanfilippo

Thyrsocyrtis hirsuta tensa Foreman, 1973, p. 442, pl. 3, figs. 13–16; pl. 12, fig. 8

Thyrsocyrtis (Pentalacorys) tensa Foreman, Sanfilippo and Riedel, 1982, p. 176, pl. 1, figs. 6, 7; pl. 3, figs. 1, 2

Remarks: In order to erect the new species *T. (P.) orthotenes*, it is necessary to restrict Foreman's definition of *T. (P.) tensa* to forms having feet that are curved with convexity inward.

Thyrsocyrtis (Pentalacorys) tetracantha (Ehrenberg)

Podocyrtis tetracantha Ehrenberg, 1873, p. 254; 1875, pl. 13, fig. 2

Thyrsocyrtis (Pentalacorys) tetracantha (Ehrenberg), Sanfilippo and Riedel, 1982, p. 176, pl. 1, figs. 11, 12; pl. 3, fig. 10

Thyrsocyrtis (Pentalacorys) triacantha (Ehrenberg)

Podocyrtis triacantha Ehrenberg, 1873, p. 254; 1875, pl. 13, fig. 4

Thyrsocyrtis (Pentalacorys) triacantha (Ehrenberg), Sanfilippo and Riedel, 1982, p. 176, pl. 1, figs. 8–10; pl. 3, figs. 3, 4

Thyrsocyrtis (Thyrsocyrtis) bromia Ehrenberg

Thyrsocyrtis bromia Ehrenberg, 1873, p. 260; 1875, pl. 12, fig. 2; Sanfilippo and Riedel, 1982, p. 172, pl. 1, figs. 17–20

Thyrsocyrtis (Thyrsocyrtis) hirsuta (Krasheninnikov)

Podocyrtis hirsutus Krasheninnikov, 1960, p. 300, pl. 3, fig. 16

Thyrsocyrtis (Thyrsocyrtis) hirsuta (Krasheninnikov), Sanfilippo and Riedel, 1982, p. 173, pl. 1, figs. 3, 4

Thyrsocyrtis (Thyrsocyrtis) rhizodon Ehrenberg

Thyrsocyrtis rhizodon Ehrenberg, 1873, p. 262; 1875, p. 94, pl. 12, fig. 1; Sanfilippo and Riedel, 1982, p. 173, pl. 1, figs. 14–16; pl. 3, figs. 12–17

Thyrsocyrtis (Thyrsocyrtis) robusta Riedel and Sanfilippo

Thyrsocyrtis hirsuta robusta Riedel and Sanfilippo, 1970, p. 526, pl. 8, fig. 1

Thyrsocyrtis (Thyrsocyrtis) robusta Riedel and Sanfilippo, Sanfilippo and Riedel, 1982, p. 174, pl. 1, fig. 5

Remarks: The abdominal segment is variable in size and the degree to which it is inflated. The length of the horn and feet, as well as the curvature of the feet, also display great variability.

Tristylospyris triceros **(Ehrenberg)**
(Pl. **P3,** figs. 7, 8)

Ceratospyris triceros Ehrenberg, 1873, p. 220; 1875, pl. 21, fig. 5

Tristylospyris triceros (Ehrenberg), Haeckel, 1887, p. 1033; Riedel, 1959, p. 292, pl. 1, figs. 7, 8; Sanfilippo et al., 1985, p. 665, fig. 10.3a, 10.3b

Remarks: This species is used in a restricted sense herein to include only forms bearing three cylindrical primary feet varying from slightly divergent to semicircularly curved, and three or more secondary feet that are shorter, varying in form from cylindroconical to thin lamellar. See also remarks for *Dorcadospyris copelata*.

Zealithapium anoectum **(Riedel and Sanfilippo)**

Lithapium anoectum Riedel and Sanfilippo, 1973, p. 516, pl. 24, figs. 6, 7

Zealithapium anoectum (Riedel and Sanfilippo), O'Connor, 1999, p. 5

Remarks: In sediments from Zone RP16 through the lower part of Zone RP19 in the three investigated sites we found sporadically a similar larger form with less regularly arranged pores, a rough to spiny surface, and often long spines projecting from the distal third of the shell (Pl. **P1,** figs. 1–4). We recorded the presence of this form using the notation "cf." It may be closely related to *Zealithapium oamaru* O'Connor, 1999, p. 5, pl. 2, figs. 6–11; pl. 5, figs. 29a–32.

Zealithapium mitra **(Ehrenberg)**

Cornutella mitra Ehrenberg, 1873, p. 221; 1875, pl. 2, fig. 8

Lithapium (?) *mitra* (Ehrenberg), Riedel and Sanfilippo, 1970, p. 520, pl. 4, figs. 6, 7

Zealithapium mitra (Riedel and Sanfilippo), O'Connor, 1999, pp. 5, 6, pl. 9, fig. 47

Zealithapium plegmacantha **(Riedel and Sanfilippo)**

Lithapium (?) *plegmacantha* Riedel and Sanfilippo, 1970, p. 520, pl. 4, figs. 2, 3

Zealithapium plegmacantha (Riedel and Sanfilippo), O'Connor, 1999, p. 5

Zygocircus cimelium **Petrushevskaya**
(Pl. **P3,** figs. 9–12)

Zygocircus cimelium Petrushevskaya in Petrushevskaya and Kozlova, 1972, p. 534, pl. 41, figs. 5, 6

Remarks: When the sagittal ring is complete, it is large and quite variable in size and shape. The arch in the five specimens observed by Petrushevskaya and Kozlova (1972) is smooth and without edges. In the Leg 199 material the lower half of the sagittal ring except for the median bar is commonly three-bladed in cross section with one of the blades directed outwardly while the upper half remains smooth and circular in cross section. The front of the ring, in the sense of Goll (1979), is generally broadly curved. The simple vertical spine arises near the midpoint of the sagittal ring height. Rare specimens may have numerous short spicules, intricate bifurcating spines, or spines terminating in spathilla, projecting from the sagittal ring. These short spines are irregular in number and position. In the upper part of some specimens remnants of thin, branching apophyses are observed reaching from the front to the back of the sagittal ring (Pl. **P3,** figs. 9, 11).

Measurements (based on 30 specimens from Cores 199-1218A-26X and 27X; 199-1219A-20H; 199-1220A-10H; and 199-1220B-9H):

Height of sagittal ring = 234–848 µm
Width of sagittal ring = 121–606 µm
Length of median bar = 20–40 µm (usually 28 µm)

Range: Due to their large size and fragility, complete specimens are rare. Their distinctiveness and high abundance is of value as a biostratigraphic marker in the late middle Eocene from Zone RP13 to Zone RP16, where broken sagittal rings are easily recognizable.

Figure F1. Magnetic susceptibility (MS) of cores from Site 1218 correlated with the MS of piston core EW9709-7P taken in the site survey area for Site 1218 (2.25 km south of Site 1218). Measurements for Site 1218 were made on the multisensor track (MST) on board the *JOIDES Resolution* (red line). MS measurements for piston core EW9709-7P were made on an MST at the Oregon State University Core Laboratory (dashed green line). Core EW9709-7P is ~15.6 m long and in this correlation its depth scale was expanded to match that of Site 1218. These correlations were checked against gamma ray attenuation density measurements and radiolarian stratigraphy in the recovered sections. Both sections are plotted vs. revised meters composite depth in Site 1218. Vertical solid line = upper limit of reliable radiolarian stratigraphy at Site 1218, vertical dashed line = upper limit of reliable radiolarian stratigraphy in piston core EW9709-7P.

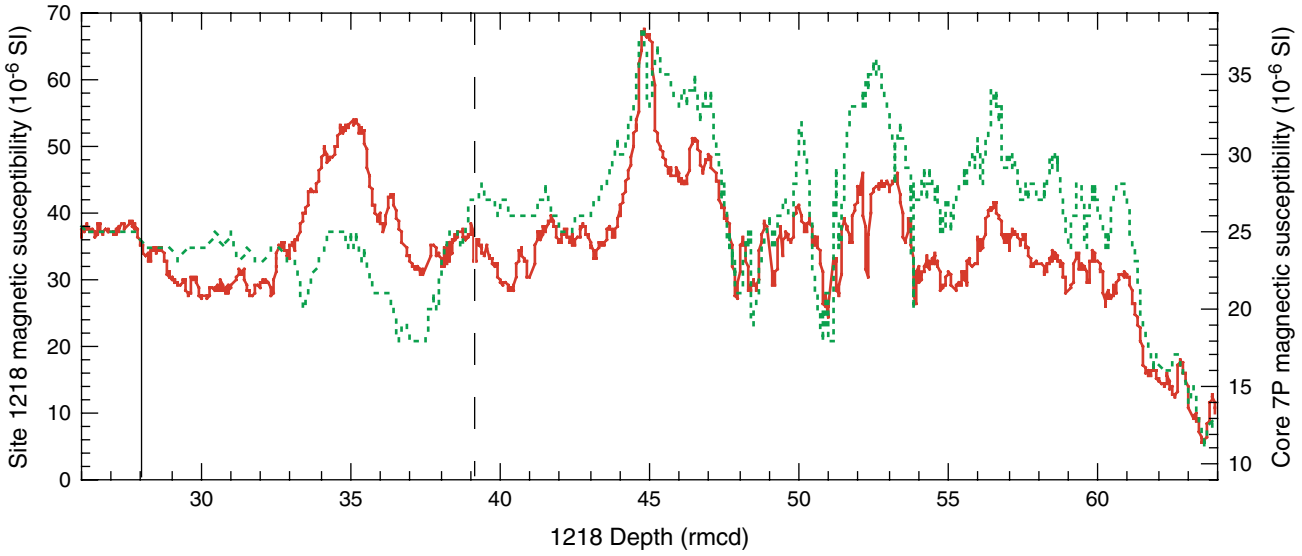

Figure F2. Magnetic susceptibility (MS) of cores from Site 1219 correlated with the MS of piston core EW9709-12P taken in the site survey area for Site 1219 (2.47 km southeast of Site 1219). Measurements for Site 1219 were made on the multisensor track (MST) on board the *JOIDES Resolution* (red line). MS measurements for piston core EW9709-12P were made on an MST at the Oregon State University Core Laboratory (dashed green line). Core EW9709-12P is ~12.7 m long and in this correlation its depth scale was expanded to match that of Site 1219. These correlations were checked against gamma ray attenuation density measurements and radiolarian stratigraphy in the recovered sections. Both sections are plotted vs. revised meters composite depth in Site 1219. Vertical solid line = upper limit of reliable radiolarian stratigraphy at Site 1219, vertical dashed line = upper limit of reliable radiolarian stratigraphy in piston core EW9709-12P.

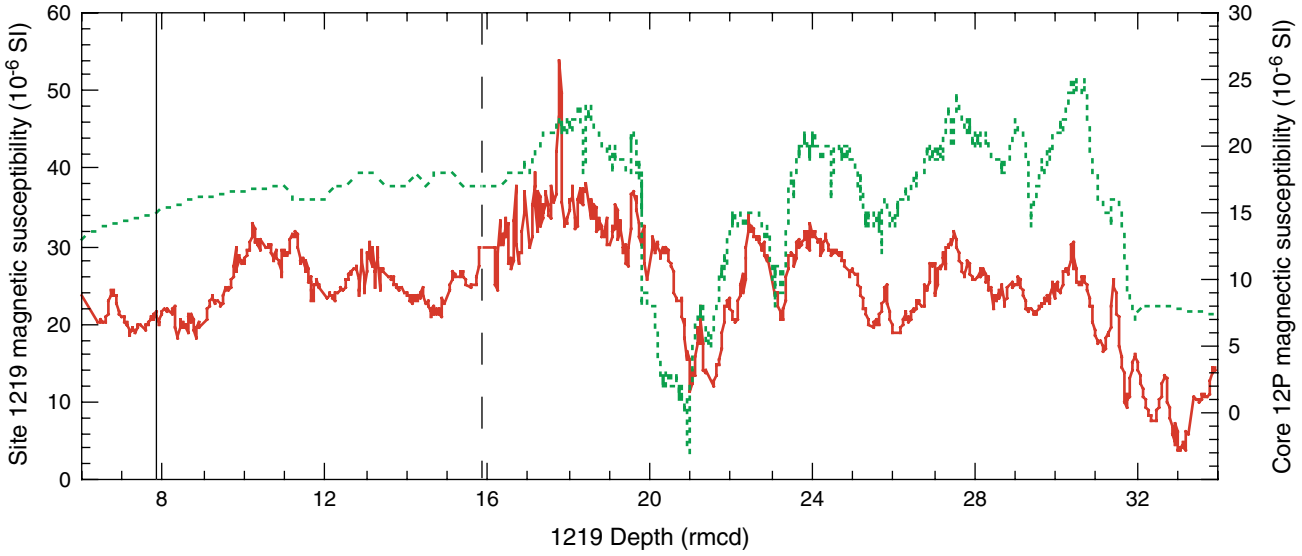

Figure F3. Correlation chart for the interval 11.7–52.6 Ma showing the position of radiolarian datums (from Table T7, p. 70). Bold type and arrows indicate those datums that define the radiolarian zonal boundaries. Paleomagnetic chrons and zonal boundaries for calcareous nannofossils and foraminifers are primarily from Berggren et al. (1995), with adjustments cited in Shipboard Scientific Party (2002a). Radiolarian zonal boundaries have been adjusted to match the new ages for the defining datums presented here. T = event top, B = event bottom, bold = zonal marker. (Continued on next three pages.)

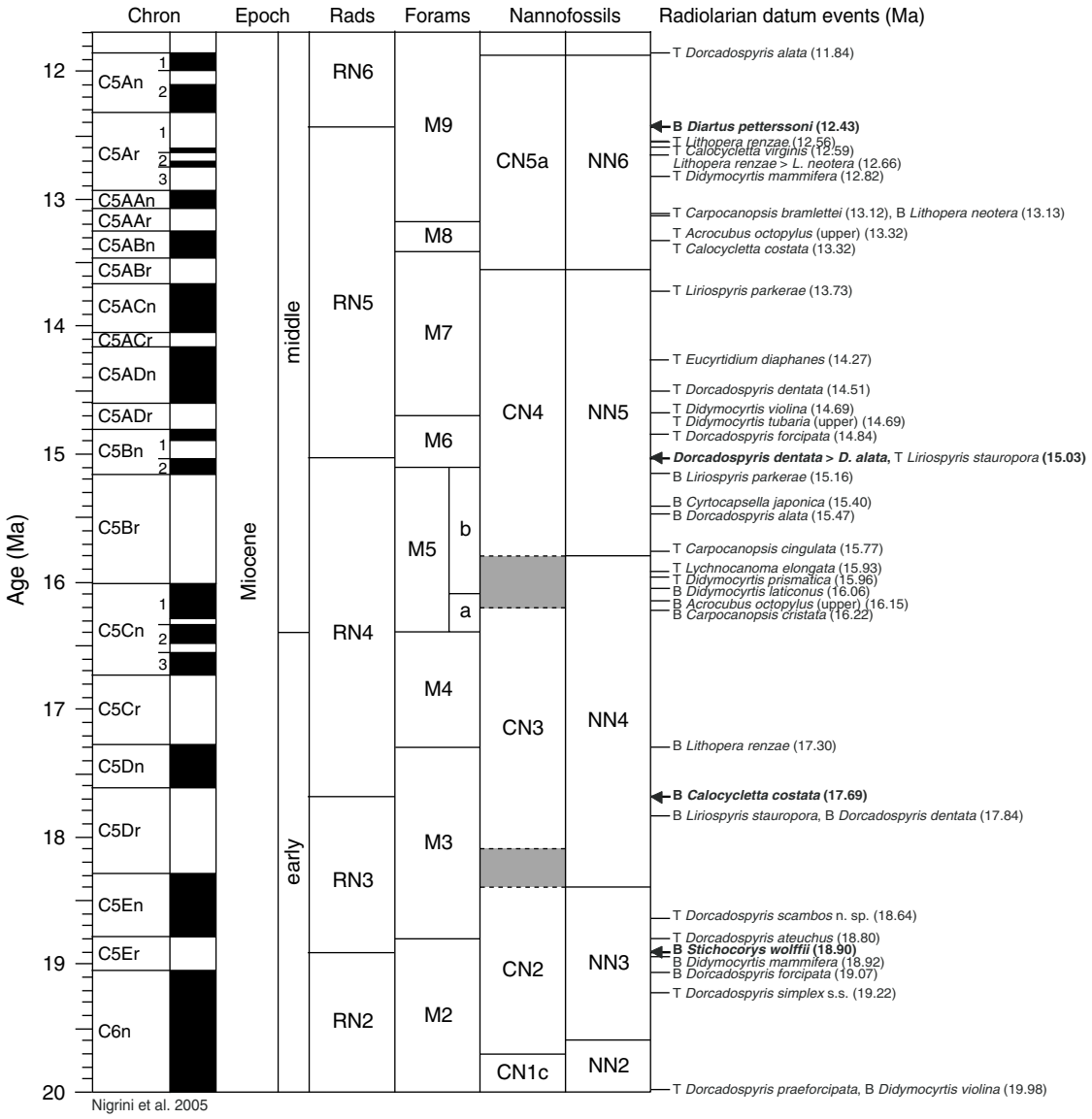

Figure F3 (continued).

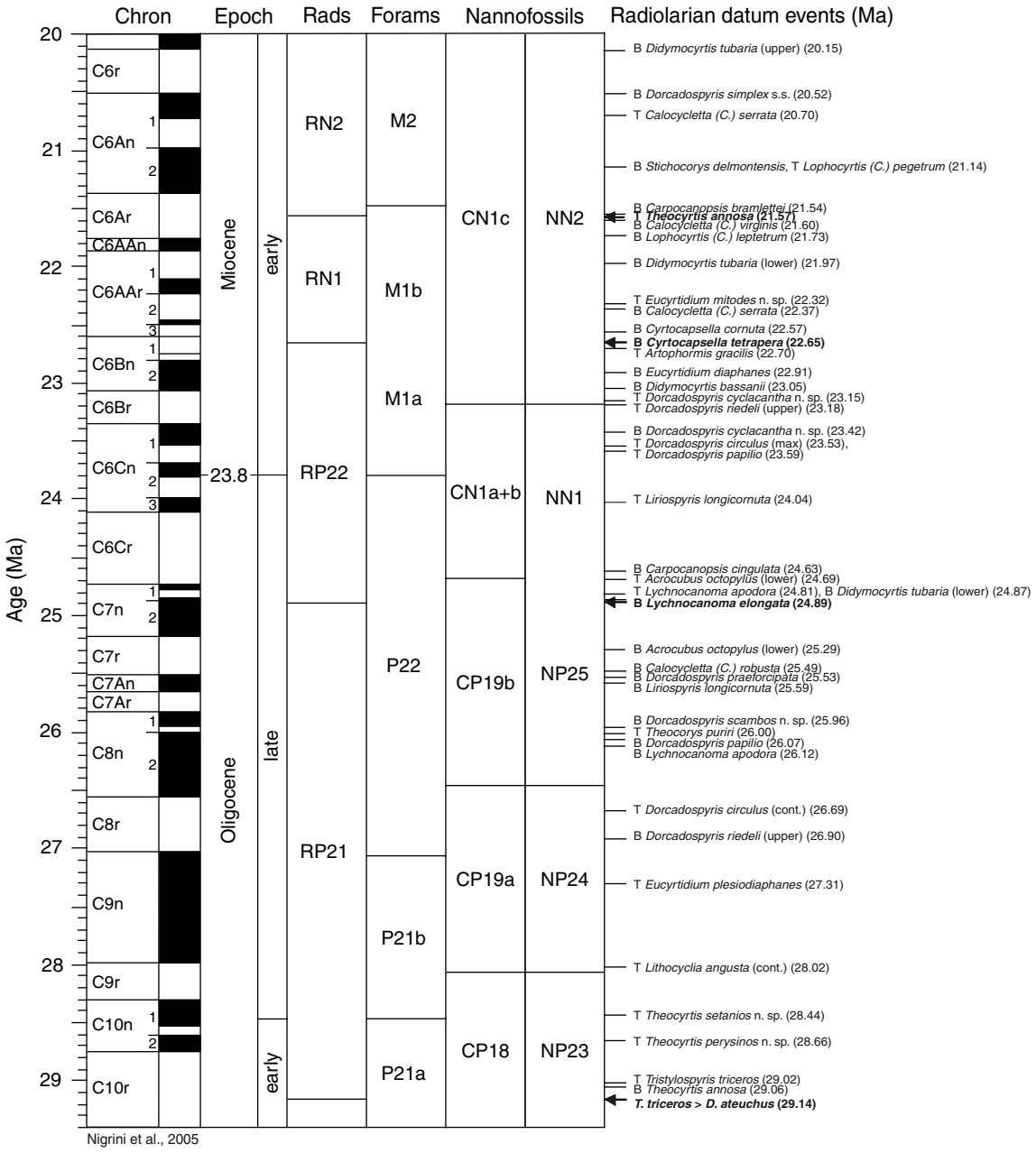

Figure F3 (continued).

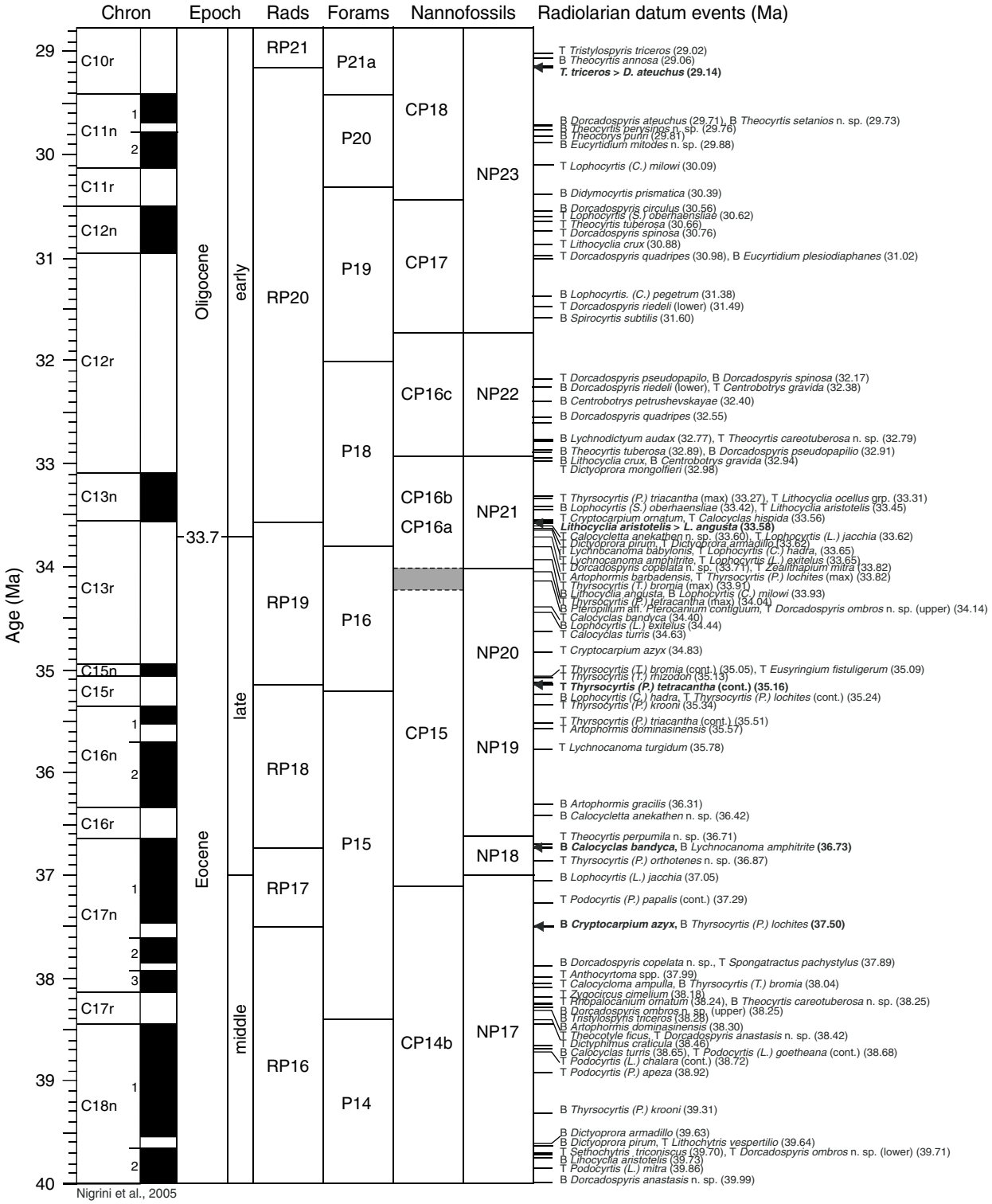

Figure F3 (continued).

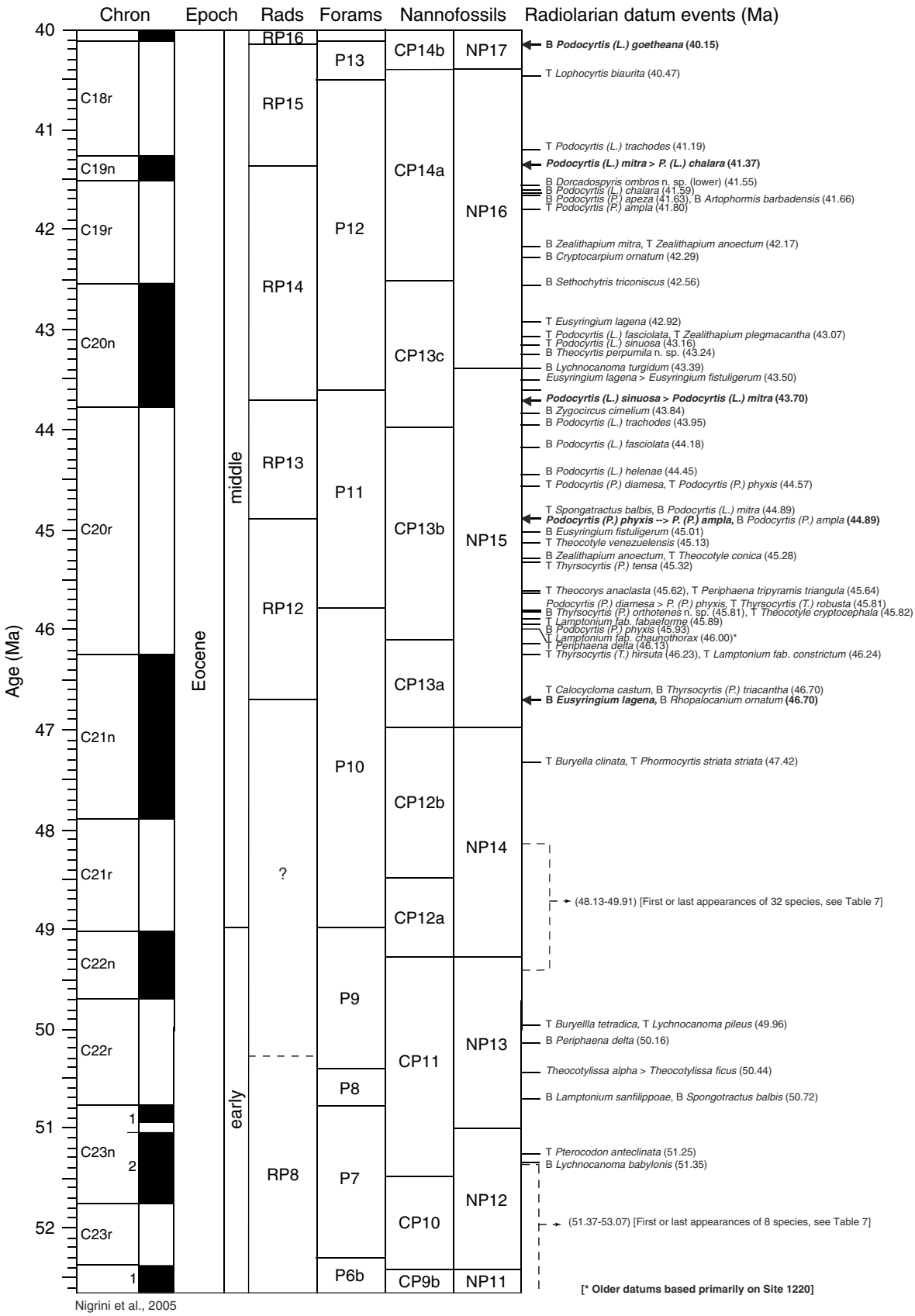

Table T1. Range chart of stratigraphically important taxa arranged alphabetically, Site 1218. (This table is available in an **oversized format.**)

Table T2. Range chart of stratigraphically important taxa arranged alphabetically, Site 1219. (This table is available in an **oversized format.**)

Table T3. Range chart of stratigraphically important taxa arranged alphabetically, Site 1220. (This table is available in an **oversized format.**)

Table T4. Range chart for piston core EW9709-7P of stratigraphically important taxa arranged alphabetically.

Core	Depth (mbsf)	Depth relative to Site 1218 (rcmd)	Abundance	Preservation	Zone (Sanfilippo and Nigrini, 1998)	Age (Ma)	*Acrocubus octopylus*	*Calocycletta (Calocycletta) robusta*	*Calocycletta (Calocycletta) virginis*	*Calocycletta (Calocyclior) caepa*	*Calocycletta (Calocyclissima) costata*	*Carpocanopsis bramlettei*	*Carpocanopsis cingulata*	*Carpocanopsis cristata*	*Cyrtocapsella cornuta*	*Cyrtocapsella japonica*	*Cyrtocapsella tetrapera*	*Diartus hughesi*	*Diartus petterssoni*	*Didymocyrtis bassanii*	*Didymocyrtis laticonus*	*Didymocyrtis mammifera*	*Didymocyrtis prismatica*	*Didymocyrtis tubaria*	*Didymocyrtis violina*	*Dorcadospyris alata*	*Dorcadospyris ateuchus*	*Dorcadospyris dentata*	*Dorcadospyris forcipata*	*Dorcadospyris scambos* n. sp.	*Eucyrtidium diaphanes*	*Liriospyris parkerae*	*Liriospyris stauropora*	*Lithopera (Lithopera) neotera*	*Lithopera (Lithopera) renzae*	*Lychnocanoma elongata*	*Stichocorys delmontensis*	*Stichocorys wolffii*
EW9709-7P	4.01	39.15	C	M	RN6	12.07	(+)		(VR)	R	(VR)			VR	F	VR	VR	–	VR		F	–				VR				–			VR	–	–	R	VR
	4.51	41.54	F	P–M		12.80	(+)		(VR)	R	(VR)	–		VR	F	VR	VR				F	VR				VR		–	(+)	(VR)	–		VR	VR	–	F	VR
	5.01	43.59	C	P	RN5	13.49	–		R	R	R	VR		VR	F	VR	VR				F	VR				VR		–	(+)	–	–	–	–	VR	–	F	VR
	6.01	47.16	F	P		15.01	F		R	–	C	VR		VR	VR	–	VR				R	–		–	–	VR		VR	+	VR	VR	–	–	–	–	–	F	R
	6.51	47.83	C	M		15.21	F		F	+	F	VR	–	VR	F	+	VR			–	F	R		VR	VR	VR		R	VR		R	–	R		+	–	F	F
	7.01	48.90	C	P–M		15.45	F	(+)	F	–	F	VR	–	VR	F	–	VR			–	R	R		VR	VR	VR		R	VR		R	–	VR		+	–	F	F
	7.51	49.91	C	P–M		15.68	F		F		F	VR	–	VR	F	–	VR			–	R	F	–	+	VR	–		R	VR		R		VR		+	–	F	F
	8.01	50.88	C	P–M		15.90	F		F		F	VR	VR	VR	F	–	R			–	VR	F	–	VR	VR	–		R	VR		R		VR		+	–	F	R
	8.51	51.24	C	P–M		15.99	F		F		F	VR	R	VR	R	–	VR			+	VR	F	+	VR	VR			R	VR	(+)	F		+		–	+	F	F
	9.01	51.90	C	P–M	RN4	16.16	–		F		F	VR	R	VR	F	–	VR			+	–	F	VR	VR	VR			R	VR	(+)	F		–		VR	+	F	F
	9.51	52.71	C	P–M		16.50	–		C		F	VR	R	–	R	–	VR			–		F	–	VR	VR			R	VR		F		VR		VR	–	F	F
	10.01	53.51	C	P–M		16.78	–		C		F	VR	R	–	R		VR			–		F	–	R	VR			VR	VR		R		VR		VR	VR	R	F
	10.51	54.41	C	P–M		17.02		–	F		R	VR	R	–	F		VR			–		F	+	R	VR			VR	VR		R		VR		VR	R	R	F
	11.01	55.17	C	M		17.22		–	F		VR	VR	R	–	F		VR			–		F	+	R	VR			R	VR	–	R		–		VR	F	R	F
	11.51	55.82	C	M		17.48		+	F		VR	VR	R		F		VR			–		F	VR	R	VR			R	VR	–	R		R		–	R	R	F
	12.01	56.39	C	P–M		17.73		+	F		VR	VR	VR		F		VR			–		F	+	R	+			VR	VR	+	R		VR			+	R	F
	12.51	56.98	F	P		17.92		VR	F		?	VR	VR		F		VR			–		R	+	VR	–		(+)	+	R	VR	R		–		VR	VR	F
	13.01	57.82	C	P–M		18.19		VR	F		?	VR	VR		F		VR			–		R	VR	VR	VR			+	R	VR	R		?		VR	R	F
	13.51	58.70	C	P–M	RN3	18.46		VR	F		–	VR	VR		F		VR			–		VR	VR	VR	+			–	R	VR	R		–		VR	R	F
	14.01	59.70	C	P–M		18.78		VR	F		–	VR	VR		F		VR			+		VR	+	VR	VR			–	R	VR	R				VR	R	R
	14.51	60.53	C	P–M		18.86		VR	F			VR	VR		F		VR			VR		VR	VR	VR	VR		+		VR	VR	R				+	F	VR
	15.01	61.99	C	P–M	RN2	19.01		VR	F			VR	VR		F		VR			+			VR	VR	+		VR		VR	VR	R				–	R	–
	15.51	64.00	C	P–M		19.21		VR	F			VR	VR		F		VR			VR			VR	R	VR		VR		?	VR	R				R	R	–

Notes: Total abundance: A = abundant, C = common, F = few, R = rare, VR = very rare, B = barren. Preservation: G = good, M = moderate, P = poor. Species abundance estimates: P = present but no abundance estimated, A = abundant (>10%), C = common (>1%–10%), F = few (0.5%–1%), VF = very few (0.1%–0.5%), MR = moderately rare (0.05%–0.1%), R = rare (0.01%–0.05%), VR = very rare (2 specimens), + = 1 specimen, – = looked for but not found. Symbols in parentheses = suspected reworking; cf = a similar but undescribed form (see text). Individual ranges are highlighted; red bars = first and last occurrences of a species. Ages are from **Pälike et al.** (this volume).

Table T5. Range chart for piston EW9709-12P of stratigraphically important taxa arranged alphabetically.

Core	Depth (mbsf)	Depth relative to Site 1218 (rcmd)	Abundance	Preservation	Zone (Sanfilippo and Nigrini, 1998)	Age (Ma)	*Acrocubus octopylus*	*Calocycletta (Calocycletta) robusta*	*Calocycletta (Calocycletta) virginis*	*Calocycletta (Calocyclior) caepa*	*Calocycletta (Calocyclissima) costata*	*Carpocanopsis bramlettei*	*Carpocanopsis cingulata*	*Carpocanopsis cristata*	*Cyrtocapsella cornuta*	*Cyrtocapsella japonica*	*Cyrtocapsella tetrapera*	*Diartus hughesi*	*Diartus petterssoni*	*Didymocyrtis bassanii*	*Didymocyrtis laticonus*	*Didymocyrtis mammifera*	*Didymocyrtis prismatica*	*Didymocyrtis tubaria*	*Didymocyrtis violina*	*Dorcadospyris alata*	*Dorcadospyris ateuchus*	*Dorcadospyris dentata*	*Dorcadospyris forcipata*	*Dorcadospyris scambos* n. sp.	*Eucyrtidium diaphanes*	*Liriospyris parkerae*	*Liriospyris stauropora*	*Lithopera (Lithopera) neotera*	*Lithopera (Lithopera) renzae*	*Lychnocanoma elongata*	*Stichocorys delmontensis*	*Stichocorys wolffii*
EW9709–12P	0.51	42.02	F	P		12.93	–		–	–	–	–		–	VR	–	–	–	–		–	–				VR				–	–		–	–		–	–
	1.01	44.78	F	P–M		13.99	R		C	VR	VR	VR		VR	F	–	VR	–	–	R	R	R		–	–	VR				–	–		–	–	(+)	F	R
	1.51	45.63	C	M–G	RN5	14.41	R		C	VR	R	VR		VR	F	VR	R			–	F	R		–	–	VR		–		VR	VR	–	–	VR		F	F
	2.01	46.12	C	M		14.65	F		C	R	R	VR		VR	F	VR	R			–	R	R		VR	VR	R		–	–	R	R	(VR)	–	R		R	F
	2.51	46.65	C	P–M		14.81	F		C	VR	F	VR		VR	F	VR	R			+	F	R		VR	VR	R		VR	–	VR	VR	–	–	VR		F	R
	3.01	46.84	C	P–M		14.89	F		C	VR	F	VR		VR	F	VR	R			VR	F	R		+	+	R		VR	VR	VR	R	R		VR		F	F
	3.51	47.18	C	M–G		15.03	F		C	R	F	VR		VR	R	VR	R			VR	R	R	–	VR	VR	VR		R	VR		VR	VR	R	R		F	F
	4.01	47.58	C	M–G		15.16	F		C	VR	F	VR		VR	F	VR	R			VR	R	R	–	VR	VR	VR		VR	VR		R	VR	R	VR		F	R
	4.51	48.11	C	M–G		15.27	F		C	VR	F	VR	–	–	F	VR	R			VR	R	R	–	VR	R	VR		R	VR		R	–	R	VR		F	R
	5.01	49.49	C	M–G		15.59	F		C	VR	F	VR	–	VR	F	–	R			VR	R	R	–	R	R	–		R	VR		R	–	VR	VR		F	R
	5.51	50.70	C	M		15.88	R		C	VR	F	VR	VR	VR	F	–	VR			VR	VR	R	–	VR	VR			R	VR		VR		VR	VR	–	F	VR
	6.01	51.48	C	M		16.01	VR		C	VR	R	VR	VR	VR	F	–	R			–	VR	R	+	R	R			R	R		VR		VR	VR	VR	F	VR
	6.51	51.78	C	M	RN4	16.15	VR		C	?	R	VR	VR	–	F	–	R			VR	–	R	VR	VR	R			R	R		VR		R	VR	+	F	R
	7.01	52.23	C	M–G		16.30	–		C	–	R	VR	VR	–	F	–	VR			+	–	VR	VR	R	R			R	VR		VR		F	VR	–	F	R
	7.51	53.10	C	M–G		16.62			C	–	R	VR	VR		F	–	VR			VR	–	VR	VR	R	R			R	VR		VR		R	VR	+	F	R
	8.01	53.69	C	M–G		16.81			C		R	VR	VR		F		VR			–		VR	VR	R	VR			R	VR		R		R	VR	R	F	R
	8.51	54.32	C	M–G		16.98		–	C		R	VR	VR		F		VR			VR		VR	VR	R	VR			R	VR		VR		R	+	R	F	R
	9.01	55.08	C	M–G		17.18		–	C		R	VR	R		F		VR			–		VR	VR	R	VR			R	VR	–	VR		R	VR	R	F	R
	9.51	55.80	C	M–G		17.46		VR	C		VR	VR	R		F		R			–		VR	VR	R	VR			R	VR	–	VR		R	–	VR	F	F
	10.01	56.67	C	M		17.81		VR	C		–	VR	R		F		R			–		VR	VR	R	VR			VR	R	–	VR		VR	–	VR	F	C
	10.51	57.62	C	M–G		18.10		F	F		–	VR	R		F		R			+		VR	VR	R	VR			–	R	+	VR		–		R	F	C
	11.01	58.49	C	M–G	RN3	18.35		F	C			VR	R		F		R			VR		VR	VR	R	VR		–		R	+	VR		–		VR	F	C
	11.51	59.46	C	M		18.69		R	F			VR	R		F		R			VR		VR	VR	R	VR		–		R	+	VR				VR	F	F
	12.01	60.57	C	M–G		18.87		R	R			VR	R		F		R			VR		VR	VR	R	VR		+		R	VR	VR				VR	F	R
	12.51	61.58	C	M	RN2	18.97		R	R			VR	R		F		VR			VR		–	VR	R	VR		VR		VR	VR	VR				VR	F	–

Notes: Total abundance: A = abundant, C = common, F = few, R = rare, VR = very rare, B = barren. Preservation: G = good, M = moderate, P = poor. Species abundance estimates: P = present but no abundance estimated, A = abundant (>10%), C = common (>1%–10%), F = few (0.5%–1%), VF = very few (0.1%–0.5%), MR = moderately rare (0.05%–0.1%), R = rare (0.01%–0.05%), VR = very rare (2 specimens), + = 1 specimen, – = looked for but not found. Symbols in parentheses = suspected reworking; cf = a similar but undescribed form (see text). Individual ranges are highlighted; red bars = first and last occurrences of a species. Ages are from **Pälike et al.** (this volume).

Table T6. Chronological list of radiolarian events (morphological first and last occurrences and evolutionary transitions) in Sites 1218, Site 1218 in combination with piston core EW9709-7P, Site 1219, Site 1219 in combination with piston core EW9709-12P, and Site 1220. (This table is available in an **oversized format.**)

Table T7. Average age (and error) for each biostratigraphic datum in Sites 1218 (in combination with EW9709-7P), 1219 (in combination with EW9709-12P), and 1220 and mean age (and error) for the entire data set. (This table is available in an **oversized format.**)

Plate P1. Codes after sample descriptions are slide designation and England Finder coordinates, respectively. Scale bars: Figs. 5–7 = 50 µm, Figs. 1–4, 8–20 = 100 µm. **1–4.** *Zealithapium* cf. *Z. anoectum* (Riedel and Sanfilippo) (Sample 199-1219A-19H-4, 45–47 cm); (1) Cs.1, N11/0; (2) M23/0; (3) Cs.2, J19/4; (4) R32/3. **5.** *Didymocyrtis bassanii* (Carnevale) (Sample 199-1219A-6H-2, 45–47 cm), W32/2. **6, 7.** *Didymocyrtis tubaria* (Haeckel) (Sample 199-1219A-6H-7, 45–47 cm); (6) B41/0; (7) EW9709-12P, 12.01 m, O12/0. **8.** *Lithocyclia*? sp. (Sample 199-1219A-16H-7, 45–47 cm), Sl.SIO, J25/0. **9.** *Acrocubus octopylus* Haeckel (Sample 199-1218A-11H-7, 45–47 cm), G24/1. **10.** *Dorcadospyris alata* (Riedel), (EW9709-12P, 2.01 m), N10/2. **11, 12.** *Dorcadospyris anastasis* Sanfilippo n. sp.; (11) Sample 199-1219A-20H-4, 45–47 cm (Cs.1, R22/4); (12) Holotype (Sample 199-1218A-26X-6, 45–47 cm), Cs.1, V27/4. **13–15.** *Dorcadospyris ateuchus* (Ehrenberg); (13) Sample 199-1219A-12H-4, 45–47 cm (R21/2); (14) Sample 199-1219A-16H-7, 45–47 cm (Sl.SIO, X7/0); (15) Sample 199-1219A-8H-4, 45–47 cm (P20/0). **16.** *Dorcadospyris circulus* (Haeckel) (Sample 199-1219A-12H-4, 45–47 cm), F28/4. **17, 18.** *Dorcadospyris cyclacantha* Moore n. sp.; (17) Sample 199-1219A-6H-7, 45–47 cm (Q33/1); (18) Holotype (Sample 199-1219A-6H-7, 45–47 cm), K46/2. **19, 20.** *Dorcadospyris copelata* Sanfilippo n. sp.; (19) Holotype (Sample 199-1219A-17H-CC), Cs.2, C6/3; (20) Sample 199-1219A-18H-1, 45–47 cm (Cs.2, B24/1).

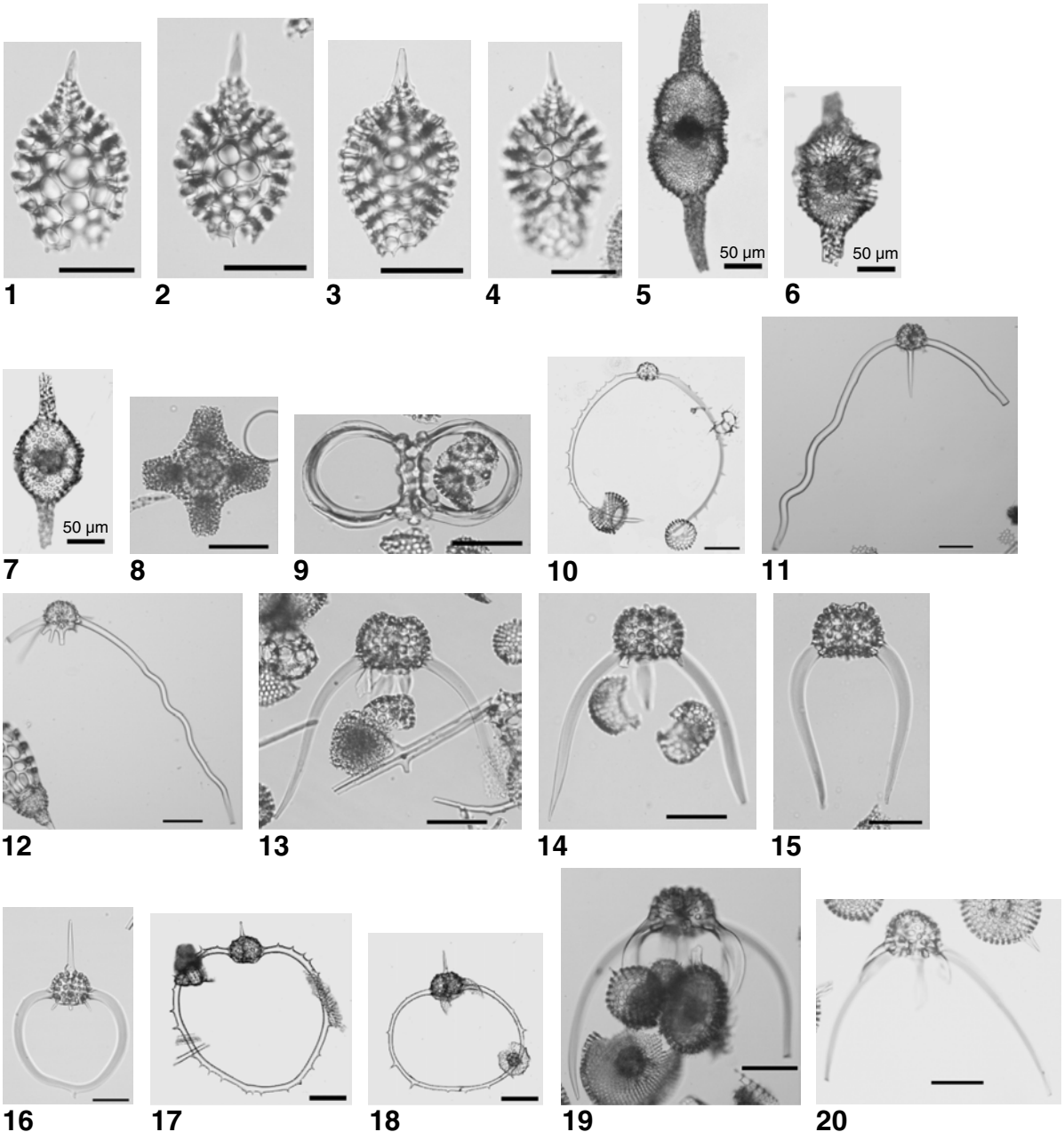

Plate P2. Codes after sample descriptions are slide designation and England Finder coordinates, respectively. Scale bars = 100 µm. **1, 2.** *Dorcadospyris copelata* Sanfilippo n. sp.; (1) basal view (Sample 199-1219A-17H-CC), Cs.2, W41/4; (2) Sample 199-1219A-17H-6, 45–47 cm (Cs.2, L30/0). **3.** *Dorcadospyris dentata* Haeckel, EW9709-7P, 11.51 m, Q23/0. **4.** *Dorcadospyris forcipata* (Haeckel), EW9709-12P, 12.01 m, O9/4. **5, 6.** *Dorcadospyris ombros* Sanfilippo n. sp.; (5) Holotype (Sample 199-1218A-25X-6, 42–44 cm), Cs.1, D49/0; (6) basal view (Sample 199-1219A-21H-7, 45–47 cm), Cs.2, M24/0. **7.** *Dorcadospyris papilio* (Riedel) (Sample 199-1218A-12H-2, 45–47 cm), A11/0. **8–13.** *Dorcadospyris praeforcipata* Moore; (8) Sample 199-1219B-6H-3, 46–48 cm (K42/2); (9) Sample 199-1218A-11H-1, 44–46 cm (S7/0); (10) Sample 199-1218A-11H-7, 45–47 cm (F17/3); (11) Sample 199-1218A-7H-5, 40–42 cm (J36/0); (12) Sample 199-1219A-8H-1, 43–45 cm (M21/0); (13) Sample 199-1218A-12H-2, 45–47 cm (J2/4). **14, 15.** *Dorcadospyris quadripes* Moore; (14) Sample 199-1220A-7H-4, 45–47 cm (M40/4); (15) Sample 199-1220A-6H-CC (Sl.B, T10/4). **16, 17.** *Dorcadospyris pseudopapilio* Moore; (16) Sample 199-1218A-22X-6, 45–47 cm (Z12/2); (17) Sample 199-1219A-16H-2, 45–47 cm (G33/2). **18, 19.** *Dorcadospyris riedeli* Moore; (18) Sample 199-1219A-6H-7, 45–47 cm (U6/1); (19) Sample 199-1218A-10H-1, 74–75 cm (M22/0).

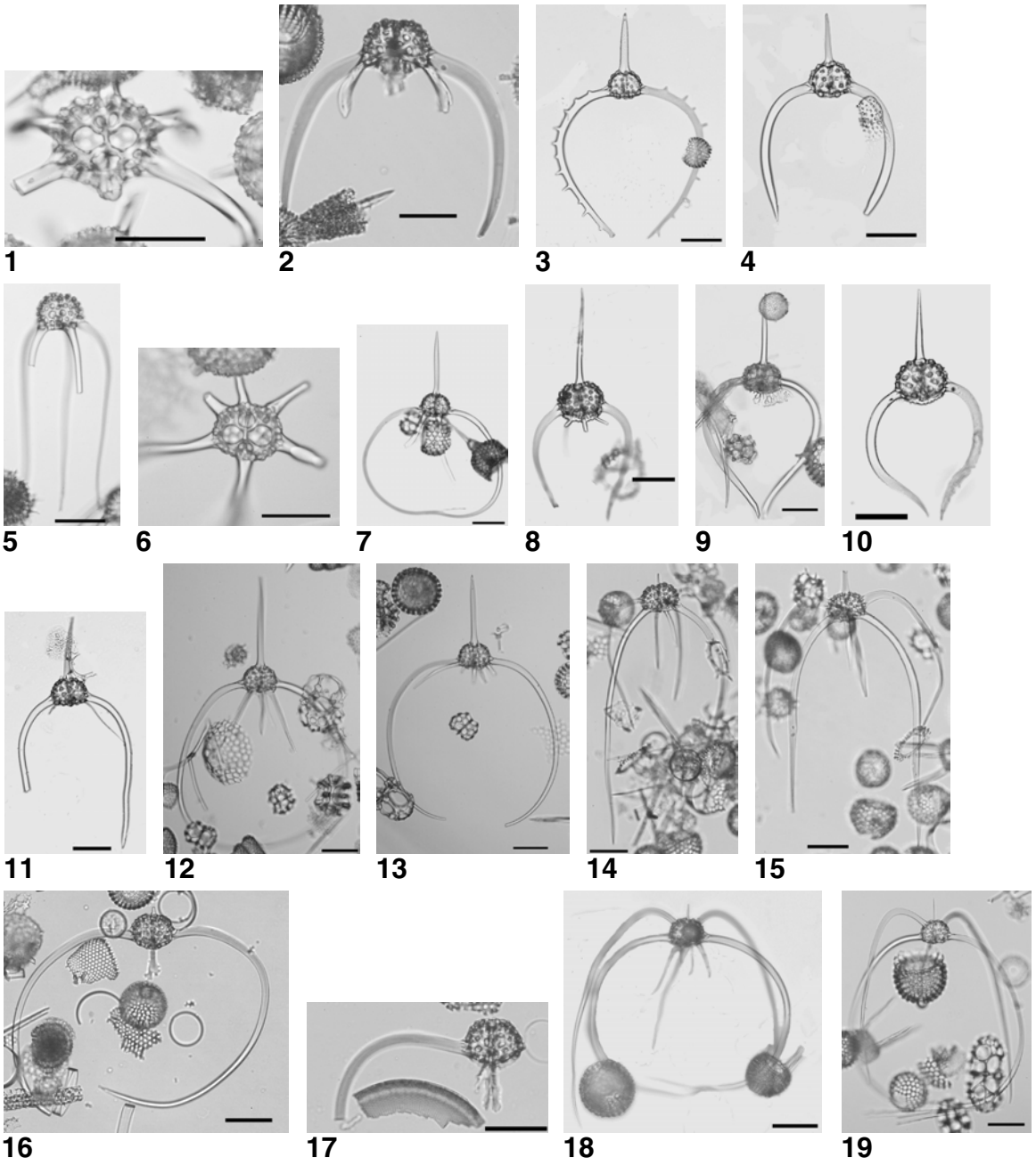

Plate P3. Codes after sample descriptions are slide designation and England Finder coordinates, respectively. Scale bars: Fig. 1 = 50 µm, Figs. 2–22 = 100 µm. **1–4.** *Dorcadospyris scambos* Moore and Nigrini n. sp.; (1) Holotype (Sample 199-1219B-6H-3, 45–47 cm), W31/0; (2) Sample 199-1219A-6H-2, 45–47 cm (G15/4); (3) EW9709-12P, 12.01 m, Y38/2; (4) Sample 199-1218A-10H-1, 74–75 cm (Y10/3). **5.** *Dorcadospyris simplex* (Riedel), s.s. (Sample 199-1219A-4H-CC), V28/0. **6.** *Liriospyris longicornuta* Goll (Sample 199-1219A-8H-2, 45–47 cm), R18/0. **7, 8.** *Tristylospyris triceros* (Ehrenberg); (7) Sample 199-1220A-10H-2, 45–47 cm (Cs.1, Y37/1); (8) Sample 199-1219A-17H-5, 32–34 cm (Cs.2, B42/2). **9–12.** *Zygocircus cimelium* Petrushevskaya; (9) Sample 199-1219A-20H-2, 45–47 cm (Cs.2, J34/2); (10) Sample 199-1218A-26X-5, 46–48 cm (Cs.1, O6/2); (11) Sample 199-1220A-10H-CC (Cs.2, W40/1); (12) Sample 199-1219A-22H-7, 46–48 cm (Cs.2, S39/2). **13, 14.** *Dorcadospyris spinosa* Moore; (13) Sample 199-1220A-7H-2, 45–47 cm (T23/3); (14) Sample 199-1219A-14H-CC (G27/2). **15, 16.** *Anthocyrtoma* spp.; (15) late form from Zone RP15 (Sample 199-1219A-21H-4, 45–47 cm), Cs.2, G34/1; (16) Sample 199-1220B-10H-2, 45–47 cm (Cs.1, X33/2). **17–19.** *Artophormis barbadensis* (Ehrenberg); (17) Sample 199-1220A-10H-6, 45–47 cm (Sl.2, L39/3); (18) Sample 199-1219A-21H-4, 45–47 cm (Cs.1, V29/3); (19) Cs.2, B12/3. **20–22.** *Artophormis gracilis* Riedel; (20) Sample 199-1218A-12H-3, 45–47 cm (R9/2); (21) Sample 199-1220A-6H-CC (Sl.B, T23/3); (22) Sample 199-1218A-12H-2, 45–47 cm (P16/4).

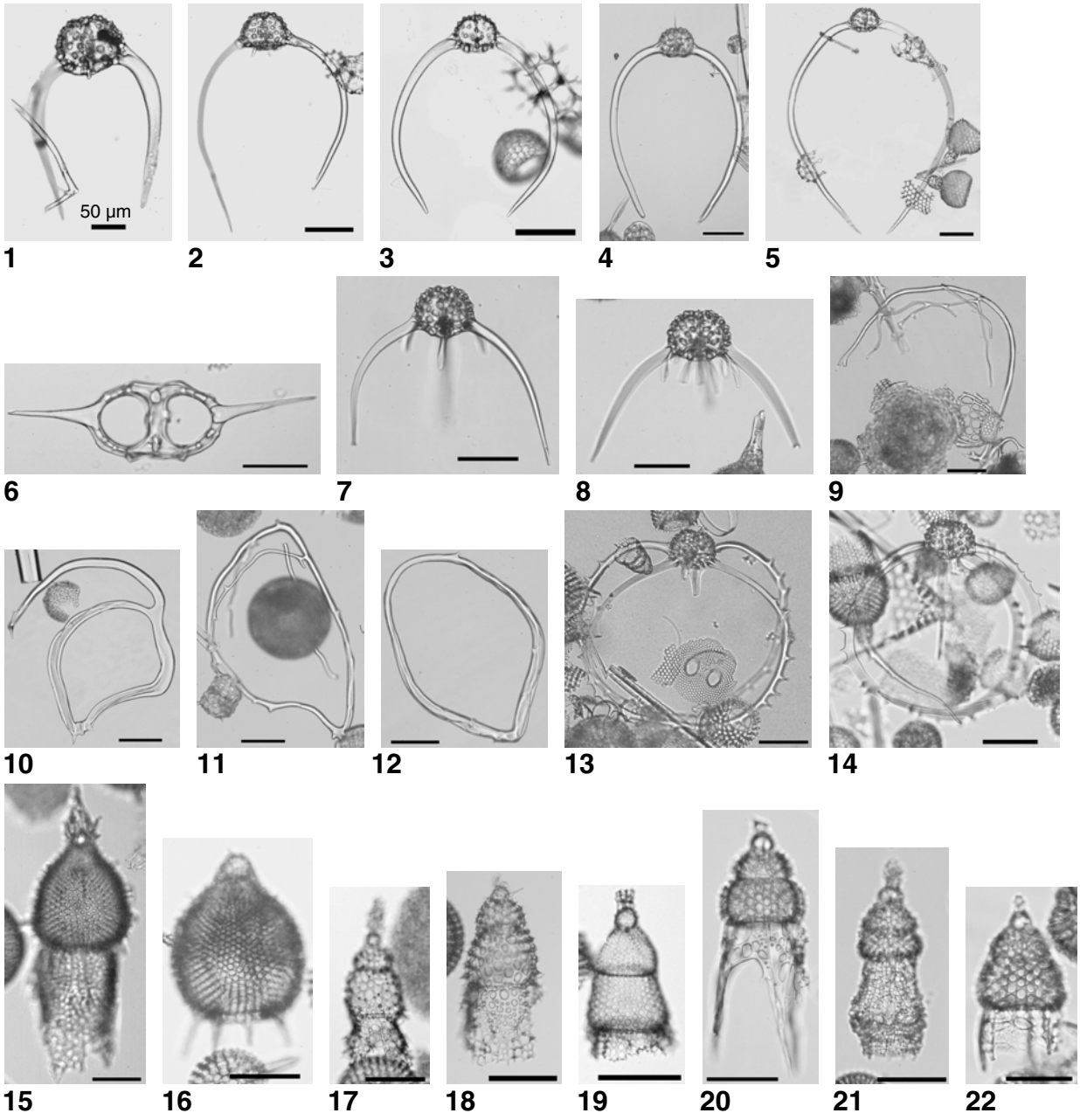

Plate P4. Codes after sample descriptions are slide designation and England Finder coordinates, respectively. Scale bars = 100 µm. **1.** *Artophormis dominasinensis* (Ehrenberg) (Sample 199-1220A-10H-2, 45–47 cm), Cs.2, S27/0. **2–4.** *Eucyrtidium mitodes* Nigrini n. sp.; (2) Sample 199-1218A-12H-6, 45–47 cm (W5/4); (3) Holotype (Sample 199-1219A-6H-3, 45–47 cm), R34/4; (4) P41/4. **5.** *Lamptonium fabaeforme chaunothorax* Riedel and Sanfilippo (Sample 199-1220B-16X-4, 46–48 cm), Sl.1, G27/1. **6.** *Lychnocanoma turgidum* (Ehrenberg) (Sample 199-1219A-21H-4, 45–47 cm), Cs.2, M16/0. **7–10.** *Pterocodon tenellus* Foreman; (7) Sample 199-1220B-18X-2, 10–12 cm (Ph.1, K48/3); (8) N28/0; (9) Sample 199-1220B-18X-3, 41–43 cm (Cs.1, V42/0); (10) X24/0. **11, 12.** *Eucyrtidium plesiodiaphanes* Sanfilippo; (11) Sample 199-1219A-12H-4, 45–47 cm (F3/2); (12) Sample 199-1220A-5H-4, 45–47 cm (J15/4). **13.** *Eusyringium fistuligerum* (Ehrenberg) (Sample 199-1218A-26X-7, 9–11 cm), Cs.1, E31/2. **14.** *Lychnocanoma apodora* Sanfilippo (Sample 199-1219A-8H-2, 45–47 cm), V8/1. **15, 16.** *Rhopalocanium ornatum* Ehrenberg; (15) Sample 199-1219A-21H-7, 45–47 cm (Cs.2, B28/0); (16) Sample 199-1219A-25X-2, 45–47 cm (Ph.1, X39/4). **17, 18.** *Theocorys puriri* O'Connor; (17) Sample 199-1219A-8H-6, 45–47 cm (Sl.SIO, N33/3); (18) Sample 199-1218A-14H-4, 45–47 cm (S9/0). **19–21.** *Theocorys spongoconus* Kling; (19) Sample 199-1219A-12H-CC (H39/2); (20) Sample 199-1218A-15H-6, 45–47 cm (F20/4); (21) Sample 199-1220A-6H-CC (N14/3).

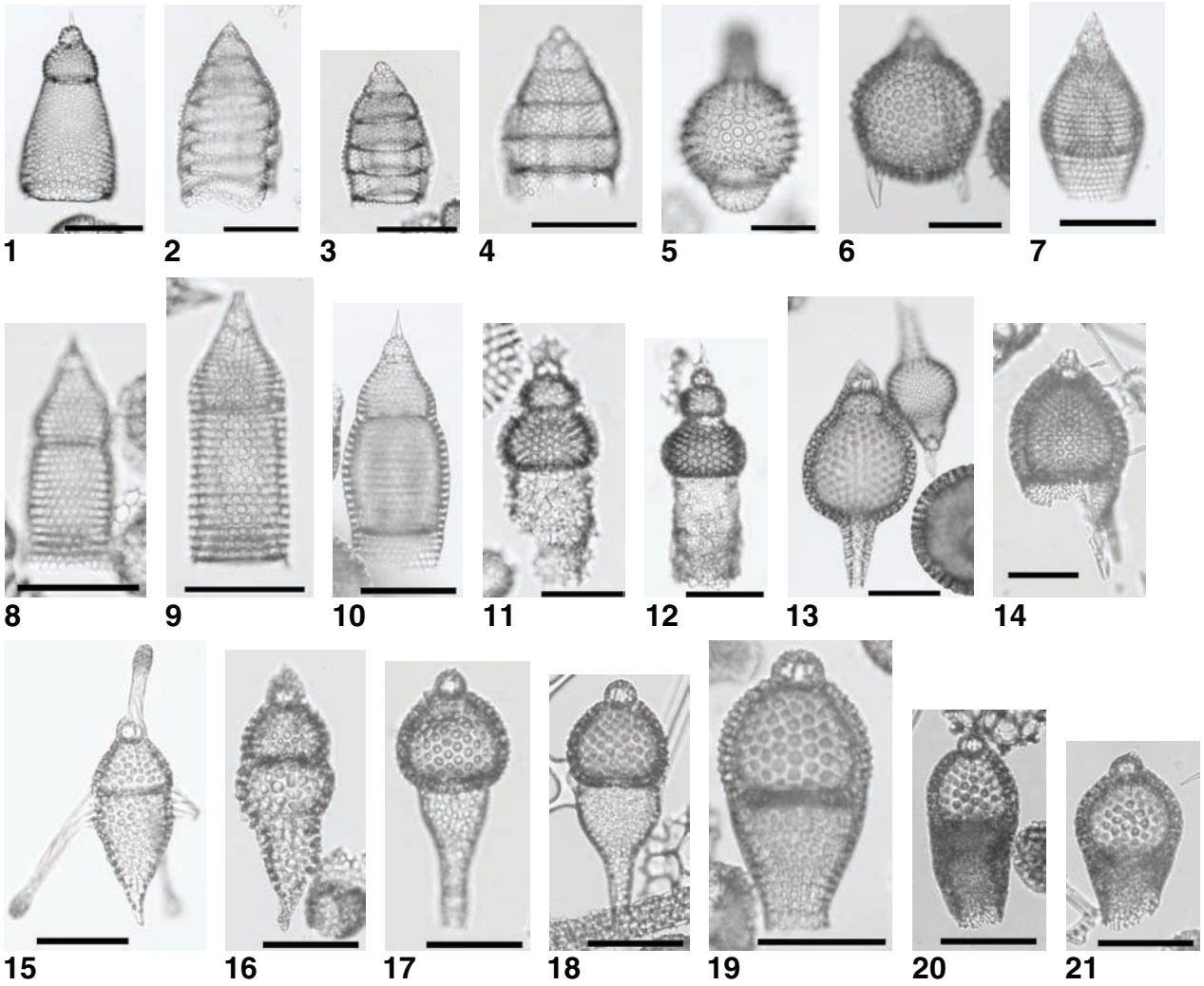

Plate P5. Codes after sample descriptions are slide designation and England Finder coordinates, respectively. Scale bars: Figs. 19, 20 = 50 µm, Figs. 1–18, 21, 22 = 100 µm. **1.** *Theocotylissa ficus* (Ehrenberg) (Sample 199-1219A-19H-6, 45–47 cm), Cs.2, B40/3. **2.** *Pteropilium* sp. aff. *Pterocanium contiguum* (Ehrenberg) (Sample 199-1219A-10H-3, 45–47 cm), T17/4. **3–5.** *Thyrsocyrtis (Pentalacorys) orthotenes* Sanfilippo n. sp.; (3) early form (Sample 199-1220B-10H-2, 45–47 cm), Cs.1, P17/0; (4) late form (Sample 199-1218A-25X-5, 63–65 cm), Cs.1, H30/0; (5) Holotype (Sample 199-1219A-19H-1, 45–47 cm), Cs.1, C21/1. **6.** *Calocycletta (Calocycletta) robusta* Moore (Sample 199-1219A-6H-7, 45–47 cm), H21/2. **7–9.** *Calocycletta (Calocycletta) anekathen* Sanfilippo and Nigrini n. sp.; (7) Sample 199-1219A-17H-5, 32–34 cm (Cs.2, L11/4); (8) K18/2; (9) Holotype (R25/3). **10.** *Podocyrtis (Podocyrtoges) diamesa* Riedel and Sanfilippo (Sample 199-1220B-11H-1, 45–47 cm), Cs.2, Q40/0. **11, 12.** *Podocyrtis (Lampterium) goetheana* (Haeckel); (11) Sample 199-1220A-10H-CC (Cs.1, L12/0); (12) Sample 199-1219A-19H-1, 45–47 cm (Cs.2, U9/3). **13.** *Podocyrtis (Podocyrtis) papalis* Ehrenberg (Sample 199-1220B-11H-1, 45–47 cm), Cs.2, U41/0. **14.** *Theocyrtis annosa* (Riedel) (Sample 199-1218A-9H-7, 74–75 cm), C37/0. **15–18.** *Theocyrtis careotuberosa* Nigrini and Sanfilippo n. sp.; (15) Holotype (Sample 199-1219A-18H-6, 45–47 cm), Cs.1, U10/3; (16) Sample 199-1218A-23X-CC (J36/3); (17) Sample 199-1220A-8H-2, 20–22 cm (Sl.1, Q7/0); (18) Sample 199-1219A-18H-5, 45–47 cm (Ph.2, C6/3). **19–22.** *Theocyrtis perpumila* Sanfilippo n. sp.; (19) late form (Sample 199-1219A-19H-5, 45–47 cm), Cs.2, O27/4; (20) Sample 199-1219A-21H-1, 45–47 cm (Cs.1, V43/2); (21) Holotype (Sample 199-1219A-21H-6, 45–47 cm), Ph.1 R10/1; (22) Sample 199-1219A-21H-1, 45–47 cm (Cs.2, M36/0).

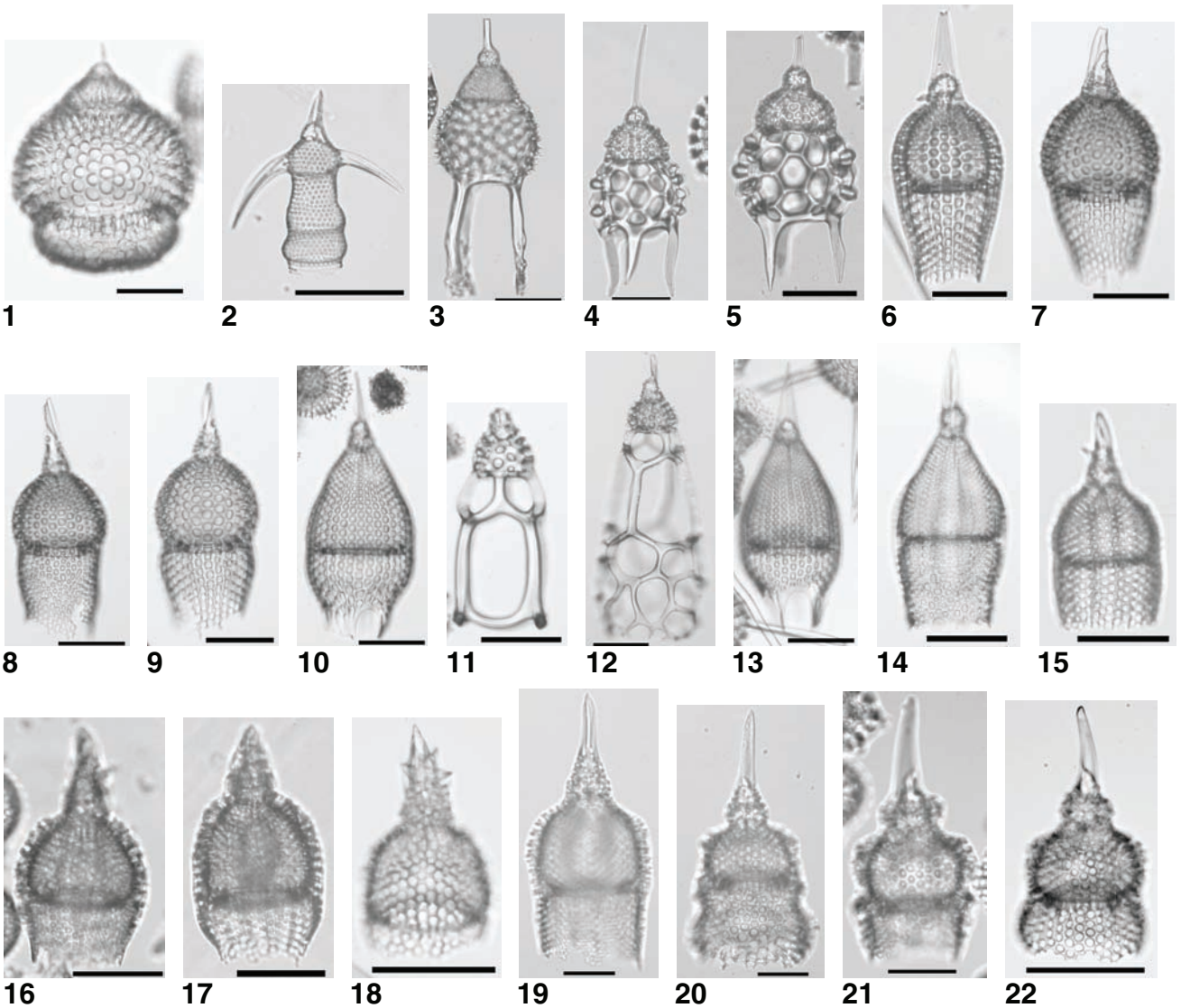

Plate P6. Codes after sample descriptions are slide designation and England Finder coordinates, respectively. Scale bars = 100 µm. **1, 2.** *Theocyrtis perysinos* Nigrini and Sanfilippo n. sp.; (1) Holotype (Sample 199-1218A-17H-6, 45–47 cm), Z19/1; (2) Sample 199-1219A-12H-7, 45–47 cm (J27/0). **3–5.** *Theocyrtis setanios* Nigrini and Sanfilippo n. sp.; (3) Sample 199-1218A-17H-2, 48–50 cm (V23/3); (4) Holotype (L6/4); (5) Sample 199-1219A-12H-5, 45–47 cm (D32/0). **6.** *Theocyrtis tuberosa* Riedel, emend. Sanfilippo et al. (Sample 199-1219A-15H-CC), U42/0. **7.** *Spirocyrtis subtilis* Petrushevskaya (Sample 199-1218A-15H-6, 45–47 cm), X20/0. **8.** *Dictyoprora* cf. *D. ovata* (Haeckel) (Sample 199-1220A-12H-2, 45–47 cm), Ph.1, U33/1. **9.** *Dictyoprora armadillo* (Ehrenberg) (Sample 199-1219A-18H-2, 45–47 cm), Ph.2, X6/3. **10, 11.** *Dictyoprora pirum* (Ehrenberg); (10) Sample 199-1219A-17H-6, 45–47 cm (Ph.1, O6/0); (11) Sample 199-1219A-17H-6, 45–47 cm (Ph.1, S31/2). **12, 13.** *Dictyoprora* spp.; (12) Sample 199-1218A-24X-4, 50–52 cm (Ph.1, K19/4); (13) Sample 199-1218A-26X-7, 9–11 cm (Ph. 2, G35/0). **14.** *Acrobotrys disolenia* Haeckel (Sample 199-1218A-7H-7, 46–48 cm), H13/2. **15.** *Acrobotrys* cf. *A. disolenia* Haeckel (Sample 199-1219A-8H-6, 45–47 cm), S29/1. **16–18.** *Botryocella* sp. gr.; (16) Sample 199-1219A-18H-2, 45–47 cm (Ph.2, V37/0); (17) Sample 199-1218A-28X-4, 46–48 cm (Ph.1, R10/0); (18) Sample 199-1219A-18H-7, 45–47 cm (Ph.1, Q28/0). **19–21.** *Botryopyle* sp. A Petrushevskaya; (19) Sample 199-1220A-11H-6, 45–47 cm (Ph.1, G26/3); (20) Sample 199-1220B-11H-CC (Ph.1, H35/0); (21) Sample 199-1220A-12H-5, 45–47 cm) (Ph.2, Q39/2). **22, 23.** *Centrobotrys petrushevskayae* Sanfilippo and Riedel; (22) Sample 199-1218A-12H-6, 45–47 cm (Y26/0); (23) Sample 199-1218A-15H-CC (O4/4). **24–26.** *Centrobotrys thermophila* Petrushevskaya; (24) Sample 199-1218A-9H-7, 74–75 cm (R31/2); (25) Sample 199-1218A-16H-CC (H37/2); (26) Q32/0.